Reviews of Geophysics

REVIEW ARTICLE
10.1029/2024RG000860

Land Reclamation Impacts on Tidal Landscape Evolution

D. S. van Maren[1,2], R. A. Schrijvershof[2,3], J. Beemster[3], C. Zhu[4], D. Xie[5], Z. Zhou[4], A. Colina Alonso[2], and A. J. F. Hoitink[3]

[1]Deltares, Delft, The Netherlands, [2]Delft University of Technology, Faculty of Civil Engineering and Geosciences, Delft, The Netherlands, [3]Hydrology and Environmental Hydraulics Group, Department of Environmental Sciences, Wageningen University, Wageningen, The Netherlands, [4]East China Normal University, State Key Lab of Estuarine and Coastal Research, Shanghai, China, [5]Zhejiang Institute of Hydraulics and Estuary, Hangzhou, China

Key Points:

- Reclamation of intertidal land strongly controls tidal dynamics and bed stability in tide-dominated coastal and estuarine environments
- Along-estuary land reclamation leads to tidal amplification but reclamation of inland areas to lower flow velocities and channel infilling
- Tidal channel networks are especially vulnerable to land reclamation, driving persistent erosion of tidal channels connecting distributaries

Correspondence to:
D. S. van Maren,
bas.vanmaren@deltares.nl

Citation:
van Maren, D. S., Schrijvershof, R. A., Beemster, J., Zhu, C., Xie, D., Zhou, Z., et al. (2025). Land reclamation impacts on tidal landscape evolution. *Reviews of Geophysics*, *63*, e2024RG000860. https://doi.org/10.1029/2024RG000860

Received 14 NOV 2024
Accepted 3 JUL 2025

Author Contributions:
Conceptualization: D. S. van Maren, R. A. Schrijvershof, J. Beemster, A. J. F. Hoitink
Data curation: D. S. van Maren, R. A. Schrijvershof, C. Zhu, D. Xie, Z. Zhou, A. Colina Alonso
Formal analysis: D. S. van Maren, J. Beemster, A. J. F. Hoitink
Methodology: D. S. van Maren, R. A. Schrijvershof, J. Beemster, A. J. F. Hoitink
Visualization: D. S. van Maren, C. Zhu
Writing – original draft: D. S. van Maren, R. A. Schrijvershof, J. Beemster, C. Zhu, D. Xie, Z. Zhou, A. Colina Alonso, A. J. F. Hoitink

Abstract In the past 1000 years, the continuous need for fertile and strategically located land has led to the reclamation of intertidal areas. The direct and short-term impact of land reclamation is a reduction in intertidal storage space and the loss of ecological value. Its long-term impact on the tidal landscape is variable but surprisingly poorly known. In this contribution, we review the impacts of land reclamation in a wide range of physical environments. Land reclamation along exposed, muddy coastlines leads to erosion or accretion, depending on local transport conditions and sediment availability. Confined muddy coasts (typically estuaries) respond by progressive infilling of tidal channels, especially when their upper reaches have been reclaimed. More gradual reclamation along the length of an estuary can lead to tidal amplification, while reclamation at the estuary mouth may additionally lead to channel erosion. The response timescales may be very long (up to centuries) especially when controlled by positive feedback mechanisms between tidal dynamics and landscape evolution. Therefore, some of the present day land reclamations will influence or possibly control the evolution of the coastal landscape in the coming decades to even centuries. In sediment-poor coastal bays, the reduction in tidal prism mainly leads to lower exchange rates and, therefore, to a reduction in water quality. The framework introduced here facilitates the assessment of the past and future impacts of land reclamations in tide-dominated environments. This understanding is crucial to predict the response of land reclamation-impacted coastal systems to accelerated sea level rise.

Plain Language Summary Fertile and low-lying coastal landscapes are often densely populated due to food supply (agriculture, aquaculture, and fisheries) and easy navigability (shipping lanes). Much of the low-lying land that is regularly inundated by the sea has been converted to agricultural land or urban environments to meet the need for land. This reclamation of land influences the tidal dynamics of the coastal environment, which in turn modifies its morphology. Through various complex tide-topography interactions identified in this paper, we explore how the location and extent of land reclamation influences tides and bed levels in various tidal environments. We especially point to the key role of sediments herein, introducing feedback mechanisms that lead to large impacts on tidal landscapes, but also long adaptation times. This is especially the case for estuaries due to their confinement and the typically large availability of sediments.

1. Introduction

1.1. Motivation

Most of the world's low-lying coastlines are densely populated, with 38% of the global population living within 100 km from the sea (Barbier, 2015) and 10% of the global population inhabiting the low-elevation coastal zone (LECZ) at an altitude less than 10 m above Mean Sea Level (McGranahan et al., 2007; Neumann et al., 2015). Population growth is also relatively large in these coastal areas, with the LECZ expected to contribute to 12% of the global population by 2060 (Neumann et al., 2015). Within the LECZ, the population density in deltaic areas is 2.6 times larger (and the urbanization rate 2 times larger) than in the non-deltaic LECZ (McGranahan et al., 2023). Humans have reshaped deltas in the past 7,000 years through various hydraulic engineering works to harness resources, protect against floods, erosion and avulsions, and encourage urbanization, agriculture and engineering (Anthony et al., 2024). These demographic developments have put the available land under pressure and have resulted in the reclamation of wetlands into agricultural or urbanized land (Fluet-Chouinard et al., 2023).

Land reclamations exist in a wide variety of types, sizes, and shapes, reflecting the coastal environments in which they are constructed, their purpose, and the period and regions of construction. Land reclamations may have

gradually encroached seaward by trapping of sediments or more suddenly by the creation of embankments in the intertidal zone, but may also be realized by closing off estuaries and embayments, or through the development of artificial islands. They may be constructed along open, exposed coastlines, but also within estuaries and lagoons. Half of the world's coastal wetlands were lost in the 20th century (~200,000 km^2; see X. Li, Bellerby, et al. (2018)). Another 13,700 km^2 of wetland was lost in the 21st century (of which 27% due to land reclamation), although a large amount of wetland loss was compensated for by the development of 9,700 km^2 of new wetland (Murray et al., 2022). In addition, 2530 km^2 of land was reclaimed in the 21st century by seaward expansion of the coastline, mostly for port facilities and industry (Sengupta et al., 2023) and concentrated in Asia, accounting for 90% of all land reclamation between 1984 and 2019 (Jung et al., 2024). The 4,000 km long shoreline of the Yellow Sea, for instance, has lost 65% of its tidal flats due to land reclamation in the past 50 years (Murray et al., 2014).

The destruction of wetlands for land reclamation purposes leads to losses of ecological value (Barbier et al., 2011; Kelleway et al., 2017), resilience against floods (Kirwan & Megonigal, 2013; Spencer et al., 2016), and connectivity (Bishop et al., 2017; Olds et al., 2018). Since resilient wetlands serve to protect the coast (Temmerman et al., 2013, 2023; Van Zelst et al., 2021; Z. Zhu et al., 2020), their destruction for land reclamation purposes negatively influences coastal safety. In fact, natural buffers that have the capacity to mitigate the effects of climate change (Kirezci et al., 2020; Neumann et al., 2015) are often sacrificed. Land reclamation may strongly influence tidal dynamics, sometimes leading to amplification of the tides (Stark et al., 2017; van Maren, Alonso, et al., 2023; van Maren, Beemster, et al., 2023; Weisscher et al., 2022) and resulting in channel erosion (Nnafie et al., 2019). With limited maintenance dredging, reclamation may also lead to basin infilling (Pierik, 2021; van Maren et al., 2016; Xie et al., 2017, 2022), thereby damping the tides (L. Li et al., 2019). The loss of net depositional areas associated with land reclamation disturbs the natural sediment balance, resulting in increasing turbidity levels (Morris & Mitchell, 2013; van Maren et al., 2016) and sediment deposition (Benninghoff & Winter, 2019; van Maren, Alonso, et al., 2023). Large-scale land reclamation can strongly reduce tidal flow velocities and associated mixing rates (J. Shi et al., 2011; C. Xu et al., 2021), exerting an unfavorable impact on water quality (R. Jia et al., 2018; Lyu et al., 2022; Yamaguchi & Hayami, 2018).

The ecological impact of land reclamation is covered in several literature reviews (Bishop et al., 2017; Gedan et al., 2009; Gittman et al., 2015; He & Silliman, 2019; Kennish, 2001). Review studies addressing the hydromorphological impacts of human control measures in estuaries have mainly focused on changing upstream sediment loads (Syvitski et al., 2005; Syvitski & Kettner, 2011; Walling, 2006) or on tidal channel deepening (Haigh et al., 2020; Talke & Jay, 2020; Winterwerp & Wang, 2013, 2021). Despite their major impact on the environment, the hydromorphological response to land reclamation has not yet received similar attention to date–only the impact of estuarine dams and weirs was recently synthesized by Figueroa and Son (2024). Through the wide range of individual case studies available, we know that the impact of reclamation works depends on their size, shape, and type (Zhong & Hu, 2021), their position within the coastal system (C. Li et al., 2016; Yang & Chui, 2017; Weisscher et al., 2022) and the sequence of their construction (G. D. Gao et al., 2014; Weisscher et al., 2022; van Maren, Beemster, et al., 2023), but also on the coastal environment in which they are constructed. However, a systematic framework relating these case studies does not yet exist, limiting generic understanding of the historic but also future response of tide-dominated environments to land reclamation.

1.2. Scope

This review focuses on the impact of land reclamations in tidal landscapes on tidal deformation and morphodynamic changes. Largely consistent with Galloway (1975) and Dalrymple and Choi (2007), who (respectively) focused on deltas and fluvial-marine systems, we define tidal landscapes as landscapes where tidal currents are responsible for the majority of sediment transport relative to river currents and waves, and thus largely control geomorphology. As will be explained in greater detail throughout this paper, such tidal landscapes are strongly impacted by reclamation works, with response timescales up to centuries. The slow but also pronounced response of tidal landscapes to land reclamations can be explained with tide-topography interactions and feedback mechanisms which will be extensively addressed later (Sections 2 and 3, respectively). Tidal environments are highly suitable for, and have thus been strongly impacted by, land reclamation because (a) their offshore profiles are gently sloping, especially when sediment supply is abundant and/or (b) they often have tidal (sub)basins which can be closed and reclaimed. Examples elaborated on in this review include:

Figure 1. Visual overview of land reclamation types in type-dominated estuaries: a centuries-old land reclamation method gradually converting intertidal area to agricultural land (Dutch-German Wadden Sea, a); a dam closing off the largest land reclamation of the world (South Sea, b); Salt ponds (South San Francisco Bay, c); a polder with former creek now functioning as drainage channel (Bangladesh, d); recent concrete embankments preparing wetlands for reclamation (Yangtze River mouth, e); and gradual conversion from salt marsh to urban area (Hangzhou Bay, f). Photos courtesy of Siebe Swart (a), Staartjes Fotografie Deventer (b), https://commons.wikimedia.org/wiki/File:South_San_Francisco_Bay_salt_ponds_and_wildlife_refuges.jpg (c), https://www.bluegoldwiki.com/index.php?curid=2281 (d), SKLEC (e), and https://map.tianditu.gov.cn (f).

1. Land reclaimed slowly over centuries by semi-natural sediment trapping on intertidal areas, followed by subsequent drainage and poldering, as common in Northwest Europe (Figure 1a).
2. Closure of estuaries and tidal basins (as progressively more common by the end of the 20th century, Figure 1b).
3. Conversion of wetlands to salt ponds or fish ponds (Figure 1c).
4. Direct occupation of supratidal wetlands and upper intertidal flats through the construction of seadikes and subsequent drainage, common practice in the 20th and 21st century (Figures 1d–1f).

The impact of land reclamation is strongly influenced by its confinement and availability of sediments. Areas with a large sediment availability are often characterized by gently sloping intertidal zones, which are suitable for reclamation. The availability of sediments also influences the response rate and gives rise to positive feedback mechanisms which may strongly extend the duration of a response (see Section 3). Furthermore, land reclamation strongly influences its environment when it is confined within a bay or estuary. We therefore distinguish three overall landscape types in this paper: (a) enclosed muddy coasts, (b) open muddy coasts, and (c) confined systems with low sediment availability. We identify the role of land reclamations by examining data of coastal response in combination with historical reclamation. In many coastal systems, this relation is obscured by concurrent human interventions that influence sediment supply, river discharge, or tidal propagation. We keep our focus on the role of land reclamations by examining data over periods in which land reclamation was the dominant intervention. For some systems, this was the period of early settlement, for which data is available in the form of navigation charts or geologic reconstructions; construction of reservoirs or deepening of channels started centuries later. The rapidly developing deltas along the Asian coastline were strongly influenced by land reclamations from the mid-20th century onward, with the impact of deepening and large-scale reservoir construction typically playing an additional (or dominant) role from the 21st century onward. This provides a time window for our review to focus on.

This review does not address land reclamation through island building (Smith et al., 2019; Subraelu et al., 2022) and land fill reclamations in general (Martín-Antón et al., 2016) due to its smaller impact on tidal hydrodynamics. Given our focus on tidal deformation and morphodynamic changes, we also exclude the more subtle effects of land reclamation on tidal dynamics of coastal seas (see e.g. Song et al. (2013) or Feng and Feng (2021)). While addressing the hydro- and morphodynamic changes in water bodies seaward of closures we do not discuss changes landward of these constructions (e.g., infilling of water bodies behind tidal barrages). We also do not evaluate the estuarine or coastal response to reservoirs constructed in the river domain, which is covered by other reviews (Syvitski et al., 2005; Syvitski & Kettner, 2011; Walling, 2006). Most of our key study sites reveal a response to reclamation before large-scale reservoir construction. However, the sediment load in rivers has been

anthropogenically influenced before the construction of reservoirs, mainly due to changes in land use (Syvitski et al., 2022). Such changes are typically only very limitedly known and, therefore, not explicitly addressed.

1.3. Methodology

This review is primarily based on information collected from scientific literature, supplemented with technical reports openly accessible through internet, obtained via a wide range of search terms. As explained in the previous section, the impact of land reclamation is obscured by additional human interventions executed simultaneously. Much land was reclaimed centuries ago during periods with limited data availability, preventing a quantitative assessment of the hydromorphological response. Data are often more abundantly available for recent reclamations. However, such recent reclamation works are often executed concurrently with other major human interventions such as the construction of upstream reservoirs and/or deepening of tidal channels for navigation purposes, obscuring the isolated impact of land reclamation.

We identify two types of systems for which data documenting the impact of land reclamation are available in the literature. The first type constitutes historic reclamations realized centuries ago in systems with important fairways for which navigation charts and water level observations are available. The second type describes reclamations sufficiently modern to be monitored, but executed before the additional effects of channel deepening or construction of upstream reservoirs additionally influenced its hydrogeomorphological response. Through this process, we have collected 54 sites in which observational data is available to quantitatively relate the landscape changes to land reclamation works (see Table 1). Within these 54 sites, we identified nine key sites for which a relatively large amount of data is available covering (a) timeseries of land reclamation areas, tidal range and channel infill volumes, and (b) maps showing the extent of the reclamations. A global map of our 54 case studies (with the nine key sites in purple) is provided in Figure 2, classified according to response type which will be detailed in Section 4. Sediment availability, especially mud, is herein an important factor (as will also be elaborated in Sections 2 and 3) and therefore we also provide the mud content (global data set from Hulskamp et al., 2023).

The results of our review are presented in four parts. First, we provide a general background to intertidal areas and the interaction between intertidal environments and the coastal system (Section 2). The impact of land reclamation may be pronounced and long-lasting because of positive feedback mechanisms that strengthen the effect of the intervention. Therefore, we introduce these concepts in Section 3. We then introduce a framework that explains how different reclamations influence their environment in Section 4. This framework is based on our interpretation of the literature documenting the response of all 54 sites. Thereafter (Section 5), we describe the response of the nine key sites in greater detail and interpret their response using our framework.

2. Tide-Topography Interaction: The Role of Intertidal Areas

2.1. Intertidal Areas

In tide-dominated environments, reclaimed land often comprise former tidal wetlands and intertidal flats. Tidal wetlands are typically inundated during spring tides and storm events, and vegetated with salt marshes in temperate regions and mangroves in tropical areas. Seaward of these wetlands, the intertidal flats are gently sloping regions that are submerged during parts of the tidal cycle. Their width is mainly determined by local hydrodynamic conditions (such as the tidal range and wave height) and the availability of sediment (S. Gao, 2019; Roberts et al., 2000). Low-energy, macro-tidal, and sediment-rich environments tend to favor the development of wide tidal flats. These flats are typically several km wide, but may extend up to several tens of kilometers along the Chinese continental shelf (N. Xu, Ma, et al., 2022) and the South American coast (Anthony et al., 2010). The relative importance of waves and tides controls the shape of the flat, with tidal dominance resulting in convex-upward flats and wave-dominance in concave-upward flats (Friedrichs, 2011). Tidal flats can be muddy or sandy, with the mud content typically increasing in the landward direction. Vegetation on tidal wetlands increases flow resistance and wave dissipation, enhancing sediment deposition and promoting elevation gain. The presence of diverse vegetation species generally increases stability of tidal wetlands and therefore enhances resilience to sea level rise (D'Alpaos et al., 2012).

Tidal flat hydrodynamics are governed by the prevailing alongshore tidal currents in deeper water and cross-shore tidal currents over the intertidal zone (Figure 3). The alongshore tidal currents in estuaries and coastal seas are primarily driven by the alongshore barotropic water level gradient. Relatively high friction over the tidal flats

Table 1
Overview of Study Sites (and References) per Response Type

Response type	System
Infilling (reclamation)	**Ems Estuary, the Netherlands** (Pierik, 2021; Schrijvershof et al., 2024; van Maren et al., 2016)
	South Bay (San Francisco Bay), United States (Foxgrover et al., 2004; B. Jaffe & Foxgrover, 2006; Fregoso et al., 2008)
	North Branch (Yangtze delta), China (Guo et al., 2021; S. Wu et al., 2019; X. Zhang et al., 2022)
	Outer Hangzhou Bay, China (Z.-j. Dai et al., 2014; L. Li et al., 2019; Y. Shi et al., 2022; Xie et al., 2017)
	Lingding Bay (Pearl River Estuary), China (Han et al., 2023; H. Wang et al., 2020; X. Zhang et al., 2022; P. Zhang et al., 2021)
	Deep bay (Pearl River Estuary), China (Yang & Chui, 2017)
	Xiangshan Bay, China (L. Li et al., 2017, L. Li, Bellerby, et al., 2018)
	Xiamen Bay, China (Y. Chen et al., 2019; J. Wang et al., 2013)
	Puba Bay, China (Y. Liu et al., 2024)
	Ribble Estuary, United Kingdom (Van Der Wal et al., 2002)
	Sydney Estuary, Australia (Birch et al., 2009; McLoughlin, 2000)
	Ord Estuary, Australia (Wolanski et al., 2001)
	Manilla Bay, the Philippines (MBSDMP, 2020; Siringan & Ringor, 1998)
Infilling (closure dams)	**South Sea, the Netherlands** (Colina Alonso et al., 2021; Elias et al., 2012; Kragtwijk et al., 2004; van Maren, Alonso, et al., 2023)
	Haringvliet Estuary, the Netherlands (Elias et al., 2017; Tonis et al., 2002; Van Der Spek & Elias, 2021)
	Grevelingen Estuary, the Netherlands (Elias et al., 2017; Van Der Spek & Elias, 2021)
	Lauwers Sea, the Netherlands (A. P. Oost, 1995; van Maren, Alonso, et al., 2023)
	Vilaine Estuary, France, the Netherlands (Traini et al., 2015)
	Yeongshan Estuary, South Korea (Williams et al., 2014)
	Keum River Estuary, South Korea (Figueroa et al., 2020; Kang et al., 2022; Kim et al., 2006)
	Nakdong Estuary, South Korea (Chang et al., 2020, 2023; Williams et al., 2013)
	Xinyanggang Estuary, China (Q. Zhu et al., 2017)
	Petitcodiac River Estuary, Canada (Van Proosdij et al., 2009)
	Avon River Estuary, Canada (Van Proosdij et al., 2009)
Tidal amplification	**Scheldt Estuary, the Netherlands** (Coen, 1988; Dam et al., 2022; Mol, 1995; van der Spek, 1997)
	Passur-Sibsa Estuary, Bangladesh (Bain et al., 2019; van Maren, Beemster, et al., 2023; Wilson et al., 2017)
	Qiantang Estuary (Xie et al., 2017; Xie et al., 2022; Y. Liu et al., 2018; L. Li et al., 2019)
	Jiaojiang Estuary, China (Sun et al., 2017)
	Thames Estuary, United Kingdom (Siggers et al., 2006)
	Humber Estuary, United Kingdom (Morris & Mitchell, 2013)
	Seine Estuary, France (Dronkers, 2016)
	Eider Estuary, Germany (Bednarczyk et al., 2008)
	Jamaica Bay, United States (Orton et al., 2020; Parejaroman et al., 2023; Swanson & Wilson, 2008)
	Boston Harbor, United States (Talke et al., 2018b)
Mouth zone erosion	**Modaomen Estuary (Pearl River Estuary), China** (L. W. Jia et al., 2013; Cai et al., 2012)
	Deep Bay (Pearl River Estuary), China (Yang & Chui, 2017)
	Yalu Estuary, China (Cheng et al., 2020)
Reduced hydrodynamic energy	**Jiaozhou Bay, China** (J. Shi et al., 2011; G. D. Gao et al., 2014, 2018; C. Xu et al., 2021; Yuan et al., 2021; Qiao et al., 2019)
	Bohai Bay, China (Ding & Wei, 2017; Liang et al., 2018; Pelling et al., 2013; C. Shen et al., 2016; X. Wang et al., 2021; Z. Wu et al., 2023; H.-Y. Yang et al., 2011; G. Zhu et al., 2021)
	Qinzhou Bay, China (Lyu et al., 2022)
	Laizhou Bay, China (Z. Wu et al., 2023)

Table 1
Continued

Response type	System
	Liaodong Bay, China (Z. Wu et al., 2023)
	Sanmen Bay, China (W. Yang et al., 2019; P. Shi et al., 2024)
	Ariake Sea, Japan (R. Jia et al., 2018; Yamaguchi & Hayami, 2018)
	Tokio Bay, Japan (Okada et al., 2011)
	Jakarta Bay, Indonesia (Ningsih et al., 2024; Rusdiansyah et al., 2018)
	Doha Bay, Qatar (Lecart et al., 2024)
Reduced cross-shore transport	Jiangsu Coast, China (Du et al., 2019; X. J. Liu et al., 2011; N. Xu, Wang, et al., 2022; Q. Zhu et al., 2016)
	Wenzhou Coast, China (R. Zhang et al., 2023)
	Ruian Coast, China (P. Chen et al., 2021)
	Eastern Wadden Sea, Germany (Dellwig et al., 2000; Flemming et al., 1994; Flemming & Nyandwi, 1994)
	Coronie Coast, Surinam (Winterwerp, Erftemeijer, et al., 2013)
	Guyana Coast, Guyana (Winterwerp, Erftemeijer, et al., 2013)
	Bang Khun Thien Coast, Thailand (Winterwerp, Erftemeijer, et al., 2013; Winterwerp et al., 2005)
	Demak Coast, Indonesia (Winterwerp, Erftemeijer, et al., 2013)

Note. The first four responses occur in estuaries (infilling estuaries due to gradual reclamation of the upper estuary or by basin closure; tidal amplification by along-estuary reclamation and funelling; and erosion of channels resulting reclamation of the estuary mouth). Reduced hydrodynamic energy occurs in sediment-poor systems such as embayments, while a reduction in cross-shore transport influences open muddy open coasts (leading to erosion or to deposition). Sites discussed in greater detail in Section 5 are in bold.

leads to a concentration of the alongshore flow in deeper channels, where bed friction is lower. The alongshore flow is thus relatively weak over wide, shallow flats. The volume changes associated with tidal filling and emptying gives rise to a cross-shore tidal current. Muddy, gently sloping tidal flats are usually shaped by those cross-shore currents rather than by longshore tidal currents (Winterwerp et al., 2022).

2.2. Influence on Tidal Dynamics

The inundation of tidal flats strongly affects tidal dynamics within coastal systems. The influence of tidal flats on tidal behavior increases with the size of the tidal flat area relative to the channel area (Friedrichs & Aubrey, 1988). Consequently, changes in tidal flats tend to have a more substantial impact in estuaries than in open coastal seas. The relationship between tidal flats and tides has been well documented in the literature and will be briefly synthesized in the following section. Key aspects herein are changes in tidal range (amplification) and changes in tidal asymmetry.

Estuarine tidal dynamics are largely determined by the balance between frictional losses and the convergence of the estuary's cross-sectional area (Dronkers, 1986; Jay, 1991; Leuven et al., 2021). Frictional dissipation occurs over the estuary bed, within the water column, and over intertidal areas and tidal wetlands, with shallow estuaries and opposing river flow promoting the greatest dissipation. In contrast, tidal amplification results from width convergence, where the narrowing (funneling) of the estuary increases the tidal amplitude (Jay, 1991). Tidal flats influence this balance in several ways. Firstly, they provide storage for incoming tides. Inundated tidal flats accommodate substantial volumes of water, (a) lowering peak water levels and (b) increasing the tidal prism. Secondly, tidal flats and wetlands increase frictional resistance due to their shallow depth and high roughness, slowing the landward propagation of the tidal wave and reducing its height and energy (Smolders et al., 2015; Stark et al., 2016). Tidal channels without tidal flats are therefore hydraulically smoother than broad channel-shoal systems with extensive tidal flats allowing faster up-estuary propagation and lower frictional losses.

Both storage and frictional losses over tidal flats influence tidal asymmetry. A tidal wave deforms as it travels through an estuary. To a first approximation, characteristics of a shallow-water wave propagate at a celerity $c = \sqrt{gh}$, with g and h denoting gravity and depth (respectively), meaning that the wave crest travels faster than the trough. This results in a shorter flood period and stronger flood currents compared to ebb currents. The shallower the estuary, the greater the difference between high and low water, enhancing deformation. The primary

10.1029/2024RG000860

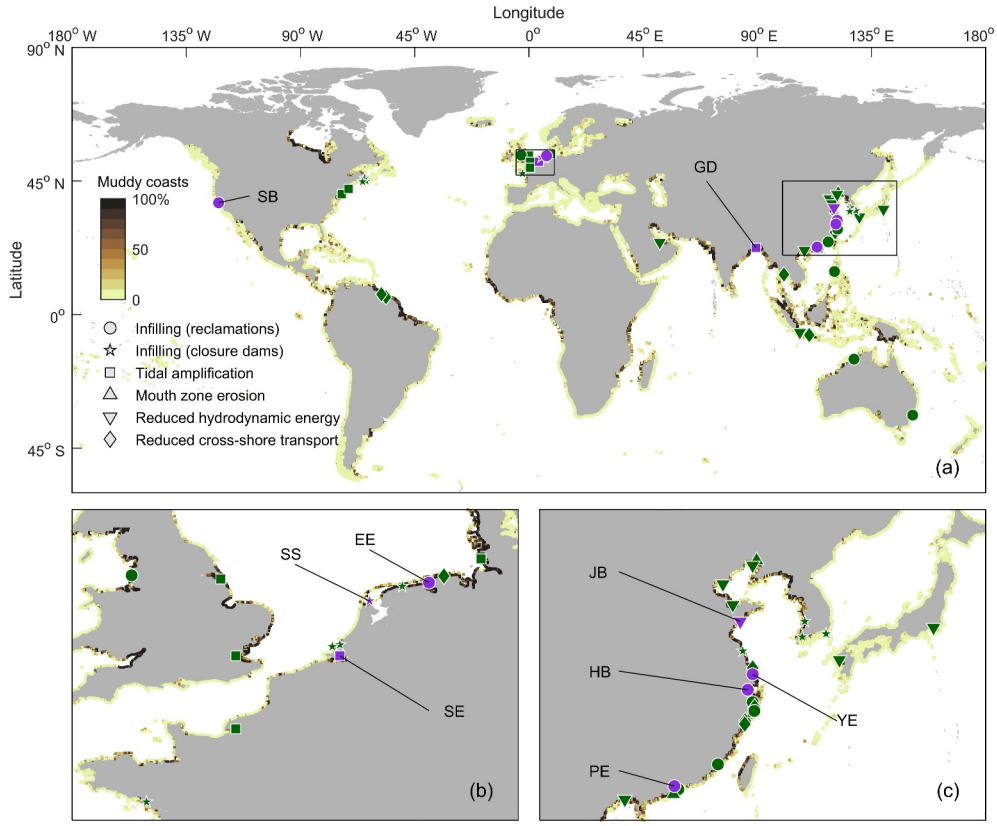

Figure 2. Overview of the 54 land reclamation sites which are part of this review–see Table 1 for more details. Purple markers are key areas (see Section 5 for abbreviations and details), green markers are areas for which less data is available. The hydromorphological response to land reclamation (as discussed in Section 4) is indicated with marker type. The coastline color provides the mud content (Hulskamp et al., 2023), with a pure mud coast in dark brown.

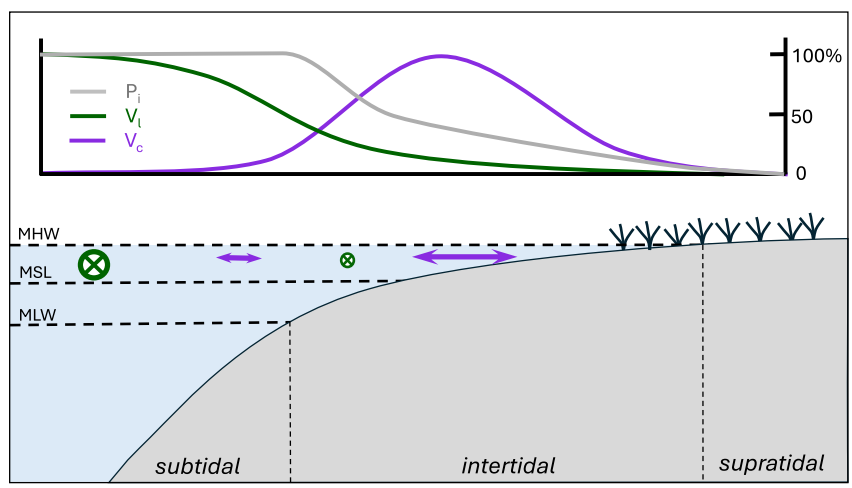

Figure 3. Sketch of typical flow velocity amplitude V and relative inundation period P_i (both ranging from 0 to 100%) over a convex-upward cross-sectional profile of a tidal flat with salt marsh. The alongshore velocity amplitude V_l (green) is highest in deep water, the cross-shore flow velocity amplitude V_c (purple) is highest over the intertidal area. The relative importance of V_l and V_c strongly site-specific, depending on the local geometry and hydrodynamic forcing. MLW is Mean Low Water, MSL is Mean Sea Level, and MHW is Mean High Water.

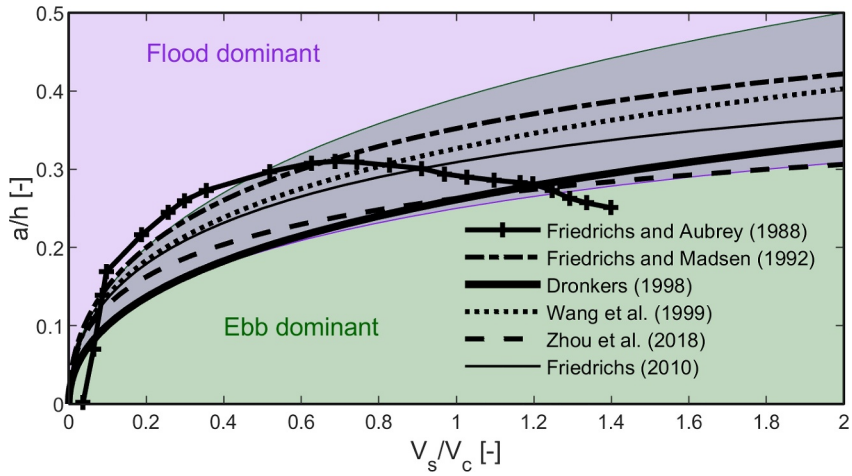

Figure 4. Dependence of flood or ebb dominance on the ratio of storage volume (V_s) to channel volume (V_c), and of tidal amplitude (a) to depth (h) according to Friedrichs and Aubrey (1988), Friedrichs and Madsen (1992), Dronkers and Scheffers (1998), Z. B. Wang et al. (1999), Friedrichs (2010), and Zhou et al. (2018). Using a database of 25 tide-dominated systems, Dronkers (2016) derived analytical expressions separating flood-dominant (purple) and ebb-dominant (green) estuaries including their overlap (deep purple) largely corresponding to the transitions defined earlier by Friedrichs, Dronkers, Wang, and Zhou.

factor counteracting this deformation is the inundation of tidal areas. When the crest of the tidal wave floods the intertidal zones, it slows the propagation of the crest more than the trough. As a result, estuaries with extensive tidal flats tend to be much less flood-dominant, or even ebb-dominant, compared to those without tidal flats (see Friedrichs & Aubrey, 1988 and Speer & Aubrey, 1985).

Since the pioneering work of Friedrichs and Aubrey (1988), a number of studies have shown flood and ebb dominance to be a function of the tidal storage volume (V_s) to channel volume (V_c) ratio, and of the tidal amplitude (a) to depth (h) ratio (Figure 4). These later studies are extended in the range of V_s/V_c but most importantly suggest a continuous increase in ebb dominance with higher V_s/V_c introducing an uncertainty which is summarized by the overlap in the expressions provided by Dronkers (2016). Figure 4 shows that deep estuaries with few tidal flats are flood-dominant (generally associated with infilling) while shallow systems with extensive tidal flats are ebb-dominant, with a tendency to export sediment. In this classification scheme flood dominance is defined as a conditions in which the tidal rise is shorter than ebb and resulting flood currents are faster than the ebb currents (here referred to as peak flow asymmetry). However, more types of tidal asymmetry exist. Flood and ebb dominance can be related to the duration of the slack tide period (slack tide duration asymmetry), but also to spatial asymmetries such as a landward decrease in velocity amplitude, giving rise to settling and scour lags. For a broad overview of tidal asymmetry, we refer to Friedrichs (2011), Dronkers (2016), and Gatto et al. (2017).

Winterwerp and Wang (2021) derived convenient analytical expressions relating tidal amplification and asymmetry to the relative size of the intertidal area F_i and to channel depth h. Their model advances on stability diagrams such as Figure 4 by computing along-estuary tidal amplification rather than using the tidal range at the mouth as a static boundary condition. The relative contribution of F_i and h are explored for a typical funnel-shaped estuary in which tides responded first to land reclamation (van der Spek, 1997) and later to deepening (van Maren, Alonso, et al., 2023)–see Section 5 for more details. In this simplified Scheldt estuary tidal amplification (Figure 5a) appears to be more sensitive to variations in water depth (x-axis) than to changes in the relative width of the intertidal area (y-axis). In contrast, the intertidal area has a stronger influence on tidal asymmetry (Figure 5b), with ebb-dominance occurring when more than 15%–20% of the cross-section consists of intertidal area (and flood-dominance when the intertidal area covers less than 15%–20%). But although the impact of intertidal area on amplification is relatively small, it does have an effect: the tides amplify at lower water depth for an estuary without intertidal area than for an estuary with extensive intertidal area (h increasing from 12 to 14 m for F_i increasing from 0 to 0.8 in Figure 5a). But, as will be elaborated in greater detail in later sections, the degree to which intertidal land is reclaimed typically varies substantially varies along the length of

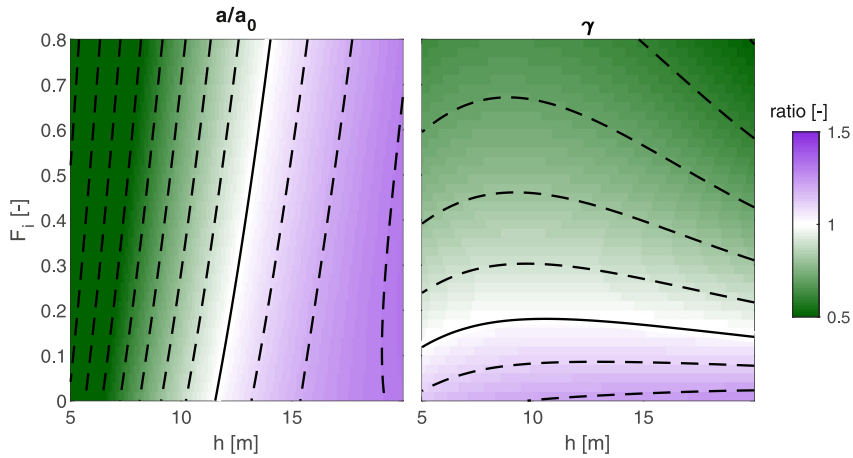

Figure 5. Increase in tidal amplification a/a_0 and tidal asymmetry γ as a function of channel depth h and intertidal area F_i for a funnel-shaped estuary, computed using the analytical model of Winterwerp and Wang (2021). Herein a/a_0 is the along-estuary tidal amplitude a relative to the amplitude at the estuary mouth a_0; $\gamma = c_{HW}/c_{LW}$ with c_{HW} the celerity of the High Water wave and c_{LW} the celerity of the Low Water wave (with a value larger than unity being flood-dominant transport). Estuarine dimensions are based on the Scheldt Estuary (see Figure 10), being 160 km long, 4 km wide at the mouth, and with an estuarine convergence length L_b of 45 km (Dronkers, 2016). The relative width of the intertidal area F_i is constant over the length of the estuary. The model is run with a large set of geometric conditions with F_i varying between 0 (i.e., no intertidal area) to 0.8 (80% intertidal area) and the channel depth h varying from 5 to 20 m. Model output is evaluated at the approximate location of Antwerp (80 km from the mouth).

an estuary. Especially in heavily engineered estuaries, F_i is therefore not constant, and an up-estuary increase in F_i will lead to tidal damping and a decrease in F_i to tidal amplification.

2.3. Residual Sediment Transport

Tidal asymmetry is a key component that controls residual sediment transport in estuaries. In general, flood-dominant estuaries tend to fill in with sediment, while ebb-dominant estuaries are likely to have a negative sediment balance. But as highlighted in the previous section multiple sources of tidal asymmetry exist. Peak flow asymmetry is generally associated with residual sand transport while slack tide duration asymmetry with the residual transport of mud (Dronkers, 1986); and settling/scour lags drive the residual transport of mud to supra and intertidal zone (cf. Postma, 1961). Therefore, deep, sandy tidal channels may export sand, while their muddy intertidal areas are filling in with sediments.

Superimposed on tide-induced barotropic transport is residual sediment transport by density-driven (baroclinic) currents. Salinity-driven circulations give rise to a landward-directed current close to the bed and since more sediment is transported close to the bed than higher up in the water column, these salinity-driven circulations lead to landward sediment transport (Burchard et al., 2018). Salinity-driven flows increase non-linearly with water depth (e.g., Geyer & MacCready, 2014) and are additionally influenced by lateral mixing between the main channel and intertidal areas (e.g., MacCready & Geyer, 2010), introducing further interactions between channel depth, intertidal area, and sediment import.

Over longer timescales, estuaries converge to near-equilibrium conditions of the bed morphology (Dronkers, 2016; Zhou et al., 2017), in which mechanisms leading to accretion or erosion roughly balance out. A change in tidal dynamics by a change in intertidal area or channel deepening disturbs this balance, and will lead to morphological adaptation toward a new equilibrium. This morphological adaptation introduces morphodynamic feedback mechanisms and long timescales, which will be discussed in greater detail in the following section.

3. Morphodynamic Feedback Mechanisms and Adaptation Timescales

3.1. Morphodynamic Feedback Loops Resulting From Land Reclamation

Key to understanding the response of tidal systems to an anthropogenic disturbance such as land reclamation is that the response may be controlled by feedback mechanisms. Such feedback loops may be negative (dampening

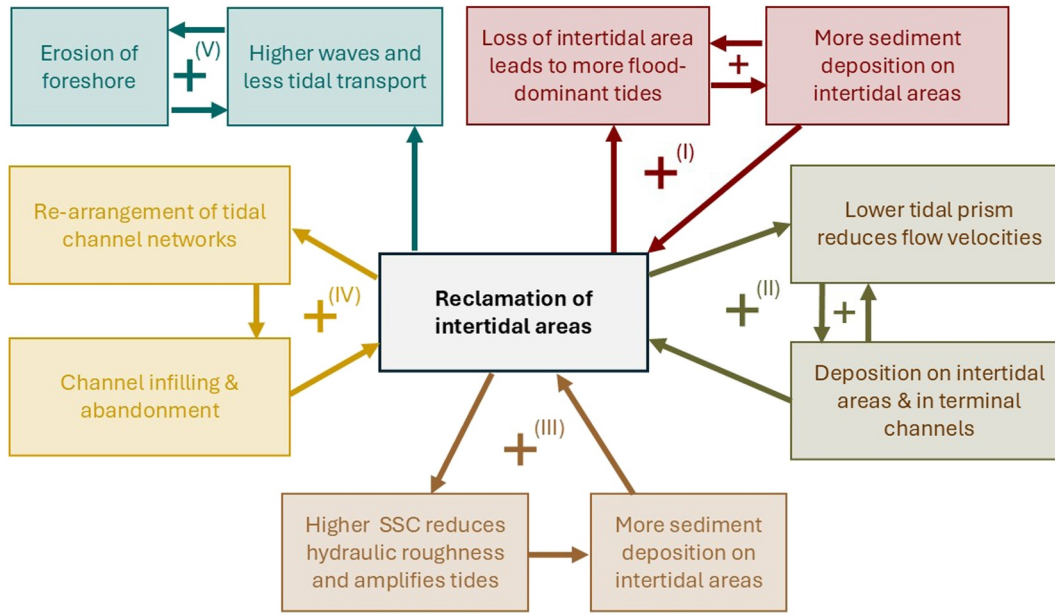

Figure 6. Positive feedback loops strengthening the initial hydromorphological response of a land reclamation in tide-dominated environments. The Roman numbers correspond to feedback loop description in the main text.

the original perturbation) or positive (amplifying the effect of a disturbance). We identified five positive feedback loops (Figure 6) that strengthen the impact of land reclamation on its environment. Positive feedback mechanisms especially influence the initial response to a land reclamation. In time, negative feedbacks emerge, stabilizing the coastal system into a new equilibrium, a state with zero residual transport when time-averaged. Note that this definition actually presents a static equilibrium, whereas the equilibrium may also be dynamic with residual transport constant or changing in time as long as sources and sinks are in equilibrium (Zhou et al., 2017). Morphodynamic equilibrium is more common in sand-dominated systems than in fine-grained environments, because muddy systems are usually governed by non-equilibrium transport (Dronkers, 2016). Most land reclamation sites occur along muddy coasts, however, because here the coastal plain is typically wide and fertile (Figure 2).

I. Increasing flood dominance
   Tides in funnel-shaped estuaries amplify with increasing width convergence (Jay, 1991), depth convergence (Leuven et al., 2023) and reduction of the intertidal area (Friedrichs & Aubrey, 1988), by which the tidal energy flux is compressed to a smaller cross-sectional area. Tides also become more flood dominant in response to loss of intertidal areas (Dronkers, 2016; Friedrichs & Aubrey, 1988; Winterwerp & Wang, 2021), as the intertidal area reduces the flood propagation celerity, whereas the ebb propagation remains little affected. Therefore, land reclamation along funnel-shaped estuaries typically leads to larger tides, because of stronger funneling and more flood-dominant tides due to loss of intertidal areas. Amplified, more flood-dominant tides strengthen up-estuary sediment transport. More sediment import, in turn, promotes sediment deposition on the intertidal areas flanking the estuary, such as demonstrated by Morris and Mitchell (2013) for the Humber, van Maren, Beemster, et al. (2023) for the Passur-Sibsa, and Z. Dai et al. (2016), Guo et al. (2022), and R. Zhang et al. (2023) for the Yangtze Estuary. This further strengthens sediment import (secondary feedback cycle in feedback loop I), but is more pronounced when the accreting intertidal flats become sufficiently high to be reclaimed (as exemplified by the Humber, Passur-Sibsa and Yangtze estuaries–see references above). The Passur-Sibsa Estuary provides an extreme example in which the tides continue to amplify to the present day, even though reclamation works were largely finished in the early 1970s (Figure 7) as a result of feedback loops I, II, and IV (see van Maren, Beemster, et al. (2023) for details).
II. Reduction in tidal prism
   Land reclamation reduces the total volume of water imported and exported at a certain cross-section over a tidal cycle, referred to as the tidal prism. Land reclamation therefore leads to a lower tidal discharge and flow

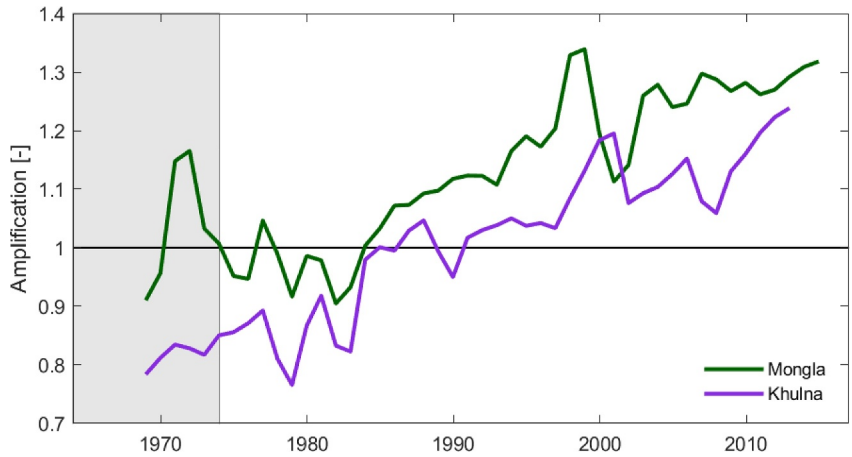

Figure 7. Amplification of the tidal range at two stations along the Passur River (Mongla and Khulna), 83 and 123 km (resp.) upstream of the estuary mouth. Amplification is defined as the annually averaged tidal range divided by the annually averaged tidal range at the mouth (Hiron Point). The gray shaded zone represents the period with most active land reclamation works (creation of polder system). The tides amplify significantly for a long period of time without any additional substantial human intervention as a result of feedback loops I, II, and IV. Water level data is from van Maren, Beemster, et al. (2023).

velocity amplitude. This flow reduction may result from gradual reclamations such as in Hangzhou Bay (Xie et al., 2017), the Ems Estuary (Schrijvershof et al., 2024) and the Passur-Sibsa Estuary (van Maren, Beemster, et al., 2023), but also along open coasts (Zhong & Hu, 2021), and especially as a result of estuarine closures (Figueroa & Son, 2024). The reduction in tidal discharge leads to sediment deposition, especially close to reclamation areas where the reduction of flow velocity is largest (Morris & Mitchell, 2013). When sediment deposits on the intertidal areas, the tidal prism is further reduced, further promoting sediment deposition. Similar to feedback loop II, this mechanism is strengthened when these intertidal areas are reclaimed, further reducing the tidal flow velocity and strengthening sediment deposition (Guo et al., 2022). The overall response of the estuary as a result of this positive feedback loop is a gradual infilling of its landward section, leading to tidal deformation and more upstream transport. The result is similar to feedback loop I and this may often occur simultaneously, but underlying transport mechanisms of feedback loop I and II are different (being controlled by tidal asymmetry and tidal prism, respectively).

III. Reduced Hydraulic Roughness

Land reclamation leads to an increase in the Suspended Sediment Concentration (SSC) through the loss of sediment sinks or stronger up-estuary transport (Dronkers, 2016; Morris & Mitchell, 2013; van Maren et al., 2016; Van Proosdij et al., 2009), especially in turbid environments. Enhanced up-estuary transport may result from stronger tidal asymmetry (as in loop I) and/or reduced tidal prism (as in loop II). Concentrations of already several 10s of mg/l may already influence the apparent hydraulic roughness of the bed through buoyancy effects, turbulence damping by fluid mud formation, smoothing of bed forms, and thickening of the viscous sublayer (Wang, 2002; Winterwerp, 2001; Winterwerp et al., 2009). Deepening of the tidal channels has been demonstrated to initiate a positive feedback mechanism in which (a) the original deepening strengthens tide-induced sediment import, (b) leading to higher sediment concentrations and therefore to lower hydraulic drag, which in turn (3) leads to more tide-induced sediment import (Dijkstra et al., 2019; van Maren, Winterwerp, & Vroom, 2015; Winterwerp & Wang, 2013), although sediment-induced reduction in vertical mixing may also reduce horizontal transport, as suggested by Wang (2002).

The increase in suspended sediment concentrations resulting from land reclamation is very likely to initiate enhanced up-estuary tidal transport similar to the effect of channel deepening, although not explicitly documented in literature. Tidal amplification is Hangzhou Bay is partly resulting from a reduction in hydraulic roughness (see Section 5 for details). Infilling of the Petitcodiac Estuary in Canada is influenced by the positive feedback related to reduced roughness after its intertidal areas had filled in with sediment in response to the construction of a causeway, partly explaining why a low-turbid but otherwise very similar tidal system nearby the Petitcodiac (the Avon Estuary) did not fill up with sediments (Van Proosdij et al., 2009). Dronkers (2016) mentions this sediment-induced feedback as a reason for tidal amplification in

the Loire, although under the influence of the combined effect of land reclamation and channel deepening. Both human interventions frequently lead to very extreme Estuarine Turbidity Maximums (ETMs) in which vertical concentration gradients dampen turbulence, thereby increasing both the propagation speed of the tidal wave and the tidal flow velocities.

IV. Re-arrangement of tidal networks
Pristine complex tidal networks are in relatively stable morphodynamic equilibrium (Hoitink et al., 2017; Iwantoro et al., 2020), but a perturbation may lead to large-scale network reorganization (Fagherazzi, 2008). In the Passur-Sibsa Estuary, land reclamation promoted tidal flow through one channel at the expense of a degenerating other channel (Bain et al., 2019). Tides amplified in one of a series of parallel estuarine channels, penetrating a neighboring parallel main channel through small connecting channels that eroded severely (van Maren, Beemster, et al., 2023). The degenerating channel filled up with sediment by loss of tidal prism whereas up-estuary transport in the other is strengthened by tidal asymmetry (van Maren, Beemster, et al., 2023). Land reclamation in the North Branch of the Yangtze Delta reduced the river flow capacity which was subsequently diverted to other distributaries; the resulting relative increase in tide-induced landward transport led to basin infilling, progressively more flood-tidal dominance (Guo et al., 2022) and redistribution of the tide-averaged flow (W. Zhang et al., 2019; Yu et al., 2020). As illustrated by these examples, the ability of tides to redistribute over different branches makes complex tidal channel networks are more sensitive to land reclamation compared to single-channel systems.

V. Erosion of muddy coasts
Many muddy coasts suffer from structural coastal erosion (Hulskamp et al., 2023). The erosion of muddy coasts in the tropics is often related to the conversion of mangroves to agriculture or aquaculture, and once erosion starts it is very persistent (Anthony & Gratiot, 2012; Besset et al., 2019; Winterwerp, Erftemeijer, et al., 2013). A mechanism likely regulating this structural erosion following conversion of mangroves forest to aqua- or agriculture was brought forward by Winterwerp, Erftemeijer, et al. (2013) and Winterwerp et al. (2020). Crucial herein is that the cross-shore profile is an equilibrium by tides bringing sediment shoreward and waves eroding the shoreline. The construction of a dike (or similar hard construction) in a muddy coastal system dominated by cross-shore tidal currents reduces the tidal prism and therefore tide-induced sediment supply. This reduction in sediment supply already leads to net erosion when wave conditions remain unchanged. However, reflection of short waves against the dike amplify the amplitude of the wind waves, further strengthening erosion of the foreshore. This deepening further reduces frictional wave dissipation, resulting in progressively more wave-driven coastal erosion until the dike collapses.

3.2. Adaptation Timescales to Land Reclamation

Morphological changes in tidal systems will asymptotically develop to a new dynamic equilibrium. This development can be described with exponential decay functions (Tonis et al., 2002; van Maren, Alonso, et al., 2023). A change in tidal range which is driven by morphological changes will experience a similar exponential decay (van Maren, Alonso, et al., 2023). The tidal range observed in the Passur-Sibsa Estuary increases linearly in time, not yet showing a reduction of the increase (Figure 7). In time, the tidal range may asymptotically develop toward a new equilibrium, as in exponential decay functions. But assuming the adaptation can be described as an exponential decay function, the associated timescales will be long (much longer than the 50 years of observations, as the system is already adapting to the land reclamation works in the 1960s).

Directly relating morphodynamic response times to land reclamation or closures through observational data is often complicated by the absence of long time series with a sufficiently high observation frequency. The various closures executed in the Netherlands provide examples where detailed and regular monitoring of bed levels started prior to interventions (in the 1920s). The closure of the Haringvliet Estuary resulted in infilling of the now low-energy environment seaward of the closure. Tonis et al. (2002) showed that the morphological decay can be described by an exponential decay function:

$$X_{(t)} = X_e + (X_0 - X_e)\, e^{-t/\tau} \tag{1}$$

in which $X_{(t)}$ is the parameter X varying over time t (such as the tidal range or deposited volume), X_e is the equilibrium value of that parameter, and τ is an adaptation timescale of parameter X. Herein τ is the e-folding

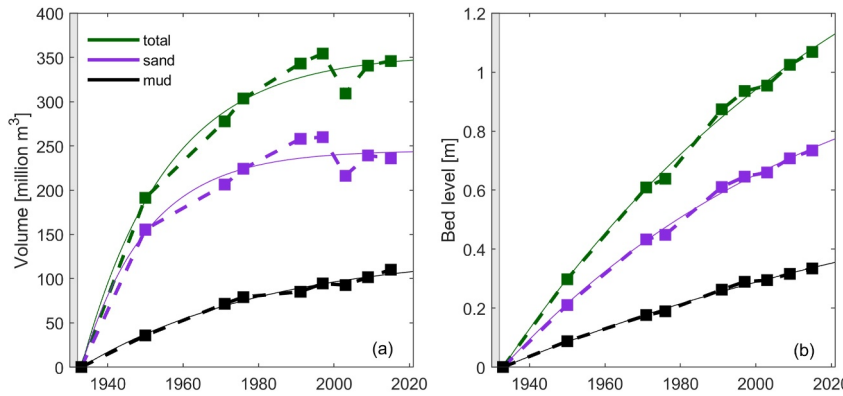

Figure 8. Example of a morphologic response to inlet closure and the associated timescales (Western Dutch Wadden Sea). Panel (a) provides the volumetric change of three combined tidal basins, panel (b) the bed level change of the intertidal flats (24% of the total area). The thick dashed lines are observations from Colina Alonso et al. (2021), the thin lines are exponential decay functions from van Maren, Alonso, et al. (2023). The gray shaded zone is the period the closure dam was constructed. The adaption time (defined as 94% of total change) is approximately 60 years for the tidal basins and 300 years for the tidal flats.

timescale, or the time over which the parameter X increases a factor e. This adaptation timescale may be alternatively defined as $T_a = 4\ln(2)\tau$, providing the time period over which 94% of X has adapted to its equilibrium value (van Maren, Alonso, et al., 2023). In the Haringvliet Estuary $\tau = 11$ years (Tonis et al., 2002) implying that 94% of the equilibrium infill is reached after 30 years. Adaptation timescales are much larger in response to closure of the South Sea (part of the Dutch Wadden Sea–see also Section 5). With 3,600 km^2, it constitutes the largest single land reclamation or inlet closure in the world. Initially, a large amount of sediment was imported from the adjacent coastal sea ("total" in Figure 8a). The adaptation timescale of T_a of all sediment combined is approximately 60 years (van Maren, Alonso, et al., 2023). However, evaluating T_a per sediment fraction (Colina Alonso et al., 2021) reveals that the import of sand reached equilibrium 50 years after closure, while the import of mud is predicted to reach equilibrium after 141 years (van Maren, Alonso, et al., 2023). This import of mud is primarily the result of the mudflats which will continue to accrete for centuries in response to closure (van Maren, Alonso, et al., 2023). This example therefore illustrates that adaptation timescales may be very long, that is, several centuries, but also that the adaptation timescales depend on the evaluated spatial scale.

4. Generalized Impact of Land Reclamation

In this section we describe the impacts of land reclamation in terms of (a) tidal response and (b) sedimentary response (infilling/erosion). The latter response is controlled by the type of coastal system (enclosed systems or open coasts), sediment availability, and the location of the reclamation within the system (especially within estuaries, displaying the greatest variety in responses). For each type of response the typical coastal environment, location of reclamation, as well as the main tidal and sedimentary changes are summarized in Table 2.

4.1. Enclosed Muddy Coasts: Estuaries, Embayments and Lagoons

Estuaries and tidal embayments or lagoons are often muddy, receiving sediments from their landward or seaward side. Several systems discussed hereafter are topographically known as bays but are in reality estuaries (receiving freshwater from one or more river systems) and may be funnel shaped similar to many estuaries. This is especially common in China–many of the Chinese bays discussed hereafter are actually estuaries. A natural, non-engineered estuary is typically funnel-shaped with a multi-channel outer estuary that transitions into a narrow tidal river, flanked by extensive intertidal flats and salt marshes or mangrove forests (depending on the climatic conditions)–see Figure 9. The incoming tidal wave amplifies because of width convergence (Jay, 1991) and tidal resonance (Talke & Jay, 2020); the tidal wave dampens due to friction and storage of water within the intertidal zone (Friedrichs & Aubrey, 1994). Therefore, shallow estuaries with extensive tidal flats tend to be dissipative, that is, the tidal wave amplitude decreases in the landward direction. With a typically mildly sloped bed, the tidal flow velocity then initially increases, followed by a decrease, resulting in a velocity maximum halfway the estuary (Dalrymple & Choi, 2007).

Table 2
Impacts of Land Reclamation in Various Settings in Terms of Main Tidal Response and Main Sedimentary Response, for Each Response Type in Section 4

Land reclamation location	Response description	Main tidal response	Main sedimentary response
Landward side of estuaries, lagoons or bays	Estuarine infilling by land reclamation-induced decreased tidal prism (type 1a, Section 4.1.1)	Decreasing tidal prism	Sedimentation
Landward side of estuaries, lagoons or bays	Estuarine infilling by closure dam-induced decreased tidal prism (type 1b, Section 4.1.2)	Decreasing tidal prism	Sedimentation
Continuous along an estuary	Tidal amplification by reduced hydraulic roughness and funelling (type 2, Section 4.1.3)	Tidal amplification	Erosion or sedimentation
Seaward side of estuaries, lagoons or bays	Mouth zone channel erosion (type 3, Section 4.1.4)	Increasing flow velocity	Erosion
Tidal flats along open muddy coasts	Reduced cross-shore transport (type 4, Section 4.2)	Decreasing tidal prism	Erosion or sedimentation
Tidal flats in sediment-poor bays	Reduced hydrodynamic energy (type 5, Section 4.3)	Decreasing flow velocity	No response

Many site-specific studies exist documenting how a land reclamation in a particular system influences the tidal range, velocities, and/or bed levels (see Table 1). Through comparison of this wide range of cases, especially the key study sites described in more detail in Section 5, we identified three response types of estuaries graphically presented in Figure 9. Land reclamation or closure (through a tidal weir the landward limit of an estuary or a closure dams in tidal basins) leads to estuarine infilling, reclamation along the estuarine length to tidal amplification, and reclamation at the mouth of the estuary to locally increasing flow velocities and bed erosion. In order to facilitate the discussion of these response types, we also refer to types 1, 2 and 3 for infilling, amplification, and channel erosion, respectively. Type 1 is subdivided into gradual land reclamations (type 1a) and inlet closures (type 1b). In the following sections, these response types will be explained in greater detail.

4.1.1. Estuarine Infilling by Land Reclamation-Induced Decrease in Tidal Prism (Type 1a)

Land reclamation typically leads to a loss of tidal prism. The resulting reduction in flow velocity will lead to infilling unless (a) the tides amplify, as for type 2 discussed hereafter, or (b) when sediment availability is low, as for sediment-poor systems. Estuarine infilling is typical for estuaries that are predominantly reclaimed at their landward reach, but may also occur for estuaries that are reclaimed along their entire length. Clear examples include Hangzhou Bay (Xie et al., 2017), the Ems Estuary (Pierik, 2021; van Maren et al., 2016), and Puba Bay (Y. Liu et al., 2024), which all fill rapidly due to the combination of reduced flow velocities and abundant sediment supply. In many other estuaries, the response may be obscured by concurrent human interventions. Sediments deposit in Lingding Bay and Deep Bay in the Pearl River Estuary in response to land reclamation, but in Lingding Bay this infilling was overcompensated by sand mining activities (Han et al., 2023). Intensive reclamation in Xiamen Bay (China) since 1955 reduced the tidal prism and flow velocities by about 40% (J. Wang et al., 2013) which led to infilling of the navigation channels (Y. Chen et al., 2019). Other examples of estuaries filling in with sediments because of up-estuary reclamation are the Ribble Estuary in the United Kingdom (Van Der Wal et al., 2002) and the Sydney Estuary in Australia (Birch et al., 2009; McLoughlin, 2000). Reclamation of 540 km^2 of mangrove area in Manilla Bay (with only 6.8 km^2 remaining; MBSDMP (2020)) is a likely driver of the rapid sedimentation rates in the bay observed in the past century (Siringan & Ringor, 1998).

Estuarine infilling may not only result from reduced flushing but also by tidal deformation. As the systems fill up with sediments, tides may become very flood dominant, strengthening up-estuary transport. Extreme examples include the Qiantang Estuary–Hangzhou Bay (Xie et al., 2017) and the Ord River (Wolanski et al., 2001), both characterized by a tidal bore. The Ord River Estuary (Wolanski et al., 2001) is rapidly silting up through tidal pumping in response to up-estuary land reclamation which intensified after the construction of upstream river dams because the buffering of river floods in the reservoir prevent regular river bed scouring. Shoaling has progressed to the point that the flood-dominant tides developed into a tidal bore (Wolanski et al., 2001). Adjacent to the Ord River is the Durack River, which has similar dimensions and flows into the same receiving basin: the macrotidal Cambridge Gulf. The Durack River Estuary is largely untouched by

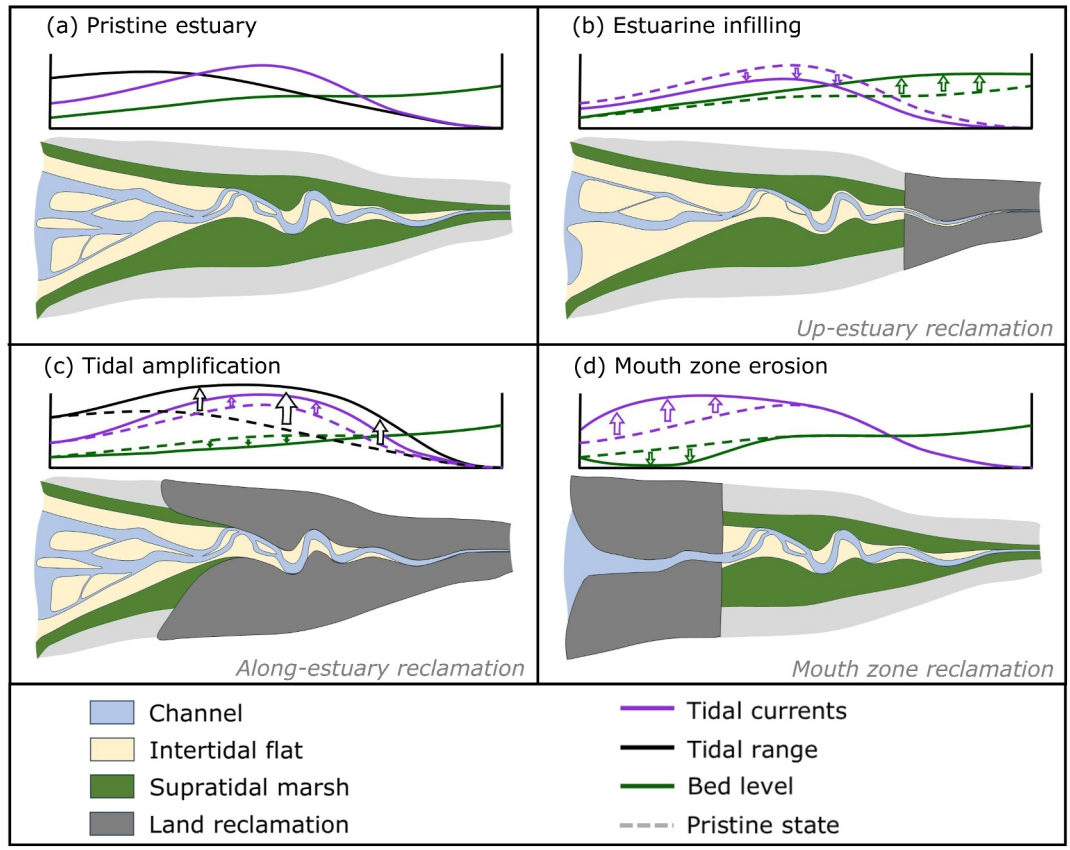

Figure 9. Conceptual response to land reclamation in an estuary, showing a schematic map and the longitudinal variation of the intensity of the three main physical parameters discussed (tidal currents, tidal range, and bed level of the tidal channel). Panel (a) sketches a typical pristine estuary with a tidal river transitioning into a multi-channel outer estuary flanked with extensive intertidal flats and supratidal marshes. The bed level (green line) gradually decreases land-inward, the tidal range (black line) initially slightly amplifies but thereafter dissipates, and the tidal current velocity (purple line) is maximal halfway the estuary. Other panels: change in planform morphology and changes in longitudinal variation of tidal currents, tidal range, and bed level as a result of up-estuary (b), along-estuary (c) and down-estuary (d) reclamation. See text for a detailed description. The dashed longitudinal distributions in panels (b–d) refer to the water level, tidal currents or bed level (depending on the color) in its pristine state (as in panel a). Only relevant longitudinal changes are visualized, therefore no tidal range changes in panels (b, d).

human interventions and is strongly ebb-asymmetric, whereas the reclaimed Ord River Estuary is very flood-dominant. The Ord River Estuary therefore clearly illustrates how land reclamation leads to infilling but also to tidal deformation.

4.1.2. Estuarine Infilling by Closure Dam-Induced Decrease in Tidal Prism (Type 1b)

An extreme example of land reclamation is the full or partial closure of a tidal inlet or estuary. Seaward of the dam, such a closure leads to a reduction in flow velocity, large infilling rates, a seaward shift of the ETM and a reduction in SSC (see the recent review by Figueroa and Son (2024)). Such closures bear resemblance to the up-estuary land reclamations discussed above, but are also profoundly different, often leading to a much stronger and sudden system change. The largest closure is that of the South Sea (van Maren, Alonso, et al., 2023), but more modest examples include the closures of the Dutch Lauwers Sea (A. P. Oost, 1995) and Grevelingen and Haringvliet estuaries (Elias et al., 2017; Tonis et al., 2002; Van Der Spek & Elias, 2021), the Vilaine Estuary in France (Traini et al., 2015) the Canadian Avon and Petitcodiac estuaries (Van Proosdij et al., 2009), the South-Korean Nakdong Estuary (Chang et al., 2023; Williams et al., 2013), the Keum River Estuary (Figueroa et al., 2020; Kim et al., 2006), and Yeongsan Estuary (Williams et al., 2014) and lastly the Xinyanggang Estuary in China (Q. Zhu et al., 2017). However, around 300 tidal sluice gates regulate the flow of larger and smaller rivers

feeding the Chinese coastline, providing a large amount of poorly documented cases, of which most are prone to mild or severe sedimentation downstream of the gate (Q. Zhu et al., 2017).

The infilling rates associated with closures are much higher than those with gradual reclamation of supratidal or intertidal areas because the low flow velocity and deep water conditions close to the dam result in a low transport capacity and therefore in large sedimentation rates. Figueroa and Son (2024) identified two types of deposits in front of an estuarine dam: closures in tide-dominated, fine-grained systems lead to the development of extensive intertidal flats attached to the shorelines, whereas middle mouth bars/barriers develop in sandy, more wave-influenced environments. An exception appears to be the Annapolis Estuary (Canada) displaying erosion downstream of a tidal barrage, probably resulting from the depletion of sediment previously provided by the upstream river (Morris, 2013).

Closures of tidal inlets, estuaries, or basins may influence the tidal range through resonance (Dykstra et al., 2024; Figueroa & Son, 2024; Talke & Jay, 2020). A tidal basin or estuary may show resonant behavior to a tidal wave with a period T when its effective length L is close to a resonance length L_r defined as (Talke & Jay, 2020)

$$L_r = \frac{(2n-1)T\sqrt{gh}}{4} \tag{2}$$

where g is the gravitational acceleration, h is the water depth, and n is 1,2,3,…The first mode ($n = 1$), known as quarter-wave resonance, is the most common form of resonance with typical values of L_r between 100 and 200 km (depending on the water depth). Examples of estuaries in which tides are probably amplifying as a result of the construction of an upstream weir include the Ems Estuary (Schuttelaars et al., 2013), the Thames Estuary (Talke & Jay, 2020), and the Vilaine Estuary (Traini et al., 2015). But also the tides in a tidal basin of the Wadden Sea in response to basin closure–see Elias et al. (2003) and Section 5.

4.1.3. Tidal Amplification by Reduced Hydraulic Roughness and Funelling (Type 2)

Many estuaries and tidal rivers experience a change (mostly an increase) in their tidal range by channel deepening (Talke & Jay, 2020; Winterwerp & Wang, 2013). Such causal relationships have only limitedly been established for land reclamations. As will be elaborated in greater detail below, land reclamation may amplify tides through loss of a reduction in hydraulic roughness and by increased funneling. The reduction in hydraulic roughness is usually attributed to a loss of intertidal storage (resulting in a cross-sectionally averaged increase in water depth), but also due to a decrease in apparent hydraulic roughness resulting from higher suspended sediment concentrations.

The loss of intertidal storage was assumed to be responsible for the amplification of the tides in the Scheldt Estuary (van der Spek, 1997) and the Passur-Sibsa Estuary (van Maren, Beemster, et al., 2023). The tides in the upper Seine Estuary amplified several meters in the past two centuries, partly because of deepening and straightening, but also because of land reclamation (Dronkers, 2016). Tides in the Eider Estuary were amplifying for a long period of time as a result of dike construction until a tidal barrage was constructed (Bednarczyk et al., 2008). Other systems in which the tidal range increased as a response to land reclamation are the Thames Estuary in the United Kingdom and Jamaica Bay in the United States. The spring tidal range in the Thames Estuary has increased 1.1 m (equivalent to 25%) in the past 100 years through a combination of deepening and land reclamations (Siggers et al., 2006). Jamaica Bay witnessed a reduction of the marsh area of 76% and the intertidal area of 73% between 1870 and 2020 relatively evenly reclaimed along its length (Orton et al., 2020). The tidal range increased from 1.16 m in 1899 to 1.64 m in 2007 (Swanson & Wilson, 2008) as a result of reduced tidal damping at the inlet and increased tidal reflection deeper into the bay (Parejaroman et al., 2023). In contrast, the tides in the strongly urbanized Boston Harbor decreased in response to land reclamation (Talke et al., 2018a), possibly related to the much smaller size of this estuary compared to other examples.

The hydrodynamic response to changes in intertidal storage depends, among others, on the location of that intertidal area. Several numerical model experiments have been performed that address the impact of the location of intertidal areas along the estuary (C. Li et al., 2016; Siemes et al., 2023; Stark et al., 2017; Weisscher et al., 2022). Although most of these studies have computed the effect of adding intertidal area, we interpret their findings in the opposite way (removing intertidal areas). When the intertidal area is removed, the tidal prism downstream of that location generally decreases, while it increases upstream of that location (Stark et al., 2017).

The response of the system depends on the exact location along the estuary of the intertidal area (Stark et al., 2017). The impact of intertidal loss on tidal dynamics appears to increase in the landward direction and especially for friction-dominated estuaries (C. Li et al., 2016), which also means that smoothing of the bed roughness (feedback III, see Figure 6) reduces the effect of intertidal storage. The effect of intertidal storage on tidal amplification is strengthened by deepening of the tidal channel in response to the increase in tidal prism (Weisscher et al., 2022).

Many estuaries in which the tidal range increases because of land reclamations fill in with sediments (such as Hangzhou Bay; Xie et al. (2017) and the Humber Estuary; Morris and Mitchell (2013)) because of a reduction in tidal flow velocity and/or increasing flood-dominant tidal currents. However, some systems experience channel erosion in combination with tidal amplification. The best-studied example of this response is the Scheldt Estuary, where Dam et al. (2022) observed pronounced sediment export, possibly resulting from weaker flood dominance (Nnafie et al., 2019). Whether reclaiming intertidal area promotes ebb or flood dominance may depend on the height of that area, with elevated areas being reclaimed promoting flood dominance and low-lying areas strengthening ebb dominance (Stark et al., 2017). Also the Sibsa Estuary was prone to erosion, probably in response to tidal amplification (van Maren, Beemster, et al., 2023). Erosion leads to channel deepening and thereby tidal amplification (see Section 2). Channel depth has a larger direct impact on tidal amplification than intertidal area (Figure 5) and therefore land reclamations may especially influence tidal amplification through channel deepening resulting from changing tidal asymmetry.

Another aspect through which along-estuary land reclamations may trigger tidal amplification is funneling. Tides amplifying in the landward direction result from width convergence (funneling) exceeding frictional losses (Jay, 1991). Along-estuary land reclamation may strengthen its landward convergence, thereby amplifying the tides. Examples of tidal amplification resulting from funneling include the Humber Estuary (Morris & Mitchell, 2013) and the Jiaojiang Estuary (Sun et al., 2017). Hangzhou Bay has experienced a slight increase in tidal range because of enhanced funneling following extensive land reclamation (Xie et al., 2017). The increase in tidal range has remained moderate because it rapidly filled up with sediments (as described in the above section). Without these rapid sedimentation rates, the tidal amplification would have been much more pronounced (L. Li et al., 2019). Also the Sibsa Estuary was more strongly funneled because only its middle to upper reaches were reclaimed while the mouth zone (the Sundarbans mangrove forest) was not, and especially the mouth zone and the middle reaches are eroding (van Maren, Beemster, et al., 2023). This has likely contributed to the dramatic increase in the tidal range in Passur-Sibsa Estuary (as shown in Figure 7).

4.1.4. Mouth Zone Channel Erosion (Type 3)

The Yalu and Modaomen estuaries (China) are both especially reclaimed along the estuary mouth, resulting in an increase in flow velocities but not in tidal amplification (Cai et al., 2012; Cheng et al., 2020; L. W. Jia et al., 2013). Both estuaries are eroding as a result of land reclamation (similar to the Scheldt Estuary). In the Yalu River Estuary (Cheng et al., 2020) the mouth zone reclamation resulted in an increase in current velocities and a decrease in flood-dominant landward transport, without amplifying tidal water levels. Further reclamation of land may transform the Yalu Estuary from a net depositional system into an erosional system (Cheng et al., 2020). The Modaomen Estuary (Pearl River Delta, China) was first extensively reclaimed (until ~1990), followed by a phase of extensive sand mining and dredging (L. W. Jia et al., 2013). The bed level started deepening autonomously around 1980, well before sand mining and other dredging activities took place. For the Modaomen, this was the result of confinement of the flow by land reclamation in the river mouth, which did not lead to tidal amplification but only to higher flow velocities.

Reducing the width of the estuary will lead to an increase in flow velocities, triggering bed scour and therefore an increase in water depth. The way an estuary (or tidal basin or bay) responds to land reclamation at its mouth can be evaluated with a choking number P (Hill, 1994; Talke & Jay, 2020):

$$P = \left(gb^2H^3T^2/C_dL\eta A^2\right)^{1/2} \tag{3}$$

where L, b, and H are the length, width, and depth of the inlet, respectively; A is the estuary surface area; T is the period of the tidal wave; C_d is a drag coefficient and η is the tidal amplitude. For small values of P the tidal wave amplitude decreases–the estuary is choked. A reduction in the width of the mouth will then lead to a reduction in

tidal prism, and therefore a decrease in tidal amplitude. Potentially, the reduction in tidal prism may lead to lower flow velocities and hence infilling and degeneration of the basin or estuary, in analogy to the stability of tidal inlets (Escoffier, 1940, 1977).

For high values ($P \gg 5$) the tidal wave amplitude and therefore tidal discharge will be limitedly influenced (no choking). For such conditions, a decreasing cross-sectional width will lead to higher flow velocities without a substantial reduction in tidal prism. The increase in water depth (because of erosion) may then lead to an increase in the tidal range. The choking number P scales with b^2/A^2, so for equal tidal characteristics and water depth, the choking number of a funnel-shaped estuary is considerably larger than that of a tidal basin. Tidal choking is therefore a much less likely process in estuaries than in tidal basins. In estuaries, bed scouring resulting from land reclamation at the mouth may then trigger tidal amplification (as in Figure 5a) and observed in the Modaomen Estuary (L. W. Jia et al., 2013)).

4.2. Reduced Cross-Shore Transport: Open Muddy Coasts (Type 4)

In many wide, gently sloping muddy environments sediment transport is primarily driven by cross-shore currents as described in Section 2 and illustrated in Figure 3. Such environments especially occur along low-energy exposed open coastlines receiving large amounts of muddy sediments (such as the Chinese coastline and the coastline downdrift of the Amazon), or lagoon systems where barriers provide shelter from waves such as the Wadden Sea. In many estuarine settings the mudflats are typically steeper and more strongly influenced by along-estuary currents. In such environments reclamation of supratidal land or parts of the intertidal area reduces cross-shore transport by reducing the tidal prism and associated flow velocity amplitudes. We identify two contrasting response types to such an interruption of cross-shore transport (both visualized in Figure 10): erosion and accretion.

The accretionary type is best generically described by Zhong and Hu (2021), see also Figures 10a and 10b. Reduction of the cross-shore flow velocity amplitude in response to reclamation leads to sedimentation (L. Chen et al., 2020; P. Chen et al., 2021; Zhong & Hu, 2021; R. Zhang et al., 2023). Such sedimentation seaward of reclamation sites is the most common response along China's coastlines, featuring extensive muddy, tide-dominated open coasts and semi-enclosed embayments. The largest stretch of muddy coast is the Jiangsu coast, but extensive mud-dominated shores are also found along the Ruian coast (P. Chen et al., 2021), and the Wenzhou coast (R. Zhang et al., 2023). Since 1984, 1.66×10^3 km^2 has been reclaimed along the muddy, tide-dominated Jiangsu coast (N. Xu, Wang, et al., 2022). Although extensive salt marshes exist in the upper intertidal and supratidal reaches, the role of vegetation is not discussed.

Land reclamation along muddy coasts may also result in erosion. Sediment transport along the 1,500 km long muddy coastline north of the Amazon is controlled by alongshore migrating mud banks which drive cyclic alterations of erosion and deposition (see (Anthony et al., 2010) for an overview). As a result, the mangrove-fringed shorelines expand during so-called "bank" phases but erode during "inter-bank" phases. The result is a dynamic coastline which is stable over longer timescales. Reclaiming land during a "bank" phase (i.e., maximal seaward extension) disrupts this long-term stability. The loss of intertidal area (through reclamation) reduces the tidal prisms, and thereby the mechanism providing sediments to the coast, explaining persistent erosion occurring along the coastlines of Guyana and Surinam (Winterwerp, Erftemeijer, et al., 2013). This cross-shore response is illustrated in Figures 10c and 10d. The long-term morphodynamic equilibrium of the intertidal zone herein depends on sediment supplied by cross-shore tidal currents flowing in and out of the supratidal zone, with waves being gradually dissipated by vegetation (Figure 10c). The full or partial reclamation of this supratidal zone weakens the landward sediment transport by cross-shore tidal currents. At the same time, reflection of wind waves against the dike leads to amplification (Klopman & Meer, 1999), strengthening wave-induced erosion of the foreshore. Both the reduction in tidally supplied sediments and the increase in wave height lead to erosion, further reducing wave energy, further promoting erosion (Figure 10d). The subsequent phase of coastal erosion necessitates strengthening dikes or seawalls in turn reflecting progressively more incoming wave energy. These self-strengthening erosion processes may lead to very persistent coastal erosion (feedback loop V in Figure 6) in relation to alongshore migrating mud banks but also in relation to conversion of mangrove forests to aquaculture ponds in the Gulf of Bangkok, Thailand and the Demak coastline in Java, Indonesia (Winterwerp, Erftemeijer, et al., 2013).

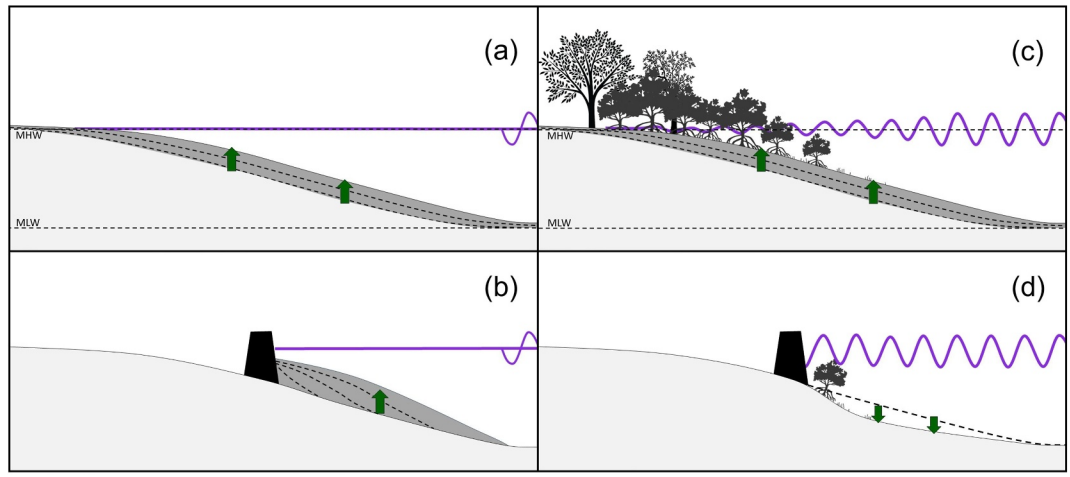

Figure 10. Schematized response of muddy open coasts (panels a, c) to land reclamation (panels b, d) based on literature describing Chinese muddy coasts (panels a, b) and the response of mangrove-mud coasts as described by Winterwerp et al. (2020) (panels c, d). The coast already expands seaward under non-reclaimed conditions along the tide-dominated Chinese coastline (a), but accretion accelerates in response to land reclamation (b, based on Zhong and Hu (2021)). In contrast, originally accreting coastlines along mangrove-mud coasts (c) have been reported to become eroding in response to coastal squeeze (d) by Winterwerp et al. (2020). Under non-reclaimed conditions wave energy is dissipated in the vegetated foreshore (c). With sufficient sediment supplied by cross-shore tidal currents sediments are deposited in the vegetated zone and the seaward tidal flats. Land reclamation (d) leads to a reduction of sediment supply by cross-shore tidal currents and an increase in wave height (a combination of less dissipation of wave energy in the vegetation foreshore and more reflection of wave energy against a sea dike). The foreshore then erodes, further reducing the width of the vegetated foreshore.

It remains unclear which conditions control reclamation along muddy open coasts to result in seaward deposition (Figures 10a and 10b) or erosion (Figures 10c and 10d). The role of waves is an explicit part of the conceptual response of Winterwerp, Erftemeijer, et al. (2013) (Figures 10c and 10d) with wave reflection strengthening erosion. Waves are also accounted for in the response described by Zhong and Hu (2021), with accretion rates decreasing with higher waves, although they do not discuss the potential effect of reflection. Both erosion and deposition seems to prevail in the Wadden Sea in response to gradual land reclamation. Along the semi-open eastern (German) Wadden Sea the reclamation of land over the past centuries has steepened the offshore profile, enhancing the hydrodynamic energy (especially resulting from waves) and therefore reducing fine sediment deposition (Flemming & Nyandwi, 1994; Mai & Bartholomä, 2000). This has resulted in erosion and coarsening of the seabed (Flemming & Nyandwi, 1994) and a relative increase in heavy metals (Dellwig et al., 2000). Therefore, the response of the eastern Wadden Sea is similar to the conceptual model in Figures 10c and 10d. In contrast, the western Wadden Sea responded to reclamation with sediment deposition, caused by both modified hydrodynamics and also the availability of sediments (Benninghoff & Winter, 2019; van Maren, Alonso, et al., 2023), more strongly resembling the conceptual model in Figures 10a and 10b. We hypothesize that a factor controlling the different response of the western and eastern Wadden Sea to land reclamation is the availability of sediments (Colina Alonso et al., 2024), with large availability (western Wadden Sea) strengthening sedimentation and smaller availability (eastern Wadden Sea) leading to erosion. But whether sediment availability is the key factor determining whether land reclamation along exposed muddy coastlines leads to erosion or to deposition requires further research.

4.3. Reduced Hydrodynamic Energy: Sediment-Poor Bays (Type 5)

We define sediment-poor here as systems in which insufficient sediment is available to morphologically adapt to changes in hydrodynamics (as for the sediment-rich examples discussed above). In sediment-rich systems, a reduction in flow velocity may, for instance, be compensated by rapid deposition, in turn leading to re-establishment of high current velocities. In sediment-poor systems, sedimentation rates are not enough to compensate for a reduction of hydrodynamic energy within timescales of centuries. Such conditions especially apply to coastal bays, where land reclamation significantly influences hydrodynamics but where sediment availability is insufficient to attain a new morphodynamic equilibrium. The sediment-poor systems discussed

below are not necessarily devoid of sediments (as exemplified by the coastal bays along China's North coast). For such cases a new equilibrium may be attained when timescales are long enough (many centuries or more).

Land reclamation in large coastal bays leads to a reduction in tidal prism and, thereby, also in flow velocities. This is evidenced by Jiaozhou Bay, Bohai Bay, Laizhou Bay, Liaodong Bay, Xiangshan Bay, Tokio Bay, and Ariaka Sea (see references in Table 1). As such, they resemble estuarine response 1a. However, a major difference is that the bed level of coastal bays is often not in equilibrium with the hydrodynamics (which alluvial estuaries typically are), but rather shaped by its geologic history. A reduction in flow velocity will therefore not lead to sedimentation rates sufficiently large to restore the original flow velocities and reach a new morphodynamic equilibrium. Land reclamation along embayments typically reduces the flow velocity, and consequently mixing rates and refresh rates. This has been documented for Bohai Bay, Laizhou Bay and Liaodong Bay by Z. Wu et al. (2023), Deep Bay (Yang & Chui, 2017), Tokio Bay (Okada et al., 2011), Arika Sea (L. W. Jia et al., 2013; Yamaguchi & Hayami, 2018), Jiaozhou Bay (J. Shi et al., 2011; C. Xu et al., 2021), Sanmen Bay (P. Shi et al., 2024), and Qinzhou Bay (Lyu et al., 2022).

Water levels in reclaimed tidal embayments with limited morphological changes may increase or decrease. The water levels in Jiaozhou Bay decreased (G. D. Gao et al., 2014) (see also Figure 12), while the water levels increased in Jakarta Bay due to funneling effects (Ningsih et al., 2024) and increased tidal choking (Rusdiansyah et al., 2018). Typically, the tides become more asymmetric and flood-dominant, as observed for Xiangshan Bay (X. Li, Bellerby, et al., 2018); Jiaozhou Bay (G. D. Gao et al., 2014)); Bohai Bay (Pelling et al., 2013) and Sanmen Bay (P. Shi et al., 2024). Herein the main tidal constituent (M_2) decreases in amplitude, while the amplitude of its overtide (M_4) often increases (as in Xiangshan Bay (X. Li, Bellerby, et al., 2018); Jiaozhou Bay (G. D. Gao et al., 2014)) and Bohai Bay (Pelling et al., 2013). Increasing storm surge levels have been reported for Bohai Bay (Ding & Wei, 2017) and Sanmen Bay (W. Yang et al., 2019), related to loss of intertidal area and increased funneling.

5. Examples of Land Reclamation Impacts

We have selected 9 key study areas (purple markers in Figure 2) for which a relatively large amount of data is available and which cover the broad range of coastal environments introduced in Section 4. These include three cases from the coastal plain of NW Europe, where land reclamation started 1,000 years ago (Sections 5.1–5.3), four cases along the rapidly expanding coastline of China, the land reclamation hotspot of the 20th and 21st century (Sections 5.6–5.9), as well as cases in the Ganges Brahmaputra delta (Section 5.4) and San Francisco Bay (Section 5.5).

5.1. Scheldt Estuary (SE), Belgium and the Netherlands

The present-day Scheldt Estuary is a classic funnel-shaped estuary of about 160 km long. It transforms from a 5 km wide meso-tidal, multi-channel, sandy outer estuary into a single-channel, muddy macro-tidal river in its upper reaches. By the 13th century most of the supratidal land in the estuary mouth (Vos, 2015) and the upper estuary (Missiaen et al., 2017) was reclaimed even though floods frequently recurred until the 17th century (de Kraker, 2015). This rapid reclamation phase was followed by a more gradual reclamation period in response to natural shoaling processes: the intertidal storage declined from 295 km^2 in 1650 to 104 km^2 in 1990 (van der Spek (1997)—see Figure 12). The secondary basins were especially efficient sediment traps (Dam et al., 2022) that were reclaimed when they reached supratidal levels (van der Spek, 1997): in total 129 million m^3 of sediments deposited in the side branches since 1860 (Dam et al., 2022). This loss of intertidal area in the Scheldt Estuary increased the tidal range (Figure 11) and the propagation speed of the incoming tidal wave (Stark et al., 2017; van der Spek, 1997; Weisscher et al., 2022).

The Scheldt Estuary as a whole has been eroding over the past 150 years (Dam et al. (2022) and Figure 12). In the period 1860–1955, 206 million m^3 was eroded in the main channel of which 111 million m^3 deposited in its side branches and 95 million m^3 was exported (mostly seaward). After 1955 the estuary reverted to net sediment import due to large-scale sediment extraction (sand mining–see Dam et al. (2022) and Elias et al. (2023)) while the tidal range further amplified due to channel deepening (van Maren, Alonso, et al., 2023). With a focus on hydromorphological impacts of land reclamation, we ignore changes after 1970, which are overwhelmingly influenced by channel deepening and dredging and disposal strategies.

10.1029/2024RG000860

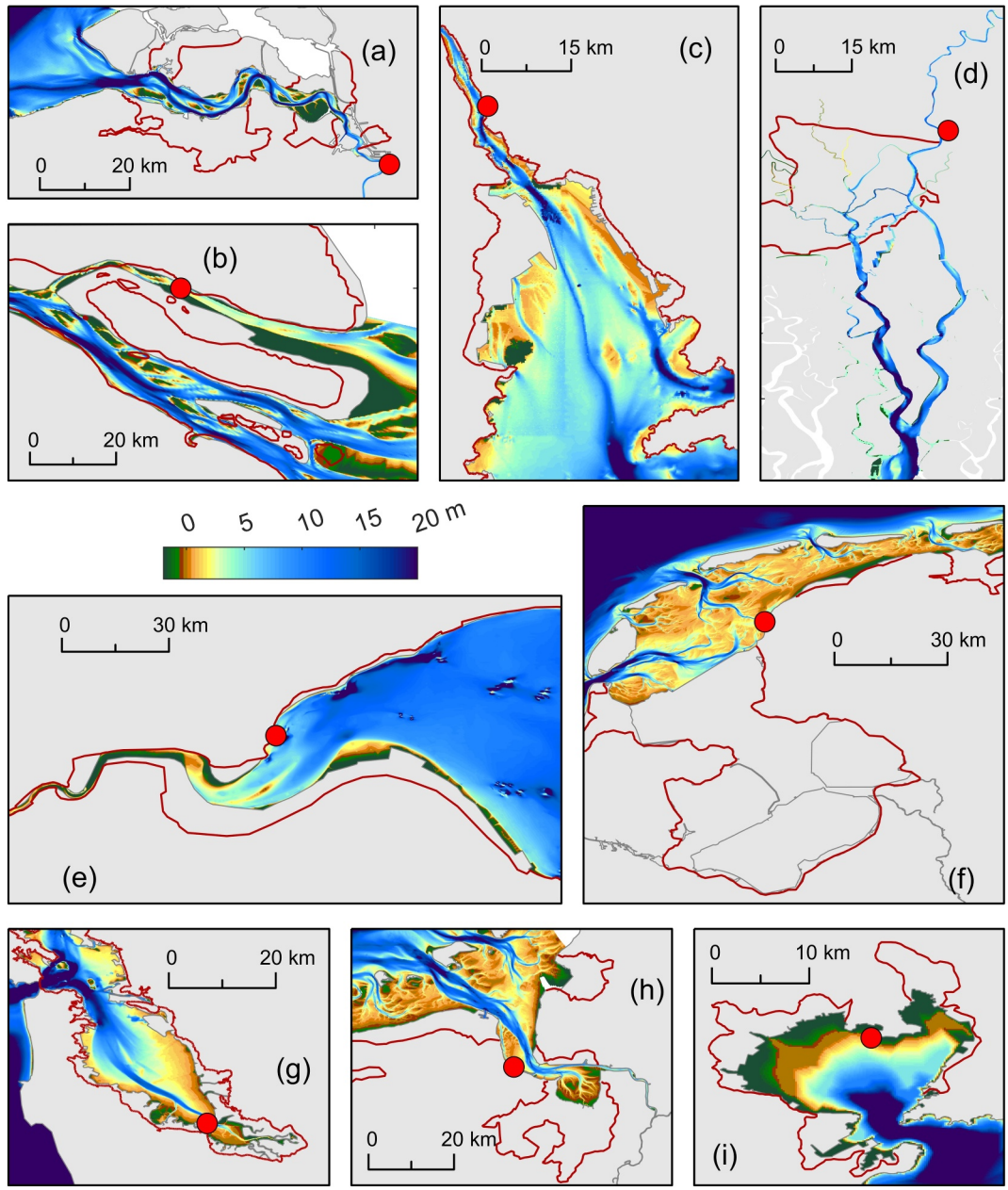

Figure 11. Bathymetry, historic coastlines (dark red lines) and water level observation stations (red circle, water level data in Figure 12) for the nine reclamation sites. The historical coastlines are from the following years: 1650 in the Scheldt Estuary (a; van der Spek, 1997) 1958 in the Yangtze Estuary (b; Guo et al., 2022), 1960 in Lingding Bay in the Pearl River Estuary (c; P. Zhang et al., 2021), 1965 in the Passur-Sibsa Estuary (d; Bain et al., 2019, with the Sibsa in the west and the Passur in the east), 1959 in Hangzhou Bay (e; Xie et al., 2017), 1500 in the western Wadden Sea (f; Van der Spek, 1995 and Rijkswaterstaat, 2021), 1858 in South San Francisco Bay (g; Grossinger, 1998), 1500 in the Ems Estuary (h; Schrijvershof et al., 2024; the strongly reclaimed inner bay is the Dollard), and 1935 in Jiaozhou Bay (i; G. D. Gao et al., 2014).

The Scheldt Estuary therefore illustrates that tides are amplifying slowly in response to human interventions along the length of the estuary (type 2). It also provides evidence of a system in which land reclamations may lead to autonomous channel deepening, contrasting with the common response of estuarine infilling.

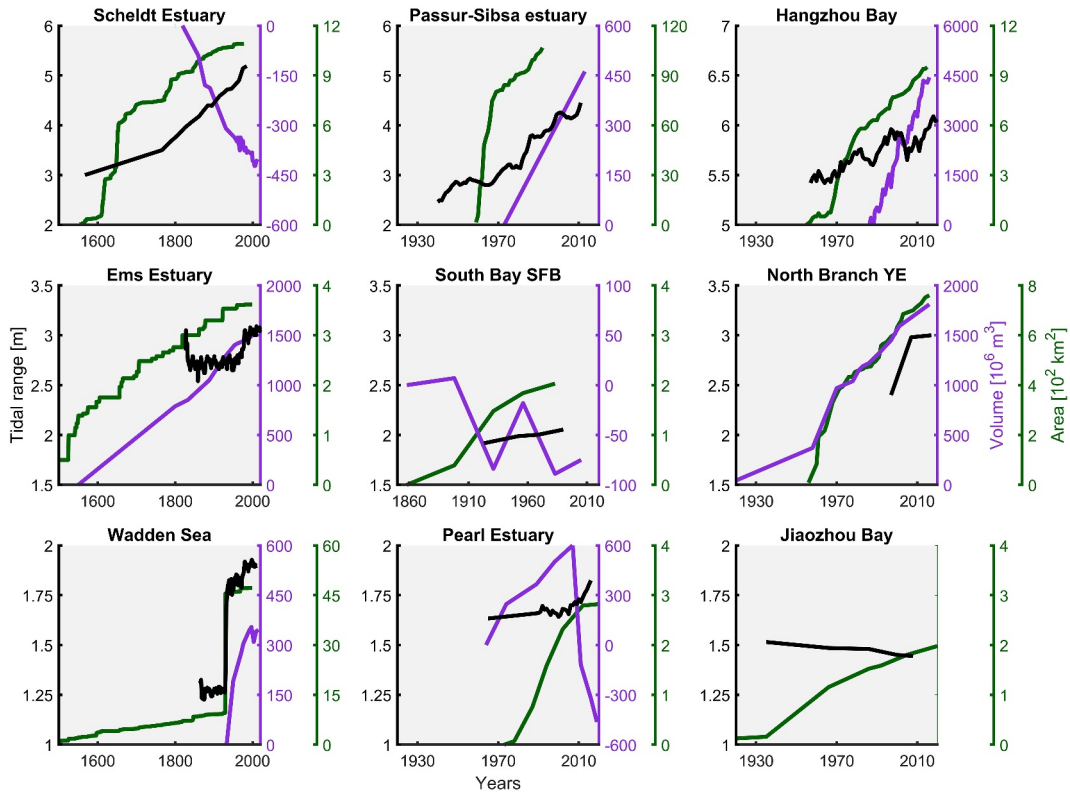

Figure 12. Cumulative channel infill volume (purple, in million m^3) and tidal range (black, in m) in response to cumulative land reclamation area (green, in km^2) for the nine main study sites. See Figure 11 for the maximal extent of the coastline and location of water level stations. Estuarine infilling by reclamation is represented by the Ems Estuary, South Bay, the North Branch of the Yangtze Estuary, Hangzhou Bay, and the Pearl Estuary (before 2010); estuarine infilling by basin closure by the Wadden Sea. Examples of coastal systems featuring tidal amplification are the Scheldt and Passur-Sibsa estuaries as well as (partly) Hangzhou Bay; river mouth channel erosion by the Pearl Estuary after 2010. A reduction of tidal energy is represented by Jiazhou Bay. Data is compiled from the following sources in (1) the Scheldt Estuary (land reclamation area from Mol (1995); infill volumes from Dam et al. (2022); tidal range at station Antwerpen from Coen (1988)); (2) the southwest Ganges delta (land reclamation area and annual tidal range at station Khulna from van Maren, Beemster, et al. (2023), channel infill volumes estimated from Wilson et al. (2017); (3) Hangzhou Bay (land reclamation area, infilling of inner Hangzhou Bay and Qiantang Estuary and annual tidal range observed at Ganpu station from Xie et al. (2017); (4) Ems Estuary (land reclamation area in Dollard Bay by Schrijvershof et al. (2024), infill volumes of the Ems Estuary compiled from Dollard volumes 1550–1985 by van Maren et al. (2016), main tidal channels 1833–1989 by Pierik (2021)) and space-covering digital maps of the entire estuary after 1989 by Elias et al. (2021), and the annual tidal range observed at station Delfzijl from the Dutch Ministry of Public Works); (5) South San Francisco Bay (reduction in marsh area from Foxgrover et al. (2004), infilling of South San Francisco Bay from Foxgrover et al. (2004) for 1858–1983 and B. Jaffe and Foxgrover (2006) for the year 2005 (covering part of South Bay), Mean Tidal Range at Dumbarton Bridge in South San Francisco Bay retrieved from Disney and Overshiner (1925) for the year 1923; Conomos (1979) for the year 1951 and https://tidesandcurrents.noaa.gov/ for later years; (6) North Channel in the Yangtze Estuary (land reclamation area from S. Wu et al. (2019); infill volumes from Guo et al. (2021), and tidal range at San He port derived from model hindcasts by X. Zhang et al. (2022); (7) Wadden Sea (land reclamation area is compiled from Schrijvershof et al. (2024), Van der Spek (1995), Niemeyer (1995); infilling of the Marsdiep basin from Colina Alonso et al. (2021) and observed annual tidal range at station Harlingen from the Dutch Ministry of Public Works); (8) Pearl Estuary (land reclamation area from X. Zhang et al. (2022); infill volumes from Han et al. (2023), and observed tidal range (defined as the sum of the M2-S2-O1-K1 harmonic constituents) at Sishengwei station (Lingding Bay) from P. Zhang et al. (2021) for 1965 and from (H. Wang et al. (2020) for 1990–2016; and (9) Jiaozhou Bay (land reclamation area from C. Xu et al. (2021) and computed tidal range (defined as the sum of the M2 and M4 harmonic constituents) at Hongdao (G. D. Gao et al., 2014).

5.2. South Sea (SS) in the Wadden Sea, the Netherlands

From the 9th century onward, the salt marshes and peatlands along the Wadden Sea coast were drained (Knottnerus, 2005; Vos, 2015) and by 1300, the larger part of the Dutch-German Wadden Sea coastline was well-protected by continuous dikes (Flemming et al., 1994; A. P. Oost, 1995; A. Oost et al., 2012). Around 15.000 km^2

of the Wadden Sea has now been reclaimed, an area larger than the present-day Wadden Sea (Reise, 2005), mostly before the year 1500 (the initial year in Figure 12). Land was reclaimed using methodologies illustrated in Figure 1a: brushwood groynes reduce hydrodynamic energy thereby promoting sedimentation which eventually becomes salt marsh; these salt marshes are converted to agricultural land by constructing sea dikes.

Land reclamation rates accelerated in the 20th century in the form of basin closures, including the South Sea in 1932 (introduced in Section 3.2) but also the Lauwers Sea (1969; 90 km^2) and the lower Elbe (1979; 150 km^2) (Reise, 2005). The closure of the South Sea instantaneously modified the tidal characteristics due to resonance of the semidiurnal tidal wave. Near the closure dam (station Harlingen), the tidal range increased by 0.5 m (Figure 12), although numerical hindcasts suggests that the increase in tidal range elsewhere exceeded one m (Vroom et al., 2012). The tidal basin morphologically responded to closure through infilling (Elias et al., 2012), especially in the channels formerly connecting the present-day Wadden Sea with the South Sea (Colina Alonso et al., 2021). The total sedimentation in response to closure was nearly 400 million m^3 (Figure 12), attaining an apparent new equilibrium in approximately 60 years (van Maren, Alonso, et al., 2023). Closure of the South Sea is therefore a Type 1b reclamation.

However, inlet closures such as the one to the South Sea possibly have an additional impact spanning much longer timescales. Many tidal flats in the Wadden Sea currently outpace the rise in sea level (Benninghoff & Winter, 2018, 2019; Z. B. Wang et al., 2018). These high sedimentation rates are probably the result of larger availability of fine sediments in response to closures and land reclamation, leading to a loss of natural sediment sinks (van Maren, Alonso, et al., 2023). On average, the fringing tidal flats accreted around 1 m since closure of the South Sea (Figure 8b), exceeding Mean Sea Level (less than 0.2 m/century; Vermeersen et al. (2018)) and the increase in tidal range (Figure 12). Locally, sedimentation rates on the tidal flats has been 3 m since closure (Baptist et al., 2019). This loss of sediment sinks is probably also driving an increase in turbidity observed in some parts of the Wadden Sea (van Maren et al., 2016).

The Wadden Sea is therefore a system that has been adapting for centuries to land reclamation (type 1a response) and more recently to inlet closures (type 1b response), especially of the inlet to the South Sea. Basin closure drives short-term (60 years) morphological change but also long-term (centuries) adaptation controlled by a larger availability of muddy sediments.

5.3. Ems Estuary (EE), Germany and the Netherlands

The Ems Estuary provides a Type-1a response to land reclamation that largely started around the year 1500. Habitation (and resulting improved drainage) of the marshlands surrounding the Ems Estuary led to subsidence and therefore vulnerability to coastal flooding, resulting in extensive marine flooding (van Maren et al., 2016; Vos & Knol, 2015). As a result, the Ems Estuary was much larger in the year 1500 than today (Schrijvershof et al., 2024). Nearly 400 km^2 of land has been reclaimed in the upper estuary since then (Figures 11h and 12). The resulting decrease in tidal prism and therefore flow velocity led to infilling of the system (1.5 x 10^9 m^3 of sediments—see Figure 12). The nearly linear infill rate suggests that the system is continuously and slowly adapting, and especially before the 20th century the reclamation of the intertidal area was the only anthropogenic driver sufficiently strong to exert a major influence on estuarine morphodynamics. The infilling of the estuary also led to the degeneration of the distinct ebb and flood channels. Over a period of 5 centuries, the flood channel has gradually expanded at the expense of the formerly dominant ebb channel because of reclamation of the upper estuary (Schrijvershof et al., 2024).

On top of the slow and gradual infilling in response to land reclamations are a number of system changes reflecting more recent interventions. The tide in the upper estuary (the lower Ems River) is amplifying in response to the construction of an upstream weir (Schuttelaars et al., 2013), several phases of channel deepening (van Maren, Alonso, et al., 2023) and a reduction of hydraulic roughness (Winterwerp, Wang, et al., 2013). The outer estuary is becoming more turbid because of creation and maintenance of navigation channels (van Maren, Van Kessel, et al., 2015), the deepening of the upper estuary (de Jonge et al., 2014) but probably especially because of the large-scale loss of sediment deposition areas in the Ems Estuary and updrift Wadden Sea (Section 5.2).

The Ems Estuary therefore provides an example of a system that fills in in response to up-estuary land reclamations, probably without strongly influencing the tidal range (type 1a). It also illustrates that historic land reclamation strongly influences estuarine morphology to date, and confirms that adaptation timescales to

reclamation may be very long (for the Ems Estuary up to several centuries). More recent human interventions such as channel deepening become prominent in the course of the 20th century, but their impact should not be confused with the slow and steady response resulting from land reclamations.

5.4. Passur-Sibsa Estuary in the Ganges Delta (GD), Bangladesh

The Ganges-Brahmaputra Delta (hereafter referred to as the GBD) is one of the most vulnerable deltas in the world (Syvitski et al., 2009; Tessler et al., 2015), but also the most populous with its 170 million inhabitants (Paszkowski et al., 2021). The eastern distributary (the Meghna Estuary) receives most of the river's sediment load while the Southwest part of the delta hardly receives sediment and is largely tide-dominated, but is also not subject to changes in fluvial sediment supply. The Southwest delta receives freshwater from the Ganges river through some old distributaries. The main distributary is the Gorai River of which the river discharge is declining slightly since the year 2000 (Ali & Hasan, 2022). But large-scale land reclamation started in the 1960s, before any changes in river discharge or sediment load in the Ganges-Brahmaputra river. Since the 1960s, 5000 km^2 of intertidal and supratidal land in the southwest delta was reclaimed (Wilson et al., 2017). The resulting loss of intertidal area influenced the tidal dynamics through two complex mechanisms, which will be illustrated with two distributaries of the Southwest delta: the Passur and the Sibsa (see Figure 11d).

Firstly, tidal channels that drain the reclaimed areas filled in with sediment due to the reduction in flow velocity. Throughout the Southwest Ganges-Brahmaputra delta, over 1,000 km of such channels filled in with sediments, while over 400 km of the primary waterways lost over 50% of their original width (Wilson et al., 2017). This resulted in the creation of 90 km^2 of new land, corresponding to deposition of 450 million m^3 (Figure 12). This infilling reduced the tidal prism, and therefore tidal flow velocities, strengthening infilling of the estuaries (van Maren, Beemster, et al. (2023) and loop II in Figure 6). The loss of intertidal storage simultaneously led to amplification of the tides in the main channels: first in the Sibsa and later in the Passur (van Maren, Beemster, et al., 2023). This increase remained linear until the present day (Figures 7 and 12), even though most of the land was reclaimed before the 1970s (van Maren, Beemster, et al., 2023). This continuous increase illustrates the importance of the progressive loss of intertidal area on tidal amplification.

The second mechanism through which the system responded to land reclamation involves interaction of the primary tidal channels (loop IV in Figure 6). The primary channels in the Southwest delta are connected through secondary channels (Bain et al., 2019). Because the amount of reclaimed land or chronology of reclamation differed between the two basins (Bain et al., 2019) the tides in one main channel amplified more than the other. But as these channels are interconnected, one primary channel may capture the tidal prism available to another, initiating a strong positive feedback loop (Bain et al., 2019; van Maren, Beemster, et al., 2023) because (a) the connecting channels erode (discharging more water) and (b) the non-amplifying main branch (the Passur) fills in with sediments while the amplifying branch (the Sibsa) erodes. Hence more and more tidal prism is conveyed through the initially amplifying branch.

The Sibsa therefore displays bed erosion and tidal amplification similar to the Scheldt Estuary providing another example of a Type-2 response. The infilling character of the Passur river in response to reduction of upstream intertidal area is typical for a Type 1a response, but with tidal amplification resulting from its connection with the Sibsa river.

5.5. South Bay (SB) in San Francisco Bay, United States

San Francisco Bay is a heavily urbanized bay with extensive intertidal flats. Its northeastern embayments (especially San Pablo Bay) have been strongly influenced by a large fluvial sediment input from 1856 to 1887 due to hydraulic gold mining, while bed levels have been strongly influenced by dredging since the 1920s and reduced upstream sediment supply due to reservoir construction since the 1950s (B. E. Jaffe et al., 2007; Barnard et al., 2013). The Central Bay area is heavily impacted by dredging and dredge disposal, borrow pits, and sand mining (Fregoso et al., 2008). South Bay (Figure 11g) is, in comparison, less influenced by dredging activities and by changes in the upstream sediment supply. However, since 1858 the area (with a water body of 410 km^2) lost 200 km^2 of marshland (80% of its 1858 size) to salt ponds, agricultural fields, and urban areas (Figure 12) while 34 km^2 (or 40% of its 1858 extent) of the intertidal area was reclaimed (Foxgrover et al., 2004). Given the relatively

minor influence of dredging works and upstream sediment load changes, we focus on the hydro-morphological effect of land reclamations in South Bay.

South Bay has undergone phases of infilling and erosion (Figure 12) with overall erosion dominating. Especially the extensive tidal flats in its middle reaches eroded, while the upper estuary and the deeper channels filled in with sediments (B. Jaffe & Foxgrover, 2006). It is not known why some of the tidal flats in South Bay were prone to erosion, but increased shipping may have provided a mechanism leading to eroding (e.g., Martins et al., 2023 and Scarpa et al., 2019). However, sedimentation was substantial in the upper estuary and channels. These accretion patterns can probably be related to the loss of the tidal prism resulting from reclamation because most of the reclaimed marshes were located in the upper estuary (Foxgrover et al., 2004). Archival data suggest that the tidal range slightly increased at the head of South Bay (Dumbarton Bridge, see Figure 12). Although such an increase may be expected because of the wetlands acting as a tidal energy sink (Holleman & Stacey, 2014), the observed increase of tidal range was comparable with the increase at the entrance of San Francisco Bay (Conomos, 1979; Disney & Overshiner, 1925).

South Bay (especially its upper reaches) therefore provides an example of a Type 1a response to reclamation: infilling with a minor change in tidal range. The response of the middle estuary is more variable, featuring alternating phases of erosion and sedimentation, probably in response to additional human interventions.

5.6. North Branch of the Yangtze Estuary (YE), China

The Yangtze River is the 5th largest river in the world in terms of discharge, annually transporting 470 million ton before the construction of upstream reservoirs (S. Yang et al., 2015). Due to its large sediment load the river formed a delta stretching over 700 km in length, controlled by tidal discharge as well as the river discharge. The Yangtze Delta expanded 1500 km^2 between 1950 and 2020, largely owing to tidal flat accretion and reclamation of the flats (Guo et al., 2021). It is heavily influenced by human interventions through damming of the upstream river, deepening of access channels, and reclamation of land (Zhao et al., 2018; C. Zhu et al., 2019). The sediment load reduced with 71–77 % as a result of infilling in upstream reservoirs (S. Yang et al., 2015; H. Yang et al., 2018). The sediment load of the Yangtze river started to decline because of reservoirs from the mid-1980s onwards, but the biggest decrease resulted from the Three Gorges Dam (2003) and subsequent megadams constructed upstream of the Three Gorges Dam. Channels were narrowed and deepened to facilitate navigation providing access to the port of Shanghai, with especially the Deep Channel Navigation Project constructed between 1998 and 2008 greatly influencing the hydrodynamics, ecology and morphology of the delta (Pan et al., 2012; C. Zhu et al., 2019, 2025). Many land reclamation activities pre-date the sediment load reduction resulting from upstream reservoirs and deepening of channels. Especially land reclamation in the northern outlet of the Yangtze Estuary (the North Branch, see Figure 11b), starting in the 1920s, profoundly influenced tidal dynamics and morphologic changes. Changes in sediment load are negligible during this period (H. Yang et al., 2018), and therefore the development of the North Branch can be primarily attributed to land reclamations.

Historically, the North Branch was an important, river-flow dominated outlet of the Yangtze River, receiving 25% of the river flow around 1900 (J. Chen & Shen, 1988). Reclamation of sand bars developing at the bifurcation region of the North and South Branches narrowed the inlet of the North Branch and reduced fluvial influence. At the same time, reclamation along the inner parts of the North Branch enhanced the width convergence, strongly amplifying the tides and even leading to the formation of tidal bores (S. Shen, 2003). The channel switched from a river-dominated system to a tide-dominated system in which large amounts of sediments accumulated as a result of flood-dominant tidal currents. Rapid infilling of the intertidal areas facilitated more land reclamation, leading to a further decrease in tidal prism and rapid degeneration of the North Branch (Z. Dai et al., 2016; Guo et al., 2022; R. Zhang et al., 2023). The North Branch now receives only 5% of the freshwater discharge (Yun, 2004)–five times less than around 1900.

The North Branch of the Yangtze Estuary therefore provides an example of a Type-1a response with pronounced morphological changes because sedimentation rates are accelerated by feedback loop I (increasing flood-dominant tides) and IV (channel competition)–see Figure 6.

5.7. Hangzhou Bay (HB), China

Hangzhou Bay is one of the largest macro-tidal estuaries worldwide (with a tidal range of 6 m, see Figure 12) with extensive tidal flats developed on the southern shore. The tides are very asymmetric and home to the world's largest tidal bore (Fan et al., 2014; Tu & Fan, 2017) as a result of the bay's funnel shape in combination with a broad inner bar amplifying and deforming the incoming tides (J. Chen et al., 1990; L. Li et al., 2019; Xie et al., 2022). The abundance of fine-grained sediments in combination with (flood-dominant) tidal currents over 2 m/s (J. Chen et al., 1990) results in tide-averaged suspended sediment concentrations up to 10 kg/m^3. Approximately 1000 km^2 of land has been reclaimed in Hangzhou Bay (Figures 11e and 12) and its upper reaches (Qiantang Estuary) since the 1950s. Reclamation influenced the tides and led to large-scale sediment infilling (4,500 million m^3 of sediment since 1990; see Figure 12 and (Xie et al., 2017)). The associated annual sediment deposition rates (around 150 million ton/year), are close to the present-day annual sediment load of the nearby Yangtze River (C. Zhu et al., 2019), constituting the main sediment source of the Hangzhou Bay deposits. But although the sediment load of the Yangtze river has been declining since the mid 1980s (S. Yang et al., 2015; H. Yang et al., 2018) there are no indications the southward sediment transport in its river plume is reducing (Xie et al., 2024). The discharge main river draining into Hangzhou Bay (the Qiantang River) has remained largely constant since beginning of observations (1979) (Xie et al., 2022). As such, Hangzhou Bay provides a tide-dominated and sediment-rich environment in which changes are primarily resulting from land reclamations.

The various reclamation works in Hangzhou Bay (see Figure 1f) minimized the natural sediment sinks of the estuary, leading to a higher sediment availability in the water column. Reclamation resulted in a weakening of the tidal flows (especially in the upper Qiantang Estuary) and due to the high availability of sediment, large sediment volumes accumulated (W. Li et al., 2024). This is typical for a type 1a estuary (rapid infilling due to loss of tidal prism) and feedback loop II in Figure 6. Both infilling and the loss of intertidal area deformed the tides, both in asymmetry and in amplitude, especially in outer Hangzhou Bay. Tidal amplification (0.6 m since 1960 at Ganpu station, see Figure 12) is mainly caused by enhanced funelling (L. Li et al., 2019): a type-2 estuarine response. This increase in tidal amplification resulting from funneling is partly compensated by more enhanced tidal dissipation resulting from the rapid infilling of the bay. Without this rapid infilling, the increase in tidal range because of funneling would have been up to two m (L. Li et al., 2019). The increase in tidal asymmetry drives two additional feedback loops (Figure 6) strengthening the effect of land reclamation: more import leads to more sedimentation on tidal flats which can be easily reclaimed (feedback loop I), and more sediment import leads to higher SSC levels which reduce the hydraulic roughness, further deforming the tides (Xie et al. (2022); feedback loop III).

Summarizing, the response of Hangzhou Bay to land reclamation is a combination of type 1a in inner Hangzhou Bay and Qiantang Estuary (rapid infilling due to loss of tidal prism) and tidal amplification in outer Hangzhou Bay (type 2) due to more pronounced funnelling. Sediments introduce various non-linear responses exacerbating the impact of land reclamations (feedback loops I, II, and III in Figure 6). Tidal amplification is partly compensated by the rapid infilling rates.

5.8. Pearl River Estuary (PE), China

The Pearl river is China's largest river after the Yangtze, annually transporting about 80 million tons of sediment. The sediment load is decreasing due to upstream dams since the 1990s (Wei et al., 2020; Z. Liu et al., 2022) but especially after 2000: it is 72 % lower in the 2020s than before 1990; Wei et al. (2020)). The Pearl River Estuary (Figure 11c) is a heavily urbanized estuary (Wei et al., 2021) consisting of four sub-estuaries, including Lingding Bay and the Modaomen Estuary. Land reclamation in the upper estuary of Lingding Bay since 1960 (Figure 12) led to a reduction in the tidal flow velocities in the lower estuary and an increase in the flow velocities in the upper estuary (Chu et al., 2022), promoting an overall infilling of the estuary (Figure 12)–a Type-1a response. In absence of contemporary major interventions, this change can be primarily attributed to land reclamation. After the year 2000 changes in Lingding Bay can no longer be directly related to land reclamation. The transition from deposition to erosion in the early 21st century (Figure 12) results from dredging. The main channel was deepened and widened in 1998 and sand mining started in 1989 but accelerated after 2007. This channel deepening in turn led to an increase in tidal amplitudes (Figure 12). Another factor influencing tidal channel stability is the pronounced decrease in sediment supply due to upstream dams (Z. Wu et al., 2016; Wei et al., 2021). Without these

upstream dams, infilling rates in response to land reclamation (until the early 21st century) would have likely been even larger.

Deep Bay (also known as Shenzhen Bay) is a tributary estuary of Lingding Bay. It has been reclaimed at its landward end and at its mouth and is filling in with sediments (Yang & Chui, 2017). Up-estuary reclamation resulted in weakening of the tidal currents (thereby probably responsible for infilling as a Type 1a response), while reclamation at the mouth accelerated tidal currents (Type 3 response). Most land reclamation in the Modaomen Estuary (another outlet of the Pearl River, south of Lingding Bay) took place in its seaward reaches to control flooding and navigation between 1983 and 1992 (L. W. Jia et al., 2013). Sand mining started in the early 1990s and channel dredging in the early 2000s. However, the main channel of the Modaomen Estuary began to deepen in the 1980s: a period in which the main anthropogenic activity was land reclamation. Deepening accelerated after 1999. But the deepening volumes (after 1999) are much larger than sand mining volumes (L. W. Jia et al., 2013; W. Zhang et al., 2015), suggesting that the reclamation works have led to scouring of the main channels in the Modaomen Estuary (Type 3 response).

In summary, up-estuary reclamation in the Pearl River Estuary led to infilling (type 1a response) in Deep Bay and Lingding Bay in a period that other interventions (dredging and reductions of the upstream sediment load) where relatively unimportant. Reclamation in the mouth of the estuary led to a type 3 response in the Modaomen Estuary (scouring of the main channel) and Deep Bay (increasing flow velocities). During subsequent periods, sand mining is responsible for pronounced deepening of the main channels leading to amplification of the tides.

5.9. Jiaozhou Bay (JB), China

Jiaozhou Bay (Figure 11i) is an embayment along China's heavily developed East Coast, and connected to the Yellow Sea. The extensive tidal flats originally flanking the inner bay have been largely reclaimed. Most of the land was reclaimed between 1935 and 1966; land reclamation speed and resulting impacts reduced after that (G. D. Gao et al., 2014). In total about 300 km^2 of land was reclaimed (Figure 12) which is almost the same as the present size of the bay (340 km^2; (G. D. Gao et al., 2014)). The water levels decreased only slightly (Figure 12), and the main hydrodynamic impact of land reclamation was a reduction in tidal prism and flow velocities (the M_2 tidal energy reduced with 50%; (G. D. Gao et al., 2014)). This led to an increase in residence time, resulting in a declining water quality (Qiao et al., 2019; J. Shi et al., 2011). There is no information available on infilling rates or bed level changes in Jiaozhou Bay, but the strong weakening of hydrodynamic energy suggests that morphological adaptation is limited. The response of Jiaozhou Bay is therefore typical for sediment-poor confined systems even though the muddy coastlines illustrate an abundance of sediments. The timescales associated with infilling are so long that the hydrodynamic response is insignificantly influenced by morphodynamic adaption.

Land reclamation also influenced the asymmetry of the tides. The M_4 tidal amplitude increased relative to the M_2 tidal amplitude, strengthening a flood-dominant tidal duration asymmetry (G. D. Gao et al., 2014) in which a longer period of high water slack compared to low water slack promotes sediment import. The impact of land reclamation on tidal asymmetry is influenced by the order of reclamation, with reclamation of the inner bay most strongly impacting the tidal duration asymmetry compared to reclamation executed at the mouth of the bay (G. D. Gao et al., 2014). But although the tidal asymmetry is flood-dominant, the net sediment transport is from the inner bay toward the ocean because the mouth of the bay is primarily coarse sediment and bedrock (S. Gao & Wang, 2002).

5.10. Synthesis

Figure 13 presents a semi-quantitative scheme composed of a hydrodynamic and a morphodynamic axis (Figure 13). For each coastal environment, the hydrodynamic and morphologic impact is provided in a relative sense (differentiating between the location of reclamation in case of estuaries, as in Section 4). Herein, we provide clusters of responses for the non-key sites: within each cluster no differentiation is made between the relative impact of each site. The relative position of the key sites relative to each other and the overall clusters of non-key sites can now be better determined. The Qiantang Estuary/Hangzhou Bay, for instance, scores higher than any other site on sedimentation rate while the South Sea (in the Wadden Sea) has the strongest reduction in tidal prism.

Most sites are in the top left quadrant (reduction in hydrodynamic energy and sedimentation) of Figure 13. Most of these examples include type 1 response (infilling resulting from a reduction in tidal prism) with a cluster for

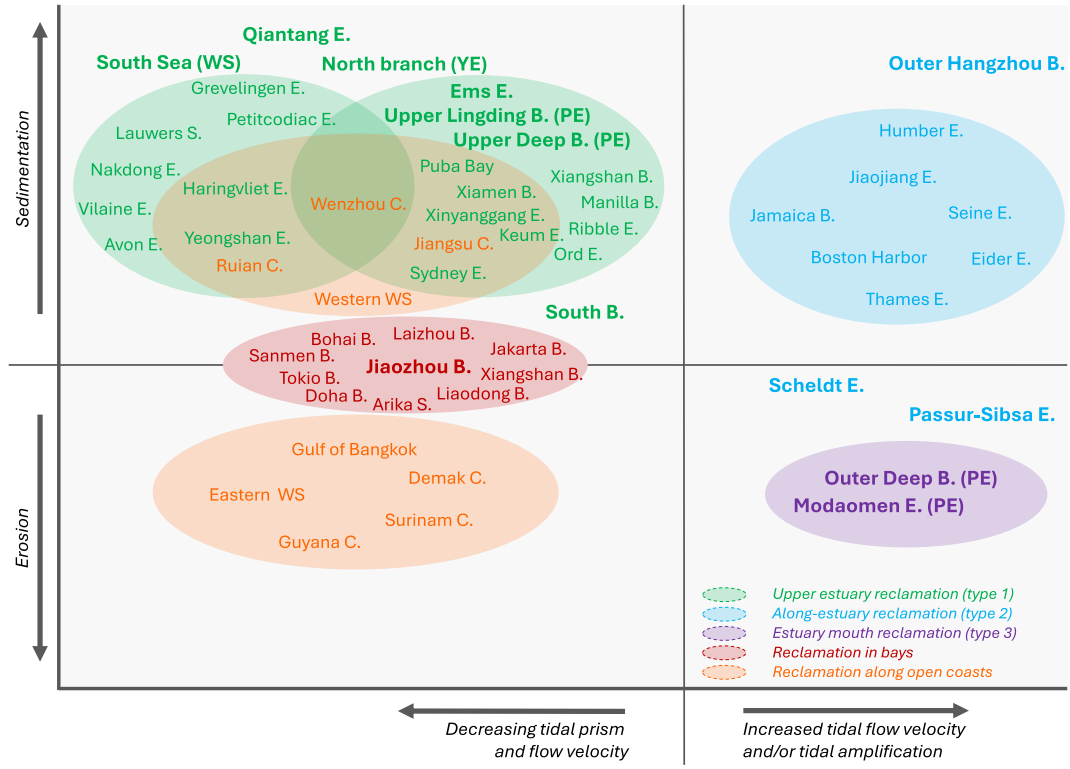

Figure 13. Response diagram summarizing the hydro-morphological impact of evaluated land reclamation differentiating per coastal environment and location of reclamation (see Table 2). Bold names refer to key sites; non-bold names to additional sites (with details in Table 2). The *x*-axis represents changes in tidal hydrodynamics (tidal amplitude, prism, and/or velocity), the *y*-axis the morphological response (sedimentation erosion). The circles represent clusters of response of case studies for which insufficient quantitative data is available to differentiate (with only some of the key sites outside clusters). Names are partly abbreviated for readability: C. = Coast, B. = Bay, E. = Estuary, PE = Pearl River Estuary, WS = Wadden Sea, YE = Yangtze Estuary.

gradual land reclamation and for closures, but also sedimentation resulting from a reduction in cross-shore flows. An increase in hydrodynamic energy (either by tidal amplification or stronger tidal flow velocities) is a less common response.

Figure 13 facilitates interpretation of observational data, and thereby helps understanding how tide-influenced coastal systems have responded in the past and therefore also how they may still respond in the future. Knowing the relationships between reclamation, hydrodynamic changes and morphological development is also important to differentiate land reclamation effects from those caused by for example, upstream reservoir construction or local channel deepening. These latter types of human interventions have received much greater scientific attention compared to that of land reclamation.

6. Summary and Outlook

In estuaries, bays and lagoons, three common response types to land reclamation have been identified. Type 1 concerns reclamation of land at the landward end of confined estuaries, which typically leads to channel infilling. This process is strengthened by positive feedback loops adding to the persistence of the intervention. Extreme examples of this type of reclamation are estuarine dams, which are constructed globally, and lead to large-scale infilling. Land reclamation along the length of an estuary, here referred to as type 2, typically leads to larger and more asymmetric tides by enhanced funneling and loss of intertidal storage space. This response is strongly governed by positive feedback loops, resulting in very persistent channel infilling, channel erosion, or tidal amplification. Reclamation at the estuary mouth, type 3, may lead to loss of tidal prism when the water body landward of the land reclamation is very large. However, for most estuaries, river mouth reclamation leads to

stronger tidal currents and, consequently, scouring of the bed; the resulting channel deepening may subsequently lead to tidal amplification.

Coastal land reclamations vary widely in terms of size, shape, and location. Their impact on the hydro-geomorphology of the system is strongly influenced by the availability of sediments and their position within the coastal system. Along open muddy coasts, they may trigger coastal erosion (limited sediment availability or pronounced wave influence) or accretion (large sediment availability), depending on local transport conditions. In more enclosed environments where sediment is insufficiently available for morphological changes to compensate for modified hydrodynamics (such as coastal embayments), the reduction in tidal prism resulting from large-scale land reclamation diminishes the tidal flow amplitudes. This, in turn, leads to lower mixing rates and longer residence times.

As part of this review, we have identified key challenges that need further scientific exploration, which are related to relatively unexplored impacts (on the SSC), process knowledge (feedback loops) and methodologies (data collection and computational aspects relating to timescales).

6.1. The Suspended Sediment Concentration

Land reclamation leads to a loss of sediment sinks and frequently to stronger up-estuary sediment transport; both would lead to an increase in SSC. Although this relation is phenomenologically described by Van Proosdij et al. (2009), Morris and Mitchell (2013), Dronkers (2016), to the authors' knowledge, only van Maren et al. (2016) and Cheng et al. (2020) quantitatively relate land reclamation to changes in turbidity. Land reclamation could even explain the global increase in SSC observed by Hou et al. (2024). According to their satellite data analysis, the globally averaged SSC increases 0.46% per year, despite the overall reduction in fluvial sediment load resulting from upstream dam construction. For 30% of the worlds deltas, the sediment load is decreasing (by e.g. upstream dams) while the offshore SSC is increasing (Hou et al., 2024). Even more, an increase in SSC was typically observed along river and tide-dominated deltas, but not along wave-dominated deltas. Hou et al. (2024) could not explain the sustained increase in SSC along deltas, but we hypothesize it may be related to land reclamation. We therefore advocate more dedicated studies relating the role of land reclamation to changes in the SSC, which may help to prevent hyperturbidity and excessive maintenance dredging and the associated loss of ecological value.

6.2. Feedback Loops

The speed, degree, and duration with which coastal systems adapt to land reclamation are strongly influenced by positive feedback loops and the availability of sediments. Despite the large-scale importance of such sediment-driven feedback loops, our understanding of these complex interactions remains limited. Advancing our scientific knowledge of such dynamics is crucial (Hoitink et al., 2020), especially when considering interventions in coastal environments. An alarming example herein is the Passur-Sibsa system, in which the tides are amplifying linearly (from 3 to 5 m–see van Maren, Beemster, et al. (2023)). Tidal amplification in response to morphological processes decays exponentially (van Maren, Alonso, et al., 2023). Given the present day linear amplification, it is likely that tidal amplification will continue for a considerable period of time, probably at least reaching the amplitudes observed in the Indian Ganges delta distributaries (over 7 m–see Chatterjee et al. (2013)). This increase in tidal amplitude, driven by sediment feedback loops, will significantly exacerbate flood risks in these heavily populated, subsiding deltas (Syvitski et al., 2009), underscoring the urgent need for both scientific understanding and careful management.

6.3. Adaptation Times and Equilibrium

The response of coastal systems may be slow, impacting the landscape evolution for centuries. This means that most systems are still presently adapting to reclamation of their intertidal areas, even if land was reclaimed decades or centuries ago. This slow response has great practical and scientific implications. Coastal systems are strongly influenced by many concurrent interventions, such as upstream dams (which lead to a reduction in upstream sediment supply and/or a change in discharge distribution), channel deepening for navigation purposes and climate change (notably sea-level rise). When predicting the impact of such interventions, the assumption is typically made that these systems start from equilibrium conditions, whereas in many cases, the morphological changes that are currently taking place are still the result of land reclamation activities in the past. In order to

separate the long term effects of land reclamations form more recent interventions we recommend to (a) put more effort into digitizing archival data (of bathymetry and water levels) to better understand long-term trends (as e.g. by Talke and Jay (2013), Talke and Jay (2017), Inayatillah et al. (2022), and Latapy et al. (2023)), and (b) account for such trends when understanding present-day or future changes resulting from changes in sediment supply, channel deepening, and climate change. Such historic changes are partly accounted for when predicting the effects of sea-level rise using aggregated models such as ASMITA (Kragtwijk et al., 2004; Van Goor et al., 2003), because they are calibrated against long-term volumetric changes. But process-based models predicting adaptation to sea-level rise (Becherer et al., 2018; van der Wegen, 2013) rarely (if ever) start from equilibrium initial conditions. Similarly, the impact of deepening on estuarine hydrodynamics, water quality, and morphology is typically evaluated with a channel depth before and after deepening (van Maren, Van Kessel, et al., 2015; van Rijn et al., 2018; Y. Wang & Shen, 2020), ignoring observations that estuarine systems are in transition resulting from land reclamation (as in this paper) or previous deepening phases with a response time of decades (van Maren, Alonso, et al., 2023).

Glossary

Reclamation	Conversion of submerged fluvial or marine environments to land by promoting sedimentation, by landfill, or by draining embanked areas
Intertidal area	The littoral zone between low tide and high tide, which is regularly inundated by the tides
Feedback mechanism	A loop system in which the system responds to an initial perturbation by amplifying it (positive feedback) or by counteracting it (negative feedback)
Tidal prism	The total volume of water imported and exported at a certain cross-section over a tidal cycle
Tidal asymmetry	A spatial or temporal deviation from a symmetric water level or flow velocity signal
Flood dominance	The most common form of tidal asymmetry where a temporal tidal asymmetry leads to sediment transport in the flood direction
Estuary	A partially enclosed water system with a free connection to the open sea or ocean, receiving fresh water from one or more rivers
Bay	A partially enclosed water system connected to a sea, lake or ocean

Acronyms

SSC	Suspended Sediment Concentration
ETM	Estuarine Turbidity Maximum
MSL	Mean Sea Level
MHW	Mean High Water
MLW	Mean Low Water
SLR	Sea Level Rise

Data Availability Statement

All data is extracted from the cited references which are all publicly available. This contribution does not present previously unpublished data. Data used for the main sites are taken from the following sources. Scheldt Estuary: van der Spek (1997), Mol (1995), Dam et al. (2022), and Coen (1988); the Yangtze Estuary: Guo et al. (2022), S. Wu et al. (2019), Guo et al. (2021), X. Zhang et al. (2022); the Pearl River Estuary: P. Zhang et al. (2021), X. Zhang et al. (2022), Han et al. (2023), and H. Wang et al. (2020); the Passur-Sibsa Estuary: Bain et al. (2019), van Maren, Beemster, et al. (2023), and Wilson et al. (2017); Hangzhou Bay: Xie et al. (2017); the Wadden Sea: Van der Spek (1995), Rijkswaterstaat (2021), Schrijvershof et al. (2024), Van der Spek (1995), Niemeyer (1995), Colina

Alonso et al. (2021); South San Francisco Bay: Grossinger (1998), Foxgrover et al. (2004), B. Jaffe and Foxgrover (2006), Disney and Overshiner (1925), and Conomos (1979); the Ems Estuary: Schrijvershof et al. (2024), van Maren et al. (2016), Pierik (2021), and Elias et al. (2021); Jiaozhou Bay: C. Xu et al. (2021) and G. D. Gao et al. (2014). Supplemental tidal data was published by NOAA (tidesandcurrents.noaa.gov) for San Francisco Bay and by the Dutch Ministry of Public Works (waterinfo.rws.nl) for the Wadden Sea and Ems Estuary.

Acknowledgments
DSM was partly funded by the Zijiang Scholar Program of East China Normal University. RAS and AJFH received funding from the Netherlands Organization for Scientific Research (NWO), within Vici project "Deltas out of shape: regime changes of sediment dynamics in tide-influenced deltas" (Grant NWO-TTW 17062). CZ acknowledges the funding from NSFC (42206169). Contributions of DX were funded by the National Natural Science Foundation of China Grant 42176170 and key project of Zhejiang Provincial Natural Science Foundation No. LZJWZ23E090003. Contributions of ZZ were supported by the National Natural Science Foundation of China Grant 42406161.

References

Ali, M. S., & Hasan, M. M. (2022). Environmental flow assessment of Gorai River in Bangladesh: A comparative analysis of different hydrological methods. *Heliyon*, *8*(7), e09857. https://doi.org/10.1016/j.heliyon.2022.e09857

Anthony, E. J., Gardel, A., Gratiot, N., Proisy, C., Allison, M. A., Dolique, F., & Fromard, F. (2010). The amazon-influenced muddy coast of South America: A review of mud-bank–shoreline interactions. *Earth-Science Reviews*, *103*(3–4), 99–121. https://doi.org/10.1016/j.earscirev.2010.09.008

Anthony, E. J., & Gratiot, N. (2012). Coastal engineering and large-scale mangrove destruction in Guyana, South America: Averting an environmental catastrophe in the making. *Ecological Engineering*, *47*, 268–273. https://doi.org/10.1016/j.ecoleng.2012.07.005

Anthony, E. J., Syvitski, J. P. M., Zăinescu, F., Nicholls, R. J., Cohen, K. M., Marriner, N., et al. (2024). Delta sustainability from the Holocene to the Anthropocene and envisioning the future. *Nature Sustainability*, *7*(10), 1–12. https://doi.org/10.1038/s41893-024-01426-3

Bain, R. L., Hale, R. P., & Goodbred, S. L. (2019). Flow reorganization in an anthropogenically modified tidal channel network: An example from the Southwestern Ganges-Brahmaputra-Meghna Delta. *Journal of Geophysical Research: Earth Surface*, *124*(8), 2141–2159. https://doi.org/10.1029/2018JF004996

Baptist, M. J., Gerkema, T., Van Prooijen, B., Van Maren, D., Van Regteren, M., Schulz, K., et al. (2019). Beneficial use of dredged sediment to enhance salt marsh development by applying a Mud Motor. *Ecological Engineering*, *127*, 312–323. https://doi.org/10.1016/j.ecoleng.2018.11.019

Barbier, E. B. (2015). Climate change impacts on rural poverty in low-elevation coastal zones. *Estuarine, Coastal and Shelf Science*, *165*, A1–A13. https://doi.org/10.1016/j.ecss.2015.05.035

Barbier, E. B., Hacker, S. D., Kennedy, C., Koch, E. W., Stier, A. C., & Silliman, B. R. (2011). The value of estuarine and coastal ecosystem services. *Ecological Monographs*, *81*(2), 169–193. https://doi.org/10.1890/10-1510.1

Barnard, P. L., Schoellhamer, D. H., Jaffe, B. E., & McKee, L. J. (2013). Sediment transport in the San Francisco Bay Coastal System: An overview. *Marine Geology*, *345*, 3–17. https://doi.org/10.1016/j.margeo.2013.04.005

Becherer, J., Hofstede, J., Gräwe, U., Purkiani, K., Schulz, E., & Burchard, H. (2018). The Wadden Sea in transition-consequences of sea level rise. *Ocean Dynamics*, *68*(1), 131–151. https://doi.org/10.1007/s10236-017-1117-5

Bednarczyk, K., Schaller, D., & Vierfuss, U. (2008). The Eider estuary. *Die Küste; Archiv für Forschung und Technik an der Nord-und Ostsee*, *74*, 307.

Benninghoff, M., & Winter, C. (2018). Decadal evolution of tidal flats and channels in the Outer Weser estuary, Germany. *Ocean Dynamics*, *68*(9), 1181–1190. https://doi.org/10.1007/s10236-018-1184-2

Benninghoff, M., & Winter, C. (2019). Recent morphologic evolution of the German Wadden Sea. *Scientific Reports*, *9*(1), 9293. https://doi.org/10.1038/s41598-019-45683-1

Besset, M., Gratiot, N., Anthony, E. J., Bouchette, F., Goichot, M., & Marchesiello, P. (2019). Mangroves and shoreline erosion in the Mekong River Delta, Viet Nam. *Estuarine, Coastal and Shelf Science*, *226*, 106263. https://doi.org/10.1016/j.ecss.2019.106263

Birch, G. F., Murray, O., Johnson, I., & Wilson, A. (2009). Reclamation in Sydney estuary, 1788–2002. *Australian Geographer*, *40*(3), 347–368. https://doi.org/10.1080/00049180903127788

Bishop, M. J., Mayer-Pinto, M., Airoldi, L., Firth, L. B., Morris, R. L., Loke, L. H., et al. (2017). Effects of ocean sprawl on ecological connectivity: Impacts and solutions. *Journal of Experimental Marine Biology and Ecology*, *492*, 7–30. https://doi.org/10.1016/j.jembe.2017.01.021

Burchard, H., Schuttelaars, H. M., & Ralston, D. K. (2018). Sediment trapping in estuaries. *Annual Review of Marine Science*, *10*(1), 371–395. https://doi.org/10.1146/annurev-marine-010816-060535

Cai, H., Savenije, H. H. G., Yang, Q., Ou, S., & Lei, Y. (2012). Influence of river discharge and dredging on tidal wave propagation: Modaomen Estuary case. *Journal of Hydraulic Engineering*, *138*(10), 885–896. https://doi.org/10.1061/(ASCE)HY.1943-7900.0000594

Chang, J., Lee, G.-h., Harris, C. K., Figueroa, S. M., & Jung, N. W. (2023). Relative contribution of the presence of an estuarine dam and land reclamation to sediment dynamics of the Nakdong Estuary. *Frontiers in Marine Science*, *10*, 1101658. https://doi.org/10.3389/fmars.2023.1101658

Chang, J., Lee, G.-H., Harris, C. K., Song, Y., Figueroa, S. M., Schieder, N. W., & Lagamayo, K. D. (2020). Sediment transport mechanisms in altered depositional environments of the anthropocene Nakdong estuary: A numerical modeling study. *Marine Geology*, *430*, 106364. https://doi.org/10.1016/j.margeo.2020.106364

Chatterjee, M., Shankar, D., Sen, G. K., Sanyal, P., Sundar, D., Michael, G. S., et al. (2013). Tidal variations in the Sundarbans Estuarine System, India. *Journal of Earth System Science*, *122*(4), 899–933. https://doi.org/10.1007/s12040-013-0314-y

Chen, J., Cangzi, L., Chongle, Z., & Walker, H. J. (1990). Geomorphological development and sedimentation in Qiantang Estuary and Hangzhou Bay. *Journal of Coastal Research*, *6*(3), 559–572. Retrieved from https://www.jstor.org/stable/4297719

Chen, J., & Shen, H. (1988). Some key points on harnessing the Changjiang estuary. *Processes of Dynamics and Geomorphology of the Changjiang Estuary*, 419–423. (in Chinese).

Chen, L., Zhou, Z., Xu, F., Jimenez, M., Tao, J., & Zhang, C. (2020). Simulating the impacts of land reclamation and de-reclamation on the morphodynamics of tidal networks. *Anthropocene Coasts*, *3*(1), 30–42. https://doi.org/10.1139/anc-2019-0010

Chen, P., Sun, Z., Zhou, X., Xia, Y., Li, L., He, Z., et al. (2021). Impacts of coastal reclamation on tidal and sediment dynamics in the Ruian coast of China. *Ocean Dynamics*, *71*(3), 323–341. https://doi.org/10.1007/s10236-021-01442-3

Chen, Y., Dong, J., Xiao, X., Ma, Z., Tan, K., Melville, D., et al. (2019). Effects of reclamation and natural changes on coastal wetlands bordering China's Yellow Sea from 1984 to 2015. *Land Degradation & Development*, *30*(13), 1533–1544. https://doi.org/10.1002/ldr.3322

Cheng, Z., Jalon-Rojas, I., Wang, X. H., & Liu, Y. (2020). Impacts of land reclamation on sediment transport and sedimentary environment in a macro-tidal estuary. *Estuarine, Coastal and Shelf Science*, *242*, 106861. https://doi.org/10.1016/j.ecss.2020.106861

Chu, N., Yao, P., Ou, S., Wang, H., Yang, H., & Yang, Q. (2022). Response of tidal dynamics to successive land reclamation in the Lingding Bay over the last century. *Coastal Engineering*, *173*, 104095. https://doi.org/10.1016/j.coastaleng.2022.104095

Coen, I. I. (1988). De eeuwige Schelde? Ontstaan en ontwikkeling van de Schelde. *Monograph of the Departement Mobiliteit en Openbare Werken, Waterbouwkundig Laboratorium*, 104. Retrieved from https://www.gs-esf.be/downloads/2018-04-03/DeEeuwigeSchelde.pdf

Colina Alonso, A., Van Maren, D., Elias, E. P., Holthuijsen, S., & Wang, Z. (2021). The contribution of sand and mud to infilling of tidal basins in response to a closure dam. *Marine Geology*, *439*, 106544. https://doi.org/10.1016/j.margeo.2021.106544

Colina Alonso, A., van Maren, D. S., Oost, A. P., Esselink, P., Lepper, R., Kösters, F., et al. (2024). A mud budget of the Wadden Sea and its implications for sediment management. *Communications Earth & Environment*, *5*(1), 153. https://doi.org/10.1038/s43247-024-01315-9

Conomos, T. J. (1979). San Francisco Bay: The urbanized estuary: Investigations into the natural history of San Francisco Bay and Delta with reference to the influence of man (no. 1977).

Dai, Z., Fagherazzi, S., Mei, X., Chen, J., & Meng, Y. (2016). Linking the infilling of the North Branch in the Changjiang (Yangtze) estuary to anthropogenic activities from 1958 to 2013. *Marine Geology*, *379*, 1–12. https://doi.org/10.1016/j.margeo.2016.05.006

Dai, Z.-j., Liu, J. T., Xie, H.-l., & Shi, W.-y. (2014). Sedimentation in the outer Hangzhou Bay, China: The influence of Changjiang sediment load. *Journal of Coastal Research*, *298*, 1218–1225. https://doi.org/10.2112/JCOASTRES-D-12-00164.1

D'Alpaos, A., Da Lio, C., & Marani, M. (2012). Biogeomorphology of tidal landforms: Physical and biological processes shaping the tidal landscape. *Ecohydrology*, *5*(5), 550–562. https://doi.org/10.1002/eco.279

Dalrymple, R. W., & Choi, K. (2007). Morphologic and facies trends through the fluvial-marine transition in tide-dominated depositional systems: A schematic framework for environmental and sequence-stratigraphic interpretation. *Earth-Science Reviews*, *81*(3–4), 135–174. https://doi.org/10.1016/j.earscirev.2006.10.002

Dam, G., van der Wegen, M., Taal, M., & van der Spek, A. (2022). Contrasting behaviour of sand and mud in a long-term sediment budget of the Western Scheldt estuary. *Sedimentology*, *69*(5), 2267–2283. https://doi.org/10.1111/sed.12992

de Jonge, V. N., Schuttelaars, H. M., van Beusekom, J. E., Talke, S. A., & de Swart, H. E. (2014). The influence of channel deepening on estuarine turbidity levels and dynamics, as exemplified by the Ems estuary. *Estuarine, Coastal and Shelf Science*, *139*, 46–59. https://doi.org/10.1016/j.ecss.2013.12.030

de Kraker, A. M. (2015). Flooding in river mouths: Human caused or natural events? Five centuries of flooding events in the SW Netherlands, 1500–2000. *Hydrology and Earth System Sciences*, *19*(6), 2673–2684. https://doi.org/10.5194/hess-19-2673-2015

Dellwig, O., Hinrichs, J., Hild, A., & Brumsack, H. J. (2000). Changing sedimentation in tidal flat sediments of the southern North Sea from the Holocene to the present: A geochemical approach. *Journal of Sea Research*, *44*(3–4), 195–208. https://doi.org/10.1016/s1385-1101(00)00051-4

Dijkstra, Y. M., Schuttelaars, H. M., Schramkowski, G. P., & Brouwer, R. L. (2019). Modeling the transition to high sediment concentrations as a response to channel deepening in the Ems River Estuary. *Journal of Geophysical Research: Oceans*, *124*(3), 1578–1594. https://doi.org/10.1029/2018jc014367

Ding, Y., & Wei, H. (2017). Modeling the impact of land reclamation on storm surges in Bohai Sea, China. *Natural Hazards*, *85*(1), 559–573. https://doi.org/10.1007/s11069-016-2586-4

Disney, L. P., & Overshiner, W. H. (1925). Tides and currents in San Francisco Bay. *Special Publication No 115. Dep. Comm., US Coast and Geod. Survey*, *121*.

Dronkers, J. (1986). Tidal asymmetry and estuarine morphology. *Netherlands Journal of Sea Research*, *20*(2–3), 117–131. https://doi.org/10.1016/0077-7579(86)90036-0

Dronkers, J. (2016). *Dynamics of coastal systems* (Vol. 41, 2nd edn). World Scientific.

Dronkers, J., & Scheffers, M. B. A. M. (1998). Morphodynamics of the Dutch Delta. In *Physics of estuaries and coastal seas, physics of estuaries and coastal seas, international biennial conference; 8th, Physics of estuaries and coastal seas* (pp. 297–304). A A Balkema. Retrieved from https://www.tib.eu/de/suchen/id/BLCP%3ACN027817695

Du, J., Shi, B., Li, J., & Wang, Y. P. (2019). Muddy Coast off Jiangsu, China: Physical, ecological, and anthropogenic processes. In *Sediment dynamics of Chinese muddy coasts and estuaries* (pp. 25–49). Elsevier. https://doi.org/10.1016/B978-0-12-811977-8.00003-0

Dykstra, S. L., Talke, S. A., Yankovsky, A. E., Torres, R., & Viparelli, E. (2024). Reflection of storm surge and tides in convergent estuaries with dams, the case of Charleston, USA. *Journal of Geophysical Research: Oceans*, *129*(9), e2023JC020498. https://doi.org/10.1029/2023jc020498

Elias, E. P., Colina Alonso, A., & van Maren, D. S. (2021). Morfologische veranderingen Eems-Dollard en Groninger wad. Deltares report.

Elias, E. P., Stive, M., Bonekamp, H., & Cleveringa, J. (2003). Tidal inlet dynamics in response to human intervention. *Coastal Engineering Journal*, *45*(4), 629–658. https://doi.org/10.1142/s0578563403000932

Elias, E. P., Van Der Spek, A., Wang, Z., & De Ronde, J. (2012). Morphodynamic development and sediment budget of the Dutch Wadden Sea over the last century. *Netherlands Journal of Geosciences - Geologie en Mijnbouw*, *91*(3), 293–310. https://doi.org/10.1017/S0016774600000457

Elias, E. P., Van Der Spek, A. J., & Lazar, M. (2017). The Voordelta, the contiguous ebb-tidal deltas in the SW Netherlands: Large-scale morphological changes and sediment budget 1965-2013; impacts of large-scale engineering. *Netherlands Journal of Geosciences*, *96*(3), 233–259. https://doi.org/10.1017/njg.2016.37

Elias, E. P., Van Der Spek, A. J. F., Wang, Z. B., Cleveringa, J., Jeuken, C. J. L., Taal, M., & Van Der Werf, J. J. (2023). Large-scale morphological changes and sediment budget of the Western Scheldt estuary 1955-2020: The impact of large-scale sediment management. *Netherlands Journal of Geosciences*, *102*, e12. https://doi.org/10.1017/njg.2023.11

Escoffier, F. F. (1940). The stability of tidal inlets. *Shore and Beach*, *8*(4), 114–115.

Escoffier, F. F. (1977). *Hydraulics and stability of tidal inlets* (Vol. 13). Waterways Experiment Station.

Fagherazzi, S. (2008). Self-organization of tidal deltas. *Proceedings of the National Academy of Sciences*, *105*(48), 18692–18695. https://doi.org/10.1073/pnas.0806668105

Fan, D., Tu, J., Shang, S., & Cai, G. (2014). Characteristics of tidal-bore deposits and facies associations in the Qiantang Estuary, China. *Marine Geology*, *348*, 1–14. https://doi.org/10.1016/j.margeo.2013.11.012

Feng, X., & Feng, H. (2021). On the role of anthropogenic activity and sea-level-rise in tidal distortion on the open coast of the yellow sea shelf. *Journal of Geophysical Research: Oceans*, *126*(3), e2020JC016583. https://doi.org/10.1029/2020jc016583

Figueroa, S. M., Lee, G.-h., Chang, J., Schieder, N. W., Kim, K., & Kim, S.-Y. (2020). Evaluation of along-channel sediment flux gradients in an anthropocene estuary with an estuarine dam. *Marine Geology*, *429*, 106318. https://doi.org/10.1016/j.margeo.2020.106318

Figueroa, S. M., & Son, M. (2024). Estuarine dams and weirs: Global analysis and synthesis. *Marine Geology*, *477*, 107388. https://doi.org/10.1016/j.margeo.2024.107388

Fluet-Chouinard, E., Stocker, B. D., Zhang, Z., Malhotra, A., Melton, J. R., Poulter, B., et al. (2023). Extensive global wetland loss over the past three centuries. *Nature*, *614*(7947), 281–286. https://doi.org/10.1038/s41586-022-05572-6

Flemming, B. W., & Davis, R., Jr. (1994). Holocene evolution, morphodynamics and sedimentology of the Spiekeroog barrier island system (southern North Sea). *Senckenbergiana Maritima*, *24*, 117–155.
Flemming, B. W., & Nyandwi, N. (1994). Land reclamation as a cause of fine-grained sediment depletion in backbarrier tidal flats (Southern North Sea). *Netherlands Journal of Aquatic Ecology*, *28*(3–4), 299–307. https://doi.org/10.1007/BF02334198
Foxgrover, A. C., Higgins, S. A., Ingraca, M. K., Jaffe, B. E., & Smith, R. E. (2004). Deposition, erosion, and bathymetric change in south San Francisco Bay: 1858–1983. *US Geological Survey Open-File Report*, *1192*, 25.
Fregoso, T. A., Foxgrover, A. C., & Jaffe, B. E. (2008). Sediment deposition, erosion, and bathymetric change in central San Francisco Bay: 1855-1979 (Vol. *1312*).
Friedrichs, C. T. (2010). Barotropic tides in channelized estuaries. In A. Valle-Levinson (Ed.), *Contemporary issues in estuarine physics* (1st ed., pp. 27–61). Cambridge University Press. https://doi.org/10.1017/CBO9780511676567.004
Friedrichs, C. T. (2011). Tidal flat morphodynamics. In *Treatise on estuarine and coastal science* (pp. 137–170). Elsevier. https://doi.org/10.1016/B978-0-12-374711-2.00307-7
Friedrichs, C. T., & Aubrey, D. G. (1988). Non-linear tidal distortion in shallow well-mixed estuaries: A synthesis. Estuarine. *Coastal and Shelf Science*, *27*(5), 521–545. https://doi.org/10.1016/0272-7714(88)90082-0
Friedrichs, C. T., & Aubrey, D. G. (1994). Tidal propagation in strongly convergent channels. *Journal of Geophysical Research*, *99*(C2), 3321–3336. https://doi.org/10.1029/93JC03219
Friedrichs, C. T., & Madsen, O. S. (1992). Nonlinear diffusion of the tidal signal in frictionally dominated embayments. *Journal of Geophysical Research*, *97*(C4), 5637–5650. https://doi.org/10.1029/92JC00354
Galloway, W. E. (1975). Process framework for describing the morphologic and stratigraphic evolution of deltaic depositional systems.
Gao, G. D., Wang, X. H., & Bao, X. W. (2014). Land reclamation and its impact on tidal dynamics in Jiaozhou Bay, Qingdao, China. Estuarine. *Coastal and Shelf Science*, *151*, 285–294. https://doi.org/10.1016/j.ecss.2014.07.017
Gao, G. D., Wang, X. H., Bao, X. W., Song, D., Lin, X. P., & Qiao, L. L. (2018). The impacts of land reclamation on suspended-sediment dynamics in Jiaozhou Bay, Qingdao, China. Estuarine. *Coastal and Shelf Science*, *206*, 61–75. https://doi.org/10.1016/j.ecss.2017.01.012
Gao, S. (2019). Chapter 10 - Geomorphology and sedimentology of tidal flats. In G. M. E. Perillo, E. Wolanski, D. R. Cahoon, & C. S. Hopkinson (Eds.), *Coastal wetlands* (2nd ed., pp. 359–381). Elsevier. https://doi.org/10.1016/B978-0-444-63893-9.00010-1
Gao, S., & Wang, Y. (2002). Sedimentary environment and tidal branch evolution characteristics of Jiaozhou Bay. *Advances in Marine Science*, *20*(3), 52–59.
Gatto, V. M., van Prooijen, B. C., & Wang, Z. B. (2017). Net sediment transport in tidal basins: Quantifying the tidal barotropic mechanisms in a unified framework. *Ocean Dynamics*, *67*(11), 1385–1406. https://doi.org/10.1007/s10236-017-1099-3
Gedan, K. B., Silliman, B., & Bertness, M. (2009). Centuries of human-driven change in Salt Marsh ecosystems. *Annual Review of Marine Science*, *1*(1), 117–141. https://doi.org/10.1146/annurev.marine.010908.163930
Geyer, W. R., & MacCready, P. (2014). The estuarine circulation. *Annual Review of Fluid Mechanics*, *46*(1), 175–197.
Gittman, R. K., Fodrie, F. J., Popowich, A. M., Keller, D. A., Bruno, J. F., Currin, C. A., et al. (2015). Engineering away our natural defenses: An analysis of shoreline hardening in the US. *Frontiers in Ecology and the Environment*, *13*(6), 301–307. https://doi.org/10.1890/150065
Grossinger, M. E. (1998). Bay area Ecoatlas v1.50b4 1998: Geographic information system of wetland habitats past and present. Retrieved from http://www.sfei.org/content/ecoatlas-version-150b4-1998
Guo, L., Xie, W., Xu, F., Wang, X., Zhu, C., Meng, Y., et al. (2022). A historical review of sediment export/import shift in the North Branch of Changjiang Estuary. *Earth Surface Processes and Landforms*, *47*(1), 5–16. https://doi.org/10.1002/esp.5084
Guo, L., Zhu, C., Xie, W., Xu, F., Wu, H., Wan, Y., et al. (2021). Changjiang Delta in the Anthropocene: Multi-scale hydro-morphodynamics and management challenges. *Earth-Science Reviews*, *223*, 103850. https://doi.org/10.1016/j.earscirev.2021.103850
Haigh, I. D., Pickering, M. D., Green, J. A. M., Arbic, B. K., Arns, A., Dangendorf, S., et al. (2020). The tides they are A-Changin': A comprehensive review of past and future nonastronomical changes in tides, their driving mechanisms, and future implications. *Reviews of Geophysics*, *58*(1), e2018RG000636. https://doi.org/10.1029/2018RG000636
Han, Z., Wang, H., Xie, H., Li, H., & Li, W. (2023). How does human activity shape the largest estuarine Bay of the Pearl River Estuary, south China (1964-2019). *Water*, *15*(23), 4143. https://doi.org/10.3390/w15234143
He, Q., & Silliman, B. R. (2019). Climate change, human impacts, and coastal ecosystems in the anthropocene. *Current Biology*, *29*(19), R1021–R1035. https://doi.org/10.1016/j.cub.2019.08.042
Hill, A. E. (1994). Fortnightly tides in a lagoon with variable choking. *Estuarine, Coastal and Shelf Science*, *38*(4), 423–434. https://doi.org/10.1006/ecss.1994.1029
Hoitink, A. J. F., Nittrouer, J. A., Passalacqua, P., Shaw, J. B., Langendoen, E. J., Huismans, Y., & Van Maren, D. S. (2020). Resilience of River deltas in the anthropocene. *Journal of Geophysical Research: Earth Surface*, *125*(3), e2019JF005201. https://doi.org/10.1029/2019JF005201
Hoitink, A. J. F., Wang, Z. B., Vermeulen, B., Huismans, Y., & Kastner, K. (2017). Tidal controls on river delta morphology. *Nature Geoscience*, *10*(9), 637–645. https://doi.org/10.1038/ngeo3000
Holleman, R. C., & Stacey, M. T. (2014). Coupling of sea level rise, tidal amplification, and inundation. *Journal of Physical Oceanography*, *44*(5), 1439–1455. https://doi.org/10.1175/jpo-d-13-0214.1
Hou, X., Xie, D., Feng, L., Shen, F., & Nienhuis, J. H. (2024). Sustained increase in suspended sediments near global river deltas over the past two decades. *Nature Communications*, *15*(1), 3319. https://doi.org/10.1038/s41467-024-47598-6
Hulskamp, R., Luijendijk, A., Van Maren, B., Moreno-Rodenas, A., Calkoen, F., Kras, E., et al. (2023). Global distribution and dynamics of muddy coasts. *Nature Communications*, *14*(1), 8259. https://doi.org/10.1038/s41467-023-43819-6
Inayatillah, A., Haigh, I. D., Brand, J. H., Francis, K., Mortley, A., Durrant, M., et al. (2022). Digitising historical sea level records in the Thames Estuary, UK. *Scientific Data*, *9*(1), 1–13. https://doi.org/10.1038/s41597-022-01223-7
Iwantoro, A. P., Van Der Vegt, M., & Kleinhans, M. G. (2020). Morphological evolution of bifurcations in tide-influenced deltas. *Earth Surface Dynamics*, *8*(2), 413–429. https://doi.org/10.5194/esurf-8-413-2020
Jaffe, B., & Foxgrover, A. (2006). Sediment deposition and erosion in South San Francisco Bay, California from 1956 to 2005. US Geological Survey Open-File Report, 1287.
Jaffe, B. E., Smith, R. E., & Foxgrover, A. C. (2007). Anthropogenic influence on sedimentation and intertidal mudflat change in San Pablo Bay, California: 1856-1983. *Estuarine, Coastal and Shelf Science*, *73*(1–2), 175–187. https://doi.org/10.1016/j.ecss.2007.02.017
Jay, D. A. (1991). Green's law revisited: Tidal long-wave propagation in channels with strong topography. *Journal of Geophysical Research*, *96*(C11), 20585–20598. https://doi.org/10.1029/91JC01633
Jia, L. W., Pan, S. Q., & Wu, C. Y. (2013). Effects of the anthropogenic activities on the morphological evolution of the Modaomen Estuary, Pearl River Delta, China. *China Ocean Engineering*, *27*(6), 795–808. https://doi.org/10.1007/s13344-013-0065-1

Jia, R., Lei, H., Hino, T., & Arulrajah, A. (2018). Environmental changes in Ariake Sea of Japan and their relationships with Isahaya Bay reclamation. *Marine Pollution Bulletin*, *135*, 832–844. https://doi.org/10.1016/j.marpolbul.2018.08.008

Jung, N. W., Lee, G.-H., Dellapenna, T. M., Jung, Y., Jo, T.-C., Chang, J., & Figueroa, S. M. (2024). Economic development drives massive global estuarine loss in the anthropocene. *Earth's Future*, *12*(4), e2023EF003691. https://doi.org/10.1029/2023EF003691

Kang, W.-U., Jo, J.-S., & Pak, S.-H. (2022). Influence of tidal flat reclamations on storm surge in the West Korean Bay of DPR Korea. *Journal of Coastal Conservation*, *26*(5), 49. https://doi.org/10.1007/s11852-022-00895-y

Kelleway, J. J., Cavanaugh, K., Rogers, K., Feller, I. C., Ens, E., Doughty, C., & Saintilan, N. (2017). Review of the ecosystem service implications of mangrove encroachment into salt marshes. *Global Change Biology*, *23*(10), 3967–3983. https://doi.org/10.1111/gcb.13727

Kennish, M. J. (2001). Anthropogenic impacts. In M. J. Kennish (Ed.), *Encyclopedia of estuaries* (pp. 29–35). Springer. https://doi.org/10.1007/978-94-017-8801-4_246

Kim, T., Choi, B., & Lee, S. (2006). Hydrodynamics and sedimentation induced by large-scale coastal developments in the Keum River Estuary, Korea. Estuarine. *Coastal and Shelf Science*, *68*(3–4), 515–528. https://doi.org/10.1016/j.ecss.2006.03.003

Kirezci, E., Young, I. R., Ranasinghe, R., Muis, S., Nicholls, R. J., Lincke, D., & Hinkel, J. (2020). Projections of global-scale extreme sea levels and resulting episodic coastal flooding over the 21st century. *Scientific Reports*, *10*(1), 11629. https://doi.org/10.1038/s41598-020-67736-6

Kirwan, M. L., & Megonigal, J. P. (2013). Tidal wetland stability in the face of human impacts and sea-level rise. *Nature*, *504*(7478), 53–60. https://doi.org/10.1038/nature12856

Klopman, G., & Meer, J. W. v. d. (1999). Random wave measurements in front of reflective structures. *Journal of Waterway, Port, Coastal, and Ocean Engineering*, *125*(1), 39–45. https://doi.org/10.1061/(asce)0733-950x(1999)125:1(39)

Knottnerus, O. S. (2005). History of human settlement, cultural change and interference with the marine environment. *Helgoland Marine Research*, *59*(1), 2–8. https://doi.org/10.1007/s10152-004-0201-7

Kragtwijk, N., Zitman, T., Stive, M., & Wang, Z. (2004). Morphological response of tidal basins to human interventions. *Coastal Engineering*, *51*(3), 207–221. https://doi.org/10.1016/j.coastaleng.2003.12.008

Latapy, A., Ferret, Y., Testut, L., Talke, S. A., Aarup, T., Pons, F., et al. (2023). Data rescue process in the context of sea level reconstructions: An overview of the methodology, lessons learned, up-to-date best practices and recommendations. *Geoscience Data Journal*, *10*(3), 396–425. https://doi.org/10.1002/gdj3.179

Lecart, M., Dobbelaere, T., Alaerts, L., Randresihaja, N. R., Mohammed, A. V., Vethamony, P., & Hanert, E. (2024). Land reclamation and its consequences: A 40-year analysis of water residence time in Doha Bay, Qatar. *PLoS One*, *19*(1), e0296715. https://doi.org/10.1371/journal.pone.0296715

Leuven, J. R., Niesten, I., Huismans, Y., Cox, J. R., Hulsen, L., van der Kaaij, T., & Hoitink, A. (2023). Peak water levels rise less than mean sea level in tidal channels subject to depth convergence by deepening. *Journal of Geophysical Research: Oceans*, *128*(4), e2022JC019578. https://doi.org/10.1029/2022jc019578

Leuven, J. R., van Keulen, D., Nienhuis, J., Canestrelli, A., & Hoitink, A. (2021). Large-scale scour in response to tidal dominance in estuaries. *Journal of Geophysical Research: Earth Surface*, *126*(5), e2020JF006048. https://doi.org/10.1029/2020jf006048

Li, C., Schuttelaars, H. M., Roos, P. C., Damveld, J. H., Gong, W., & Hulscher, S. J. (2016). Influence of retention basins on tidal dynamics in estuaries: Application to the Ems estuary. *Ocean & Coastal Management*, *134*, 216–225. https://doi.org/10.1016/j.ocecoaman.2016.10.010

Li, L., Guan, W., He, Z., Yao, Y., & Xia, Y. (2017). Responses of water environment to tidal flat reduction in Xiangshan Bay: Part II locally resuspended sediment dynamics. *Estuarine, Coastal and Shelf Science*, *198*, 114–127. https://doi.org/10.1016/j.ecss.2017.08.042

Li, L., Guan, W., Hu, J., Cheng, P., & Wang, X. H. (2018). Responses of water environment to tidal flat reduction in Xiangshan Bay: Part I hydrodynamics. *Estuarine, Coastal and Shelf Science*, *206*, 14–26. https://doi.org/10.1016/j.ecss.2017.11.003

Li, L., Ye, T., Wang, X. H., He, Z., & Shao, M. (2019). Changes in the hydrodynamics of Hangzhou Bay due to land reclamation in the past 60 years. In *Sediment dynamics of Chinese muddy coasts and estuaries* (pp. 77–93). Elsevier. https://doi.org/10.1016/B978-0-12-811977-8.00005-4

Li, W., Zhang, Y., Hu, P., Chen, F., & He, Z. (2024). Evolutions of hydrodynamics and sediment transport pattern in the Qiantang estuary (China) in response to multidecadal embankment constructions. *Estuarine, Coastal and Shelf Science*, *309*, 108965. https://doi.org/10.1016/j.ecss.2024.108965

Li, X., Bellerby, R., Craft, C., & Widney, S. E. (2018). Coastal wetland loss, consequences, and challenges for restoration. *Anthropocene Coasts*, *1*(1), 1–15. https://doi.org/10.1139/anc-2017-0001

Liang, H., Kuang, C., Olabarrieta, M., Song, H., Ma, Y., Dong, Z., et al. (2018). Morphodynamic responses of Caofeidian channel-shoal system to sequential large-scale land reclamation. *Continental Shelf Research*, *165*, 12–25. https://doi.org/10.1016/j.csr.2018.06.004

Liu, X. J., Gao, S., & Wang, Y. P. (2011). Modeling profile shape evolution for accreting tidal flats composed of mud and sand: A case study of the central Jiangsu coast, China. *Continental Shelf Research*, *31*(16), 1750–1760. https://doi.org/10.1016/j.csr.2011.08.002

Liu, Y., Ma, C., Fan, D., Sun, Q., Chen, J., Li, M., & Chen, Z. (2018). The Holocene environmental evolution of the inner Hangzhou Bay and its significance. *Journal of Ocean University of China*, *17*(6), 1301–1308. https://doi.org/10.1007/s11802-018-3562-2

Liu, Y., Xia, X., Wang, X., Cai, T., & Zheng, J. (2024). Human-induced rapid siltation within a macro-tidal bay during past decades. *Frontiers in Marine Science*, *11*, 1325003. https://doi.org/10.3389/fmars.2024.1325003

Liu, Z., Fagherazzi, S., Liu, X., Shao, D., Miao, C., Cai, Y., et al. (2022). Long-term variations in water discharge and sediment load of the Pearl River Estuary: Implications for sustainable development of the Greater Bay area. *Frontiers in Marine Science*, *9*, 983517. https://doi.org/10.3389/fmars.2022.983517

Lyu, H., Song, D., Zhang, S., Wu, W., & Bao, X. (2022). Compound effect of land reclamation and land-based pollutant input on water quality in Qinzhou Bay, China. *Science of the Total Environment*, *826*, 154183. https://doi.org/10.1016/j.scitotenv.2022.154183

MacCready, P., & Geyer, W. R. (2010). Advances in estuarine physics. *Annual Review of Marine Science*, *2*(1), 35–58. https://doi.org/10.1146/annurev-marine-120308-081015

Mai, S., & Bartholomä, A. (2000). The missing mud flats of the Wadden Sea: A reconstruction of sediments and accommodation space lost in the wake of land reclamation. *Proceedings in Marine Science*, *2*, 257–272. https://doi.org/10.1016/s1568-2692(00)80021-2

Martín-Antón, M., Negro, V., del Campo, J. M., López-Gutiérrez, J. S., & Esteban, M. D. (2016). Review of coastal land reclamation situation in the world. *Journal of Coastal Research*, *75*(75), 667–671. https://doi.org/10.2112/si75-133.1

Martins, D., Alves da Silva, A., Duarte, J., Canário, J., & Vieira, G. (2023). Changes in vessel traffic disrupt tidal flats and saltmarshes in the Tagus Estuary, Portugal. *Estuaries and Coasts*, *46*(5), 1141–1156. https://doi.org/10.1007/s12237-023-01198-7

MBSDMP. (2020). *Manila bay sustainable development master plan: Manilla bay atlas* (p. 296). National Economic and Development Authority.

McGranahan, G., Balk, D., & Anderson, B. (2007). The rising tide: Assessing the risks of climate change and human settlements in low elevation coastal zones. *Environment and Urbanization*, *19*(1), 17–37. https://doi.org/10.1177/0956247807076960

McGranahan, G., Balk, D., Colenbrander, S., Engin, H., & MacManus, K. (2023). Is rapid urbanization of low-elevation deltas undermining adaptation to climate change? A global review. *Environment and Urbanization*, *35*(2), 527–559. https://doi.org/10.1177/09562478231192176
McLoughlin, L. C. (2000). Shaping Sydney harbour: Sedimentation, dredging and reclamation 1788-1990s. *Australian Geographer*, *31*(2), 183–208. https://doi.org/10.1080/713612246
Missiaen, T., Jongepier, I., Heirman, K., Soens, T., Gelorini, V., Verniers, J., et al. (2017). Holocene landscape evolution of an estuarine wetland in relation to its human occupation and exploitation: Waasland scheldt polders, northern Belgium. *Netherlands Journal of Geosciences*, *96*(1), 35–62. https://doi.org/10.1017/njg.2016.24
Mol, G. (1995). De Westerschelde: Een resultaat van menselijke ingrepen. *Rijkswaterstaat Rijksinstituut voor Kust en Zee Directie Zeeland*.
Morris, R. (2013). Geomorphological analogues for large estuarine engineering projects: A case study of barrages, causeways and tidal energy projects. *Ocean & Coastal Management*, *79*, 52–61. https://doi.org/10.1016/j.ocecoaman.2012.05.010
Morris, R., & Mitchell, S. (2013). Has loss of accommodation space in the Humber Estuary led to elevated suspended sediment concentrations? *Journal of Frontiers in Construction Engineering*, *2*, 1–9.
Murray, N. J., Clemens, R. S., Phinn, S. R., Possingham, H. P., & Fuller, R. A. (2014). Tracking the rapid loss of tidal wetlands in the Yellow Sea. *Frontiers in Ecology and the Environment*, *12*(5), 267–272. https://doi.org/10.1890/130260
Murray, N. J., Worthington, T. A., Bunting, P., Duce, S., Hagger, V., Lovelock, C. E., et al. (2022). High-resolution mapping of losses and gains of Earth's tidal wetlands. *Science*, *376*(6594), 744–749. https://doi.org/10.1126/science.abm9583
Neumann, B., Vafeidis, A. T., Zimmermann, J., & Nicholls, R. J. (2015). Future coastal population growth and exposure to sea-level rise and coastal flooding - A global assessment. *PLoS One*, *10*(3), e0118571. https://doi.org/10.1371/journal.pone.0118571
Niemeyer, H. D. (1995). Long-term morphodynamical development of the east Frisian Islands and Coast. In *Coastal engineering 1994* (pp. 2417–2433). Kobe, Japan: American Society of Civil Engineers. https://doi.org/10.1061/9780784400890.176
Ningsih, N. S., Hanifah, F., Yani, L. F., & Rachmayani, R. (2024). Simulated response of seawater elevation and tidal dynamics in Jakarta Bay to coastal reclamation. *Ocean Dynamics*, *74*(3), 211–221. https://doi.org/10.1007/s10236-024-01598-8
Nnafie, A., De Swart, H. E., De Maerschalck, B., Van Oyen, T., Van Der Vegt, M., & Van Der Wegen, M. (2019). Closure of secondary basins causes channel deepening in estuaries with moderate to high friction. *Geophysical Research Letters*, *46*(22), 13209–13216. https://doi.org/10.1029/2019GL084444
Okada, T., Nakayama, K., Takao, T., & Furukawa, K. (2011). Influence of freshwater input and bay reclamation on long-term changes in seawater residence times in Tokyo bay, Japan. *Hydrological Processes*, *25*(17), 2694–2702. https://doi.org/10.1002/hyp.8010
Olds, A. D., Nagelkerken, I., Huijbers, C. M., Gilby, B. L., Pittman, S. J., & Schlacher, T. A. (2018). Connectivity in coastal seascapes. *Seascape Ecology*, 261–292.
Oost, A., Hoekstra, P., Wiersma, A., Flemming, B. W., Lammerts, E., Pejrup, M., et al. (2012). Barrier island management: Lessons from the past and directions for the future. *Ocean & Coastal Management*, *68*, 18–38. https://doi.org/10.1016/j.ocecoaman.2012.07.010
Oost, A. P. (1995). Dynamics and sedimentary development of the Dutch Wadden Sea with emphasis on the Frisian inlet; a study of the barrier islands, ebb-tidal deltas and drainage basins. *Geologica Ultraiectina*, *126*, 518.
Orton, P. M., Sanderson, E. W., Talke, S. A., Giampieri, M., & MacManus, K. (2020). Storm tide amplification and habitat changes due to urbanization of a lagoonal estuary. *Natural Hazards and Earth System Sciences*, *20*(9), 2415–2432. https://doi.org/10.5194/nhess-20-2415-2020
Pan, L., Ding, P., & Ge, J. (2012). Impacts of deep waterway project on morphological changes within the north passage of the Changjiang estuary, China. *Journal of Coastal Research*, *28*(5), 1165–1176. https://doi.org/10.2112/jcoastres-d-11-00129.1
Parejaroman, L. F., Orton, P. M., & Talke, S. A. (2023). Effect of Estuary urbanization on tidal dynamics and high tide flooding in a coastal lagoon. *Journal of Geophysical Research: Oceans*, *128*(1), e2022JC018777. https://doi.org/10.1029/2022JC018777
Paszkowski, A., Goodbred, S., Borgomeo, E., Khan, M. S. A., & Hall, J. W. (2021). Geomorphic change in the Ganges-Brahmaputra-Meghna delta. *Nature Reviews Earth & Environment*, *2*(11), 763–780. https://doi.org/10.1038/s43017-021-00213-4
Pelling, H., Uehara, K., & Green, J. M. (2013). The impact of rapid coastline changes and sea level rise on the tides in the Bohai sea, China. *Journal of Geophysical Research: Oceans*, *118*(7), 3462–3472. https://doi.org/10.1002/jgrc.20258
Pierik, H. J. (2021). Landscape changes and human-landscape interaction during the first millennium AD in the Netherlands. *Netherlands Journal of Geosciences*, *100*, e11. https://doi.org/10.1017/njg.2021.8
Postma, H. (1961). Transport and accumulation of suspended matter in the Dutch Wadden Sea. *Netherlands Journal of Sea Research*, *1*(1–2), 148–190. https://doi.org/10.1016/0077-7579(61)90004-7
Qiao, L., Liang, S., Song, D., Wu, W., & Wang, X. H. (2019). Jiaozhou Bay. In x. h. Wang (Ed.), *Sediment dynamics of Chinese muddy coasts and estuaries* (pp. 5–23). Elsevier. https://doi.org/10.1016/B978-0-12-811977-8.00002-9
Reise, K. (2005). Coast of change: Habitat loss and transformations in the Wadden Sea. *Helgoland Marine Research*, *59*(1), 9–21. https://doi.org/10.1007/s10152-004-0202-6
Rijkswaterstaat. (2021). Morfologische veranderingen: Duurzame bescherming en ontwikkeling van dynamische Waddenzeenatuur. *Brochure NN1221ZB003*.
Roberts, W., Le Hir, P., & Whitehouse, R. (2000). Investigation using simple mathematical models of the effect of tidal currents and waves on the profile shape of intertidal mudflats. *Continental Shelf Research*, *20*(10–11), 1079–1097. https://doi.org/10.1016/s0278-4343(00)00013-3
Rusdiansyah, A., Tang, Y., He, Z., Li, L., Ye, Y., & Yahya Surya, M. (2018). The impacts of the large-scale hydraulic structures on tidal dynamics in open-type bay: Numerical study in Jakarta Bay. *Ocean Dynamics*, *68*(9), 1141–1154. https://doi.org/10.1007/s10236-018-1183-3
Scarpa, G. M., Zaggia, L., Manfè, G., Lorenzetti, G., Parnell, K., Soomere, T., et al. (2019). The effects of ship wakes in the Venice lagoon and implications for the sustainability of shipping in coastal waters. *Scientific Reports*, *9*(1), 19014. https://doi.org/10.1038/s41598-019-55238-z
Schrijvershof, R., Van Maren, D. S., van der Wegen, M., & Hoitink, A. (2024). Land reclamation controls multi-centennial evolution of the Ems estuary. *Earth's Future*, *12*(11). https://doi.org/10.1029/2024ef005080
Schuttelaars, H. M., de Jonge, V. N., & Chernetsky, A. (2013). Improving the predictive power when modelling physical effects of human interventions in estuarine systems. *Ocean & Coastal Management*, *79*, 70–82. https://doi.org/10.1016/j.ocecoaman.2012.05.009
Sengupta, D., Choi, Y. R., Tian, B., Brown, S., Meadows, M., Hackney, C. R., et al. (2023). Mapping 21st century global coastal land reclamation. *Earth's Future*, *11*(2), e2022EF002927. https://doi.org/10.1029/2022EF002927
Shen, C., Shi, H., Zheng, W., Li, F., Peng, S., & Ding, D. (2016). Study on the cumulative impact of reclamation activities on ecosystem health in coastal waters. *Marine Pollution Bulletin*, *103*(1–2), 144–150. https://doi.org/10.1016/j.marpolbul.2015.12.028
Shen, S. (2003). Tidal bore in the north branch of the Changjiang estuary. In *Proceedings of the international conference on estuaries and coasts, Hangzhou, China* (pp. 8–11).
Shi, J., Li, G., & Wang, P. (2011). Anthropogenic influences on the tidal prism and water exchanges in Jiaozhou Bay, Qingdao, China. *Journal of Coastal Research*, *27*, 57–72. https://doi.org/10.2112/JCOASTRES-D-09-00011.1

Shi, P., Yang, W., Xu, X., & Zhang, F. (2024). Response of hydrodynamic environment to land reclamation in Sanmen Bay, China over the last half-century. *Frontiers in Marine Science*, *11*, 1448565. https://doi.org/10.3389/fmars.2024.1448565
Shi, Y., Huang, C., Shi, S., & Gong, J. (2022). Tracking of land reclamation activities using landsat observations: an example in Shanghai and Hangzhou Bay. *Remote Sensing*, *14*(3), 464. https://doi.org/10.3390/rs14030464
Siemes, R. W. A., Duong, T. M., Willemsen, P. W. J. M., Borsje, B. W., & Hulscher, S. J. M. H. (2023). Morphological response of a highly engineered Estuary to altering channel depth and restoring wetlands. *Journal of Marine Science and Engineering*, *11*(11), 2150. https://doi.org/10.3390/jmse11112150
Siggers, G., Spearman, J., Littlewood, M., & Donovan, B. (2006). One hundred years of morphological change in the Thames estuary. Impacts on tide levels and implications for flood risk management to 2100.
Siringan, F., & Ringor, C. (1998). Changes in bathymetry and their implications to sediment dispersal and rates of sedimentation in Manila Bay. *Science Diliman*, *10*(2), 12–26.
Smith, L., Cornillon, P., Rudnickas, D., & Mouw, C. B. (2019). Evidence of environmental changes caused by Chinese island-building. *Scientific Reports*, *9*(1), 5295. https://doi.org/10.1038/s41598-019-41659-3
Smolders, S., Plancke, Y., Ides, S., Meire, P., & Temmerman, S. (2015). Role of intertidal wetlands for tidal and storm tide attenuation along a confined estuary: A model study. *Natural Hazards and Earth System Sciences*, *15*(7), 1659–1675. https://doi.org/10.5194/nhess-15-1659-2015
Song, D., Wang, X. H., Zhu, X., & Bao, X. (2013). Modeling studies of the far-field effects of tidal flat reclamation on tidal dynamics in the east China seas. *Estuarine, Coastal and Shelf Science*, *133*, 147–160. https://doi.org/10.1016/j.ecss.2013.08.023
Speer, P., & Aubrey, D. (1985). A study of non-linear tidal propagation in shallow inlet/estuarine systems part ii: Theory. *Estuarine, Coastal and Shelf Science*, *21*(2), 207–224. https://doi.org/10.1016/0272-7714(85)90097-6
Spencer, T., Schuerch, M., Nicholls, R. J., Hinkel, J., Lincke, D., Vafeidis, A., et al. (2016). Global coastal wetland change under sea-level rise and related stresses: The DIVA Wetland Change Model. *Global and Planetary Change*, *139*, 15–30. https://doi.org/10.1016/j.gloplacha.2015.12.018
Stark, J., Smolders, S., Meire, P., & Temmerman, S. (2017). Impact of intertidal area characteristics on estuarine tidal hydrodynamics: A modelling study for the Scheldt Estuary. *Estuarine, Coastal and Shelf Science*, *198*, 138–155. https://doi.org/10.1016/j.ecss.2017.09.004
Stark, J., van Oyen, T., Meire, P., & Temmerman, S. (2016). Observations of tidal propagation and storm surge attenuation in a large tidal marsh. In *Effects of intertidal ecosystems on estuarine hydrodynamics and flood wave attenuation: A multi-scale study* (Vol. 21).
Subraelu, P., Ebraheem, A. A., Sherif, M., Sefelnasr, A., Yagoub, M., & Rao, K. N. (2022). Land in water: The study of land reclamation and artificial islands formation in the UAE coastal zone: A remote sensing and GIS perspective. *Land*, *11*(11), 2024. https://doi.org/10.3390/land11112024
Sun, Z.-l., Huang, S.-j., Jiao, J.-g., Nie, H., & Lu, M. (2017). Effects of cluster land reclamation projects on storm surge in Jiaojiang Estuary. *China. Water Science and Engineering*, *10*(1), 59–69. https://doi.org/10.1016/j.wse.2017.03.003
Swanson, R. L., & Wilson, R. E. (2008). Increased tidal ranges coinciding with Jamaica Bay development contribute to marsh flooding. *Journal of Coastal Research*, *24*(6), 1565–1569. https://doi.org/10.2112/07-0907.1
Syvitski, J. P. M., Ángel, J. R., Saito, Y., Overeem, I., Vörösmarty, C. J., Wang, H., & Olago, D. (2022). Earth's sediment cycle during the anthropocene. *Nature Reviews Earth & Environment*, *3*(3), 179–196. https://doi.org/10.1038/s43017-021-00253-w
Syvitski, J. P. M., & Kettner, A. (2011). Sediment flux and the Anthropocene. *Philosophical Transactions of the Royal Society A: Mathematical, Physical and Engineering Sciences*, *369*(1938), 957–975. https://doi.org/10.1098/rsta.2010.0329
Syvitski, J. P. M., Kettner, A. J., Overeem, I., Hutton, E. W. H., Hannon, M. T., Brakenridge, G. R., et al. (2009). Sinking deltas due to human activities. *Nature Geoscience*, *2*(10), 681–686. https://doi.org/10.1038/ngeo629
Syvitski, J. P. M., VÃrÃsmarty, C. J., Kettner, A. J., & Green, P. (2005). Impact of humans on the flux of terrestrial sediment to the global coastal ocean. *Science*, *308*(5720), 376–380. https://doi.org/10.1126/science.1109454
Talke, S. A., & Jay, D. A. (2013). Nineteenth century North American and Pacific tidal data: Lost or just forgotten? *Journal of Coastal Research*, *29*(6a), 118–127. https://doi.org/10.2112/jcoastres-d-12-00181.1
Talke, S. A., & Jay, D. A. (2017). *Archival water-level measurements: Recovering historical data to help design for the future* (Vol. 8). Civil and Environmental Engineering Faculty Publications and Presentations.
Talke, S. A., & Jay, D. A. (2020). Changing tides: The role of natural and anthropogenic factors. *Annual Review of Marine Science*, *12*(1), 121–151. https://doi.org/10.1146/annurev-marine-010419-010727
Talke, S. A., Kemp, A., & Woodruff, J. (2018a). Relative sea level, tides, and extreme water levels in Boston harbor from 1825 to 2018. *Journal of Geophysical Research: Oceans*, *123*(6), 3895–3914. https://doi.org/10.1029/2017jc013645
Talke, S. A., Kemp, A. C., & Woodruff, J. (2018b). Relative sea level, tides, and extreme water levels in Boston Harbor from 1825 to 2018. *Journal of Geophysical Research: Oceans*, *123*(6), 3895–3914. https://doi.org/10.1029/2017JC013645
Temmerman, S., Horstman, E. M., Krauss, K. W., Mullarney, J. C., Pelckmans, I., & Schoutens, K. (2023). Marshes and mangroves as nature-based coastal storm buffers. *Annual Review of Marine Science*, *15*(1), 95–118. https://doi.org/10.1146/annurev-marine-040422-092951
Temmerman, S., Meire, P., Bouma, T. J., Herman, P. M. J., Ysebaert, T., & De Vriend, H. J. (2013). Ecosystem-based coastal defence in the face of global change. *Nature*, *504*(7478), 79–83. https://doi.org/10.1038/nature12859
Tessler, Z. D., Vörösmarty, C. J., Grossberg, M., Gladkova, I., Aizenman, H., Syvitski, J. P. M., & Foufoula-Georgiou, E. (2015). Profiling risk and sustainability in coastal deltas of the world. *Science*, *349*(6248), 638–643. https://doi.org/10.1126/science.aab3574
Tonis, I., Stam, J., & Van De Graaf, J. (2002). Morphological changes of the Haringvliet estuary after closure in 1970. *Coastal Engineering*, *44*(3), 191–203. https://doi.org/10.1016/S0378-3839(01)00026-6
Traini, C., Proust, J.-N., Menier, D., & Mathew, M. (2015). Distinguishing natural evolution and human impact on estuarine morpho-sedimentary development: A case study from the Vilaine Estuary, France. Estuarine. *Coastal and Shelf Science*, *163*, 143–155. https://doi.org/10.1016/j.ecss.2015.06.025
Tu, J., & Fan, D. (2017). Flow and turbulence structure in a hypertidal estuary with the world's biggest tidal bore. *Journal of Geophysical Research: Oceans*, *122*(4), 3417–3433. https://doi.org/10.1002/2016jc012120
Van der Spek, A. (1995). Reconstruction of tidal inlet and channel dimensions in the Frisian Middelzee, a former tidal basin in the Dutch Wadden Sea. *Special Publication of the International Association of Sedimentologists*, *24*, 239–258.
van der Spek, A. (1997). Tidal asymmetry and long-term evolution of Holocene tidal basins in the Netherlands: Simulation of palaeo-tides in the Schelde estuary. *Marine Geology*, *141*(1–4), 71–90. https://doi.org/10.1016/S0025-3227(97)00064-9
Van Der Spek, A. J., & Elias, E. P. (2021). Half a century of morphological change in the Haringvliet and Grevelingen ebb-tidal deltas (SW Netherlands) - Impacts of large-scale engineering 1964-2015. *Marine Geology*, *432*, 106404. https://doi.org/10.1016/j.margeo.2020.106404
Van Der Wal, D., Pye, K., & Neal, A. (2002). Long-term morphological change in the Ribble Estuary, northwest England. *Marine Geology*, *189*(3–4), 249–266. https://doi.org/10.1016/S0025-3227(02)00476-0

van der Wegen, M. (2013). Numerical modeling of the impact of sea level rise on tidal basin morphodynamics. *Journal of Geophysical Research: Earth Surface*, *118*(2), 447–460. https://doi.org/10.1002/jgrf.20034

Van Goor, M., Zitman, T., Wang, Z., & Stive, M. (2003). Impact of sea-level rise on the morphological equilibrium state of tidal inlets. *Marine Geology*, *202*(3–4), 211–227. https://doi.org/10.1016/s0025-3227(03)00262-7

van Maren, D., Alonso, A., Engels, A., Vandenbruwaene, W., De Vet, P., Vroom, J., & Wang, Z. B. (2023). Adaptation timescales of estuarine systems to human interventions. *Frontiers in Earth Science*, *11*, 1111530. https://doi.org/10.3389/feart.2023.1111530

van Maren, D., Beemster, J., Wang, Z., Khan, Z., Schrijvershof, R., & Hoitink, A. (2023). Tidal amplification and river capture in response to land reclamation in the Ganges-Brahmaputra delta. *Catena*, *220*, 106651. https://doi.org/10.1016/j.catena.2022.106651

van Maren, D., Oost, A., Wang, Z., & Vos, P. (2016). The effect of land reclamations and sediment extraction on the suspended sediment concentration in the Ems Estuary. *Marine Geology*, *376*, 147–157. https://doi.org/10.1016/j.margeo.2016.03.007

van Maren, D., Van Kessel, T., Cronin, K., & Sittoni, L. (2015). The impact of channel deepening and dredging on estuarine sediment concentration. *Continental Shelf Research*, *95*, 1–14. https://doi.org/10.1016/j.csr.2014.12.010

van Maren, D., Winterwerp, J., & Vroom, J. (2015). Fine sediment transport into the hyper-turbid lower Ems River: The role of channel deepening and sediment-induced drag reduction. *Ocean Dynamics*, *65*(4), 589–605. https://doi.org/10.1007/s10236-015-0821-2

Van Proosdij, D., Milligan, T., Bugden, G., & Butler, K. (2009). A tale of two macro tidal estuaries: Differential morphodynamic response of the intertidal zone to causeway construction. *Journal of Coastal Research*, 772–776.

van Rijn, L., Grasmeijer, B., & Perk, L. (2018). Effect of channel deepening on tidal flow and sediment transport: Part I—Sandy channels. *Ocean Dynamics*, *68*(11), 1457–1479. https://doi.org/10.1007/s10236-018-1204-2

Van Zelst, V. T. M., Dijkstra, J. T., Van Wesenbeeck, B. K., Eilander, D., Morris, E. P., Winsemius, H. C., et al. (2021). Cutting the costs of coastal protection by integrating vegetation in flood defences. *Nature Communications*, *12*(1), 6533. https://doi.org/10.1038/s41467-021-26887-4

Vermeersen, B. L., Slangen, A. B., Gerkema, T., Baart, F., Cohen, K. M., Dangendorf, S., et al. (2018). Sea-level change in the Dutch Wadden Sea. *Netherlands Journal of Geosciences*, *97*(3), 79–127. https://doi.org/10.1017/njg.2018.7

Vos, P. (2015). *Origin of the Dutch coastal landscape: Long-term landscape evolution of the Netherlands during the holocene, described and visualized in national, regional and local palaeogeographical map series* (PhD thesis). Utrecht University.

Vos, P., & Knol, E. (2015). Holocene landscape reconstruction of the Wadden Sea area between Marsdiep and Weser: Explanation of the coastal evolution and visualisation of the landscape development of the northern Netherlands and Niedersachsen in five palaeogeographical maps from 500 BC to present. *Netherlands Journal of Geosciences - Geologie en Mijnbouw*, *94*(2), 157–183. https://doi.org/10.1017/njg.2015.4

Vroom, J., Elias, E. P., Lescinski, J., & Wang, Z. B. (2012). Assessment of the effects of the Zuider Sea closure on the hydrodynamics of the Wadden Sea inlets. In *Proceedings of the 33rd international conference on coastal engineering 2012*.

Walling, D. (2006). Human impact on land–ocean sediment transfer by the world's rivers. *Geomorphology*, *79*(3–4), 192–216. https://doi.org/10.1016/j.geomorph.2006.06.019

Wang, H., Zhang, P., Hu, S., Cai, H., Fu, L., Liu, F., & Yang, Q. (2020). Tidal regime shift in Lingdingyang Bay, the Pearl River Delta: An identification and assessment of driving factors. *Hydrological Processes*, *34*(13), 2878–2894. https://doi.org/10.1002/hyp.13773

Wang, J., Hong, H., Zhou, L., Hu, J., & Jiang, Y. (2013). Numerical modeling of hydrodynamic changes due to coastal reclamation projects in Xiamen Bay, China. *Chinese Journal of Oceanology and Limnology*, *31*(2), 334–344. https://doi.org/10.1007/s00343-013-2109-z

Wang, X. (2002). Tide-induced sediment resuspension and the bottom boundary layer in an idealized estuary with a muddy bed. *Journal of Physical Oceanography*, *32*(11), 3113–3131. https://doi.org/10.1175/1520-0485(2002)032<3113:tisrat>2.0.co;2

Wang, X., Xiao, X., Xu, X., Zou, Z., Chen, B., Qin, Y., et al. (2021). Rebound in China's coastal wetlands following conservation and restoration. *Nature Sustainability*, *4*(12), 1076–1083. https://doi.org/10.1038/s41893-021-00793-5

Wang, Y., & Shen, J. (2020). A modeling study on the influence of sea-level rise and channel deepening on estuarine circulation and dissolved oxygen levels in the tidal James River, Virginia, USA. *Journal of Marine Science and Engineering*, *8*(11), 950. https://doi.org/10.3390/jmse8110950

Wang, Z. B., Elias, E. P., Van Der Spek, A. J., & Lodder, Q. J. (2018). Sediment budget and morphological development of the Dutch Wadden Sea: Impact of accelerated sea-level rise and subsidence until 2100. *Netherlands Journal of Geosciences*, *97*(3), 183–214. https://doi.org/10.1017/njg.2018.8

Wang, Z. B., Jeuken, C., & de Vriend, H. (1999). Tidal asymmetry and residual sediment transport in estuaries (Vol. *Z2749*).

Wei, X., Cai, S., Ni, P., & Zhan, W. (2020). Impacts of climate change and human activities on the water discharge and sediment load of the Pearl River, southern China. *Scientific Reports*, *10*(1), 16743. https://doi.org/10.1038/s41598-020-73939-8

Wei, X., Cai, S., & Zhan, W. (2021). Impact of anthropogenic activities on morphological and deposition flux changes in the Pearl River Estuary, China. *Scientific Reports*, *11*(1), 16643. https://doi.org/10.1038/s41598-021-96183-0

Weisscher, S. A., Baar, A. W., Van Belzen, J., Bouma, T. J., & Kleinhans, M. G. (2022). Transitional polders along estuaries: Driving land-level rise and reducing flood propagation. *Nature-Based Solutions*, *2*, 100022. https://doi.org/10.1016/j.nbsj.2022.100022

Williams, J. R., Dellapenna, T., Lee, G.-h., & Louchouarn, P. (2014). Sedimentary impacts of anthropogenic alterations on the Yeongsan Estuary, South Korea. *Marine Geology*, *357*, 256–271. https://doi.org/10.1016/j.margeo.2014.08.004

Williams, J. R., Dellapenna, T. M., & Lee, G.-h. (2013). Shifts in depositional environments as a natural response to anthropogenic alterations: Nakdong Estuary, South Korea. *Marine Geology*, *343*, 47–61. https://doi.org/10.1016/j.margeo.2013.05.010

Wilson, C., Goodbred, S., Small, C., Gilligan, J., Sams, S., Mallick, B., & Hale, R. (2017). Widespread infilling of tidal channels and navigable waterways in the human-modified tidal deltaplain of southwest Bangladesh. *Elementa: Science of the Anthropocene*, *5*, 78. https://doi.org/10.1525/elementa.263

Winterwerp, J. C. (2001). Stratification effects by cohesive and noncohesive sediment. *Journal of Geophysical Research*, *106*(C10), 22559–22574. https://doi.org/10.1029/2000JC000435

Winterwerp, J. C., Albers, T., Anthony, E. J., Friess, D. A., Manchego, A. G., Moseley, K., et al. (2020). Managing erosion of mangrove-mud coasts with permeable dams: Lessons learned. *Ecological Engineering*, *158*, 106078. https://doi.org/10.1016/j.ecoleng.2020.106078

Winterwerp, J. C., Borst, W. G., & De Vries, M. B. (2005). Pilot study on the erosion and rehabilitation of a mangrove mud Coast. *Journal of Coastal Research*, *212*, 223–230. https://doi.org/10.2112/03-832A.1

Winterwerp, J. C., Erftemeijer, P. L. A., Suryadiputra, N., Van Eijk, P., & Zhang, L. (2013). Defining eco-morphodynamic requirements for rehabilitating eroding mangrove-mud coasts. *Wetlands*, *33*(3), 515–526. https://doi.org/10.1007/s13157-013-0409-x

Winterwerp, J. C., Lely, M., & He, Q. (2009). Sediment-induced buoyancy destruction and drag reduction in estuaries. *Ocean Dynamics*, *59*(5), 781–791. https://doi.org/10.1007/s10236-009-0237-y

Winterwerp, J. C., Van Kessel, T., van Maren, D. S., & Van Prooijen, B. C. (2022). Fine sediment in open water: From fundamentals to modeling. *World Scientific*.

Winterwerp, J. C., & Wang, Z. B. (2013). Man-induced regime shifts in small estuaries I: Theory. *Ocean Dynamics*, *63*(11–12), 1279–1292. https://doi.org/10.1007/s10236-013-0662-9

Winterwerp, J. C., & Wang, Z.-B. (2021). Hydrosedimentological response to estuarine deepening: Conceptual analysis. *Journal of Waterway, Port, Coastal, and Ocean Engineering*, *147*(5), 04021023. https://doi.org/10.1061/(ASCE)WW.1943-5460.0000660

Winterwerp, J. C., Wang, Z. B., Van Braeckel, A., Van Holland, G., & Kosters, F. (2013). Man-induced regime shifts in small estuaries II: A comparison of rivers. *Ocean Dynamics*, *63*(11–12), 1293–1306. https://doi.org/10.1007/s10236-013-0663-8

Wolanski, E., Moore, K., Spagnol, S., D'adamo, N., & Pattiaratchi, C. (2001). Rapid, human-induced siltation of the macro-tidal Ord River Estuary, Western Australia. *Estuarine, Coastal and Shelf Science*, *53*(5), 717–732. https://doi.org/10.1006/ecss.2001.0799

Wu, S., Chen, R., & Meadows, M. E. (2019). Evolution of an estuarine Island in the Anthropocene: Complex dynamics of Chongming Island, Shanghai, P.R. China. *Sustainability*, *11*(24), 6921. https://doi.org/10.3390/su11246921

Wu, Z., Saito, Y., Zhao, D., Zhou, J., Cao, Z., Li, S., et al. (2016). Impact of human activities on subaqueous topographic change in Lingding Bay of the Pearl River Estuary, China, during 1955–2013. *Scientific Reports*, *6*(1), 37742. https://doi.org/10.1038/srep37742

Wu, Z., Zhou, C., Wang, P., & Fei, Z. (2023). Responses of tidal dynamic and water exchange capacity to coastline change in the Bohai Sea, China. *Frontiers in Marine Science*, *10*, 1118795. https://doi.org/10.3389/fmars.2023.1118795

Xie, D., Bing Wang, Z., Huang, J., & Zeng, J. (2022). River, tide and morphology interaction in a macro-tidal estuary with active morphological evolutions. *Catena*, *212*, 106131. https://doi.org/10.1016/j.catena.2022.106131

Xie, D., Chen, Y., Pan, C., Zhang, S., Wei, W., Wang, Z. B., et al. (2024). Response of suspended sediment dynamics to human activities in the transitional zone between Changjiang estuary and Hangzhou Bay. *Frontiers in Marine Science*, *11*, 1440754. https://doi.org/10.3389/fmars.2024.1440754

Xie, D., Pan, C., Wu, X., Gao, S., & Wang, Z. B. (2017). Local human activities overwhelm decreased sediment supply from the Changjiang River: Continued rapid accumulation in the Hangzhou Bay-Qiantang Estuary system. *Marine Geology*, *392*, 66–77. https://doi.org/10.1016/j.margeo.2017.08.013

Xu, C., Zhou, C., Ma, K., Wang, P., & Yue, X. (2021). Response of water environment to land reclamation in Jiaozhou Bay, China over the last 150 years. *Frontiers in Marine Science*, *8*, 750288. https://doi.org/10.3389/fmars.2021.750288

Xu, N., Ma, Y., Yang, J., Wang, X. H., Wang, Y., & Xu, R. (2022). Deriving tidal flat topography using ICESat-2 laser altimetry and Sentinel-2 imagery. *Geophysical Research Letters*, *49*(2), 1–10. https://doi.org/10.1029/2021GL096813

Xu, N., Wang, Y., Huang, C., Jiang, S., Jia, M., & Ma, Y. (2022). Monitoring coastal reclamation changes across Jiangsu Province during 1984-2019 using landsat data. *Marine Policy*, *136*, 104887. https://doi.org/10.1016/j.marpol.2021.104887

Yamaguchi, S., & Hayami, Y. (2018). Impact of Isahaya dike construction on DO concentration in the Ariake Sea. *Journal of Oceanography*, *74*(6), 565–586. https://doi.org/10.1007/s10872-017-0454-9

Yang, H., Yang, S., Xu, K., Milliman, J., Wang, H., Yang, Z., et al. (2018). Human impacts on sediment in the Yangtze River: A review and new perspectives. *Global and Planetary Change*, *162*, 8–17. https://doi.org/10.1016/j.gloplacha.2018.01.001

Yang, H.-Y., Chen, B., Barter, M., Piersma, T., Zhou, C.-F., Li, F.-S., & Zhang, Z.-W. (2011). Impacts of tidal land reclamation in Bohai Bay, China: Ongoing losses of critical Yellow Sea waterbird staging and wintering sites. *Bird Conservation International*, *21*(3), 241–259. https://doi.org/10.1017/S0959270911000086

Yang, S., Xu, K., Milliman, J., Yang, H., & Wu, C. (2015). Decline of Yangtze River water and sediment discharge: Impact from natural and anthropogenic changes. *Scientific Reports*, *5*(1), 1–14. https://doi.org/10.1038/srep12581

Yang, W., Feng, X., & Yin, B. (2019). The impact of coastal reclamation on tidal and storm surge level in Sanmen Bay, China. *Journal of Oceanology and Limnology*, *37*(6), 1971–1982. https://doi.org/10.1007/s00343-019-8247-1

Yang, Y., & Chui, T. F. M. (2017). Hydrodynamic and transport responses to land reclamation in different areas of semi-enclosed subtropical bay. *Continental Shelf Research*, *143*, 54–66. https://doi.org/10.1016/j.csr.2017.06.008

Yu, X., Zhang, W., & Hoitink, A. (2020). Impact of river discharge seasonality change on tidal duration asymmetry in the Yangtze River estuary. *Scientific Reports*, *10*(1), 6304. https://doi.org/10.1038/s41598-020-62432-x

Yuan, Y., Jalon-Rojas, I., & Wang, X. H. (2021). Response of water-exchange capacity to human interventions in Jiaozhou Bay, China. *Estuarine, Coastal and Shelf Science*, *249*, 107088. https://doi.org/10.1016/j.ecss.2020.107088

Yun, C. (2004). Recent evolution of the Yangtze River estuary and its mechanisms. In *Processes of dynamics and geomorphology of the changjiang Estuary* (p. 302). (in Chinese).

Zhang, P., Yang, Q., Wang, H., Cai, H., Liu, F., Zhao, T., & Jia, L. (2021). Stepwise alterations in tidal hydrodynamics in a highly human-modified estuary: The roles of channel deepening and narrowing. *Journal of Hydrology*, *597*, 126153. https://doi.org/10.1016/j.jhydrol.2021.126153

Zhang, R., Chen, Y., Chen, P., Zhou, X., Wu, B., Chen, K., et al. (2023). Impacts of tidal flat reclamation on suspended sediment dynamics in the tidal-dominated Wenzhou Coast, China. *Frontiers in Marine Science*, *10*, 1097177. https://doi.org/10.3389/fmars.2023.1097177

Zhang, W., Feng, H., Zhu, Y., Zheng, J., & Hoitink, A. (2019). Subtidal flow reversal associated with sediment accretion in a delta channel. *Water Resources Research*, *55*(12), 10781–10795. https://doi.org/10.1029/2019wr025945

Zhang, W., Xu, Y., Hoitink, A., Sassi, M., Zheng, J., Chen, X., & Zhang, C. (2015). Morphological change in the Pearl River Delta, China. *Marine Geology*, *363*, 202–219. https://doi.org/10.1016/j.margeo.2015.02.012

Zhang, X., Lin, J., Huang, H., Deng, J., & Chen, A. (2022). Analysis on the dynamics of coastline and reclamation in Pearl River Estuary in China for nearly last half century. *Water*, *14*(8), 1228. https://doi.org/10.3390/w14081228

Zhao, J., Guo, L., He, Q., Wang, Z. B., Van Maren, D., & Wang, X. (2018). An analysis on half century morphological changes in the Changjiang Estuary: Spatial variability under natural processes and human intervention. *Journal of Marine Systems*, *181*, 25–36. https://doi.org/10.1016/j.jmarsys.2018.01.007

Zhong, Z., & Hu, Z. (2021). The impact of reclamation on tidal flat morphological equilibrium. *Frontiers in Marine Science*, *8*, 769077. https://doi.org/10.3389/fmars.2021.769077

Zhou, Z., Coco, G., Townend, I., Gong, Z., Wang, Z., & Zhang, C. (2018). On the stability relationships between tidal asymmetry and morphologies of tidal basins and estuaries. *Earth Surface Processes and Landforms*, *43*(9), 1943–1959. https://doi.org/10.1002/esp.4366

Zhou, Z., Coco, G., Townend, I., Olabarrieta, M., Van Der Wegen, M., Gong, Z., et al. (2017). Is "morphodynamic equilibrium" an oxymoron? *Earth-Science Reviews*, *165*, 257–267. https://doi.org/10.1016/j.earscirev.2016.12.002

Zhu, C., Guo, L., Van Maren, D., Tian, B., Wang, X., He, Q., & Wang, Z. (2019). Decadal morphological evolution of the mouth zone of the Yangtze Estuary in response to human interventions. *Earth Surface Processes and Landforms*, *44*(12), 2319–2332. https://doi.org/10.1002/esp.4647

Zhu, C., van Maren, D. S., Guo, L., Xie, W., Xing, C., Wang, Z. B., & He, Q. (2025). Water and sediment exchange between the anthropogenically modified distributaries of the Yangtze estuary. *Catena*, *250*, 108729. https://doi.org/10.1016/j.catena.2025.108729

Zhu, G., Xie, Z., Xu, H., Liang, M., Cheng, J., Gao, Y., & Zhang, L. (2021). Land reclamation pattern and environmental regulation guidelines for port clusters in the Bohai Sea, China. *PLoS One*, *16*(11), e0259516. https://doi.org/10.1371/journal.pone.0259516

Zhu, Q., Wang, Y., Gao, S., Zhang, J., Li, M., Yang, Y., & Gao, J. (2017). Modeling morphological change in anthropogenically controlled estuaries. *Anthropocene*, *17*, 70–83. https://doi.org/10.1016/j.ancene.2017.03.001

Zhu, Q., Wang, Y. P., Ni, W., Gao, J., Li, M., Yang, L., et al. (2016). Effects of intertidal reclamation on tides and potential environmental risks: A numerical study for the southern Yellow Sea. *Environmental Earth Sciences*, *75*(23), 1472. https://doi.org/10.1007/s12665-016-6275-0

Zhu, Z., Vuik, V., Visser, P., Soens, T., Van Wesenbeeck, B., Van De Koppel, J., et al. (2020). Historic storms and the hidden value of coastal wetlands for nature-based flood defence. *Nature Sustainability*, *3*(10), 853–862. https://doi.org/10.1038/s41893-020-0556-z